Novel drugs for tuberculosis: pharmacological and biochemical characterization in suitable test systems

Von der Fakultät für Lebenswissenschaften

der Technischen Universität Carolo-Wilhelmina

zu Braunschweig

zur Erlangung des Grades einer

Doktorin der Naturwissenschaften

(Dr. rer. nat.)

genehmigte
D i s s e r t a t i o n

von Hanaa Ahmad Nabel Abdelazez Wanas
aus Damietta, Ägypten

1. Referentin oder Referent: Prof. Dr. Mahavir Singh
2. Referentin oder Referent: Prof. Dr. Stefan Dübel
eingereicht am: 10.10.2012
mündliche Prüfung (Disputation) am: 11.12.2012

Druckjahr 2013

Vorveröffentlichungen der Dissertation

Teilergebnisse aus dieser Arbeit wurden mit Genehmigung der Fakultät für Lebenswissenschaften, vertreten durch den Mentor der Arbeit, in folgenden Beiträgen vorab veröffentlicht:

Tagungsbeiträge (Conference contributions):

1. [Poster presentation, 8th International Conference of Pathogenesis of Mycobacterial Infections, Saltsjöbaden, Stockholm, Sweden (2011).]

Wanas, H., Niggemann, J., Sasse, F. and Singh, M. *In vitro* antimycobacterial activity and cellular toxicity of lipophilic pyrazinoate esters.

2. [Poster presentation, 4th International Ph.D. Symposium, Braunschweig (2010).]

Wanas, H., Bhuju, S., Singh M. Novel drugs for tuberculosis: Pharmacological and biochemical characterization in suitable test systems.

The supervision from the Egyptian side was through:

Prof. Dr. Salwa Elmesiry
Professor of Pharmacology
Faculty of Medicine, Cairo University

Prof. Dr. Sohir Abo El-Azm
Professor of Pharmacology
Faculty of Medicine, Cairo University

Prof. Dr. Aida Khatab
Professor of Pharmacology
Faculty of Medicine, Cairo University

Acknowledgements

First and foremost, I would like to thank ALLAH, the lord of the world, the source of all knowledge and the knower of everything who helped me to finish this work.

I wish I could express my most sincere thanks, deep respect and appreciation to **Prof. Dr. Mahavir Singh** for his generous help, professional guidance and careful review of the work. I would like to thank him for his supervision and support from the preliminary to the concluding level that enabled me to develop an understanding of the subject. Also, all thanks for my Egyptian supervisors, **Prof. Dr. Salwa Elmesiry**, **Prof. Dr. Sohir Abo El-Azm** and **Prof. Dr. Aida Khatab** for their faithful support during all steps of the work.

I am heartily thankful to **Dr. Matthias Stehr** for his continuous guidance and supervision during many steps of my practical work. I wish to express my most sincere thanks and deep gratitude to **Dr. Florence Sasse** and all his staff members for their faithful support in performing the cell culture work. I would like to express my deepest thanks to **Dr. Jutta Niggemann** for her generous help during the synthesis of the pyrazinamide analogues. Special thanks for **Dr. Pere-Joan Cardona Iglesias** and **Dr. Cristina Vilaplana**, Experimental Tuberculosis Unit, Spain for helping in the mice experiments. I have furthermore to thank my colleagues at Helmholtz Zentrum für Infektionsforschung (HZI), **Dr. Sabin Buhju**, **Dr. Ayssar El Amin** and **Ibrahim Sabra** for their innovative and constructive advices and discussions. I would also like to thank all staff members in **Lionex GmbH** and special thanks to **Dr. Wulf Oehlmann** for his help and technical support and providing the place to perform the mycobacterial work. I wish also to convey my gratitude to all the current **Genomanalytik (GMAK)** and former colleagues in the **Dept. of Genome Analysis (GNA)** for providing me with a good working atmosphere.

I cannot forget to extend my deepest gratitude to the **Egyptian Culture Affair and Mission Sector under the Egyptian Government** beside the **Deutscher Akademischer Austauschdienst (DAAD)** for the award of doctoral scholarship during the first two years in my work. And also, all thanks for the **Pharmacology Dept., Medical school, Cairo University** for recommending me to have this scholarship.

I owe the deepest thanks to my parents, my daughter **(Hoda)**, my son **(Omar)**, my **sisters**, my **brother** and my **friends** for their love, care, pray, support, patience, and encouragement during the whole my life. Without them, I would have never the chance to achieve lots of things.

Finally, I am deeply thankful and profoundly grateful to my beloved husband **(Alaa-Eldin)** for his help, patience, motivation and enthusiasm. I could not have imagined having a better life partner than him.

Hanaa Wanas

Contents

1. Introduction

Tuberculosis (TB) is a major global public health problem around the world. It remains one of the leading infectious causes of morbidity and mortality. *Mycobacterium tuberculosis* (*M. tb*) is estimated to have infected one-third of the world's population (*WHO: Tuberculosis facts, 2007*). Annually, around 9 million people develop an active form of the disease with subsequent nearly 2 million deaths worldwide (*Geraldes Santos et al., 2007)*. Regionally, the majority of TB cases in 2008 existed in Asia (55%) and Africa (30%), with noticeable decrease of cases in the Eastern Mediterranean (7%), Europe (5%), and the Americas (3%) (*Haydel, 2010)*.

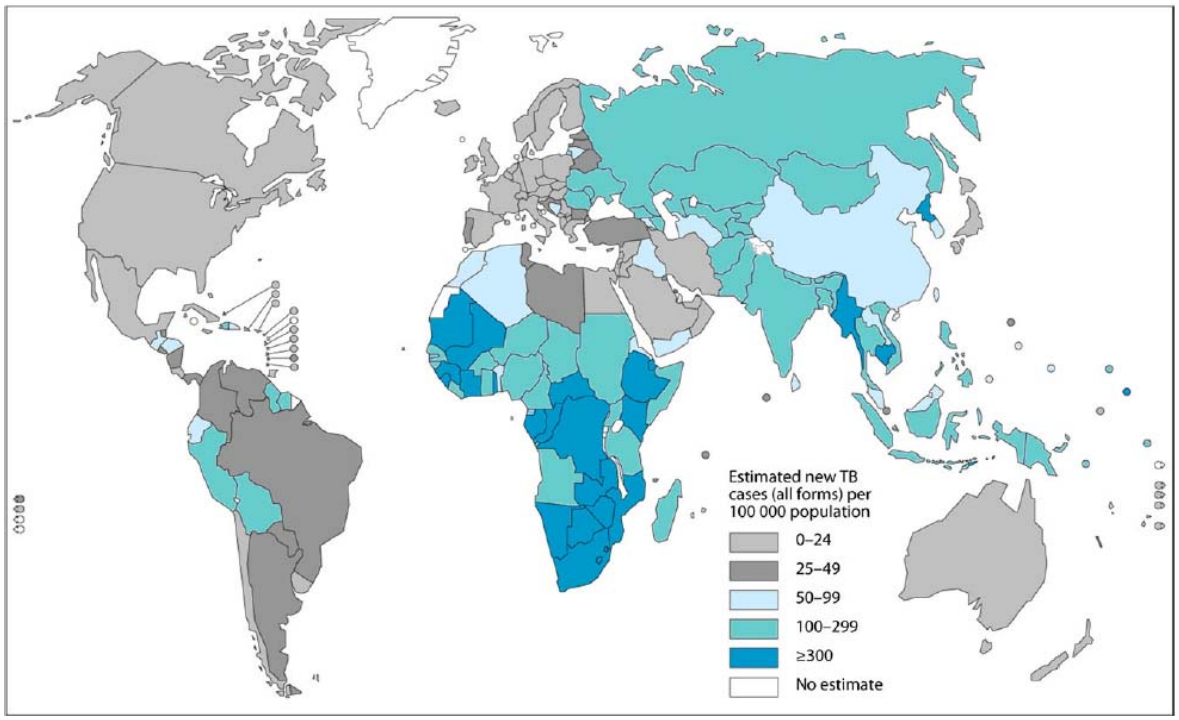

Fig. (1): Estimated TB incidence rates, 2010. Source: (*WHO: Global tuberculosis control, 2011*)

TB infects mainly the lung parenchyma (pulmonary TB) however; extra-pulmonary TB represents also a common clinical feature in which the bacillus penetrates other organs such as lymph nodes, abdomen, pleura, genitourinary tract, skin, joints, bones, meninges, pericardium, larynx, breast and female genital tract (*Sharma & Mohan, 2004*). Fever, loss of weight, and a typical cough with blood and sputum are the usual manifestations of the disease. Bacille Calmette-Guérin (BCG) vaccine, which is an alive attenuated strain of *M. bovis*, is the only currently used vaccine (*Daele & Calenbergh, 2005*). The widespread use of the vaccine is

controversial as it failed to decrease the pandemic of TB. In addition; recent data suggested that BCG might also have accelerated the development of even more virulent forms of TB. On the other hand, it could be valuable in preventing the less frequent severe forms in children such meningitis and systemic disease (*Marriner et al., 2011*) (*Young & Dye, 2006*).

TB is an air born infection which is transmitted as a highly infectious aerosol. The fate of the initial exposure to *M. tb* varies from immediate elimination of the organism by the host's innate immune response to infected individuals developing active primary TB (*Flynn & Chan, 2001*). However, the most of exposed cases develop a latent infection with no clinical symptoms. These patients have the risk of 5-10 % to develop the active form during their life even with the absence of any cause of immunosuppression (*Clark-Curtiss & Haydel, 2003*).

Other aspect that contributed markedly to aggravate the situation is the co-infection with human immunodeficiency virus (HIV) in which TB and HIV synergistically influence the progress of each other's. HIV positive individuals have a 60-fold greater risk to develop active TB (*Corbett et al., 2003*). The treatment of the dual infection is more complicated due to the negative interaction between antiviral and anti-TB drugs, especially rifampicin (RIF) which accelerates the metabolism of several antiviral drugs. Furthermore, the immunosuppression with HIV enhances the rate of TB relapse (*Aaron et al, 2004*). Currently, around one-third of HIV positive individuals are co-infected with TB (*Haydel, 2010)*.

1.1 Tuberculosis treatment and drug resistance:

1.1.1 Recommended treatment and current anti-TB antibiotics:

As recommended by the world health organization (WHO), the standard treatment initiated during the first two months by daily administration of the first-line anti-TB drugs; isoniazid (INH), RIF, pyrazinamide (PZA), and ethambutol. In the continuation phase, INH and RIF are administered for additional 4 to 12 months. (*WHO: treatment of tuberculosis guidelines, 2010*). This standardized treatment regimen is a part of (DOTS), the Directly Observed Treatment Short-course. This strategy was developed to shorten the length of the illness, to lower the mortality rate and to avoid the development of drug resistance. It depends on five principal elements: political commitment for financing, proper case detection with appropriate laboratory techniques, standard chemotherapeutic treatment, a monitoring system and a direct observation of the treatment (*Daele & Calenbergh, 2005*).

First-line anti-TB antibiotics (Table-1) work mainly against actively replicating *M. tb*, thus reducing the spread of infection to other individuals during the first two months of treatment. The sterilizing property of RIF during the short-course antibiotic regimen is referred to its activity against dormant bacteria (*Haydel, 2010)*. PZA has a powerful activity against dormant and slow replicating *M. tb* under acidic and hypoxic conditions inside macrophages and in the pulmonary caseous lesions (*Zhang et al., 2003*) (*Zhang & Mitchison, 2003*). When resistance to INH is suspected, adding ethambutol to the first-line drug regimen is recommended to prevent RIF-resistance (*American thoracic society and infectious diseases society of America, 2003*).

Table (1): First line anti-tuberculosis drugs (*Haydel, 2010*).

First-line drug	Antibiotic class	Route	Activity	Mechanism of action	Genes and products related to resistance
Isoniazid	Pyridine hydrazide	Oral	Bactericidal	Inhibition of cell wall synthesis (mycolic acid)	*1- katG*: catalaseperoxidase 2- *inhA*: enoyl-ACP Reductase 3- *ndh*: NADH dehydrogenase II
Rifampicin	Rifamycin	Oral	Bactericidal	Inhibition of RNA synthesis (RNAP)	*rpoB*: β-subunit of RNA polymerase
Pyrazinamide	Nicotinamide analogue	Oral	Bacteriostatic / bactericidal	Acidification of the cytoplasm & disruption of the cell wall function	*pncA*: nicotinamidase/ pyrazinamidase
Ethambutol	Ethylenediamine derivative	Oral	Bacteriostatic	Inhibition of cell wall synthesis (arabinogalactan)	*embCAB*: arabinosyl transferase

The second-line drugs (table-2) are introduced to the drug regimen with the resistance to the first-line. Each member of the second-line has its own problems, either lower potency, higher toxicity or the expensive cost (*Dorman & Chaisson, 2007*) (*Moore-Gillon, 2001*).

Table (2): Second line anti-tuberculosis drugs (*Haydel, 2010*).

second-line drug	Antibiotic class	Route	Activity	Mechanism of action	Genes and products related to resistance
Streptomycin	Aminoglycoside	IM	Bactericidal	Inhibition of protein synthesis	1- rpsL: S12 ribosomal protein 2- rrs: 16S rRNA
Kanamycin/ Amikacin	Aminoglycoside	IM	Bactericidal	Inhibition of protein synthesis	rrs: 16S rRNA
Capreomycin	Polypeptide	IM	Bactericidal	Inhibition of protein synthesis	1- rrs: 16S rRNA 2- tlyA: Putative rRNA methyltransferase
Levofloxacin	Fluoroquinolone	Oral or IV	Bactericidal	Inhibition of DNA replication	gyrA: DNA gyrase subunit A
Moxifloxacin	Fluoroquinolone	Oral or IV	Bactericidal	Inhibition of DNA replication	gyrA: DNA gyrase subunit A
Gatifloxacin	Fluoroquinolone	Oral or IV	Bactericidal	Inhibition of DNA replication	gyrA: DNA gyrase subunit A
Ethionamide	Thioamide	Oral	Bacteriostatic	Inhibition of mycolic acid (cell wall) synthesis	1- inhA: Enoyl-ACP reductase 2- etaA/ethA: Flavin monooxygenase
Cycloserine	Isoxazolidinone	Oral	Bacteriostatic	Inhibition of peptidoglycan (cell wall) synthesis	Unknown (alrA: D-alanine racemase in Mycobacterium smegmatis)
Para-aminosalicylic acid	Salicyclic acid	Oral	Bacteriostatic	Inhibition of folic acid synthesis	thyA: thymidylate synthase

1.1.2 Emergence of drug resistance:

Drug-resistance in tuberculosis could be either initial due to infection with already resistant strains or acquired resistance that comes from the selection for resistance due to inadequate, interrupted treatment. Acquired resistance can originate also from treatment with drugs that the strain already are resistant to; this intensifies the development of resistance to even more drugs (*Andrews et al., 2008*).

Each year, 424,000 individual develop multi-drug resistant TB (MDR-TB), which is defined as resistance to at least two of the best first-line anti-TB antibiotics, INH and RIF.

The estimated cure rate with MDR-TB infection ranges between 60-80%, which is to be compared to > 95% for fully susceptible strains (*Haydel, 2010*). MDR-TB infection can be fatal even in HIV negative patients due to the lack of a good second-line drug (*Leimane et al., 2005*).

This situation had contributed to the promotion of the emergence of extensively drug-resistant TB (XDR-TB), the definition that was 1st announced in March 2006. XDR-TB is not only resistant to first-line but also to any fluoroquinolone as well as one or more of the injectable drugs; kanamycin, amikacin and capreomycin (*Gandhi et al., 2006*). The number of countries that reported at least one case of XDR-TB has jumped from 20 in 2007 to 57 in 2009, thus highlighting its spread. The cure rate between these patients ranges between 30-60%. Furthermore, they should be subjected to strict monitoring and support to prevent more drug resistance that could make the disease untreatable (*Haydel, 2010*). In 2012, the third case over world of totally drug resistant TB has been diagnosed in India. The first 2 cases were discovered in Indonesia and Iran in 2007 and 2009 respectively (*Rowland, 2012*)

1.2. The urgency of new anti-TB drugs development:

It is obvious that, the performance of the current stuff for TB diagnosis and treatment limits the competent implementation of the DOTS strategy which actually covers only 20 to 25% of all patients worldwide (*O'Brien & Nunn, 2001*) (*Balganesh et al., 2004*).

The two prominent features of the current anti-TB regimen, which makes it far from ideal, are combination and long therapy for at least 6 months. The combination therapy is mandatory not only to prevent the emergence of drug resistant mutants, but also due to the different contribution of the individual drugs in the combination to eradicate the microbe in its different states, either rapidly dividing, slow or non-replicating or intracellular (*Balganesh et al., 2004*). The therapy of six months is needed to minimize the risk of relapses produced by the persisters, the bacilli that remain in the host for relatively long periods despite appropriate drug treatment (*Fenhalls et al., 2002*).

This kind of lengthy multidrug regimen usually associated with lack of patient compliance that usually leads to emergence of drug resistance. Development of drug resistance is frequent when observed treatment is not available, when recommended regimens are not used, and with using drugs with poor bioavailability (*O'Brien & Nunn, 2001*).

With the diagnosis of MDR-TB or XDR-TB, the patient will be subjected to very expensive regimen schedules consisting of 20 tablets per day and intramuscular injection for at least 18 to 24 months. Such regimens are associated with overwhelming, toxic side effects, as well as the psychological and social anxieties (*Haydel, 2010*).

The minimum requirement for a new antituberculosis drug is to decrease the duration of therapy. This would enable DOTS to reach higher percentage of patients and to improve patient compliance with better control of the disease. The ideal drug to reach this goal would be a compound that has cidal activity against replicating and non- replicating bacilli, extra and intracellular. When this far goal will be reached, the new compound will be introduced into the regimen replacing one or two of the existing members. Studying the pharmacokinetic/pharmacodynamic properties of the new compound and also the frontline antituberculosis drugs would help to design a more competent dosing regimen that can shorten the duration of therapy (*Balganesh et al., 2004*).

The use of RIF, the most effective drug in reducing patient bacillary burdens for drug-susceptible TB, is one of the most pressing reasons in new anti-TB drug discovery (*Marriner et al., 2011*). RIF is a powerful inducer of many cytochrome P450 (CYP) enzymes particularly P450 (CYP) 3A4. This eventually will inactivate other drugs thus reducing effective serum concentrations and exposure. On the other hand, RIF reduces the bioavailability of concomitantly administrated drugs by up-regulating membrane transporters (P-glycoproteins) which often work as cellular efflux pumps in the gastrointestinal tract (*Sousa et al., 2008*). RIF might be substituted by rifabutin in HIV-coinfected patients receiving antiretroviral drugs whose serum levels are affected by RIF induction of CYP3A4. However, current clinical assessment does not completely support substitution of RIF with rifabutin (*Davies et al., 2007*). (Fig. 2) summarizes the desired profiles needed in a new TB drug and the characteristic features contributing to achieve these profiles.

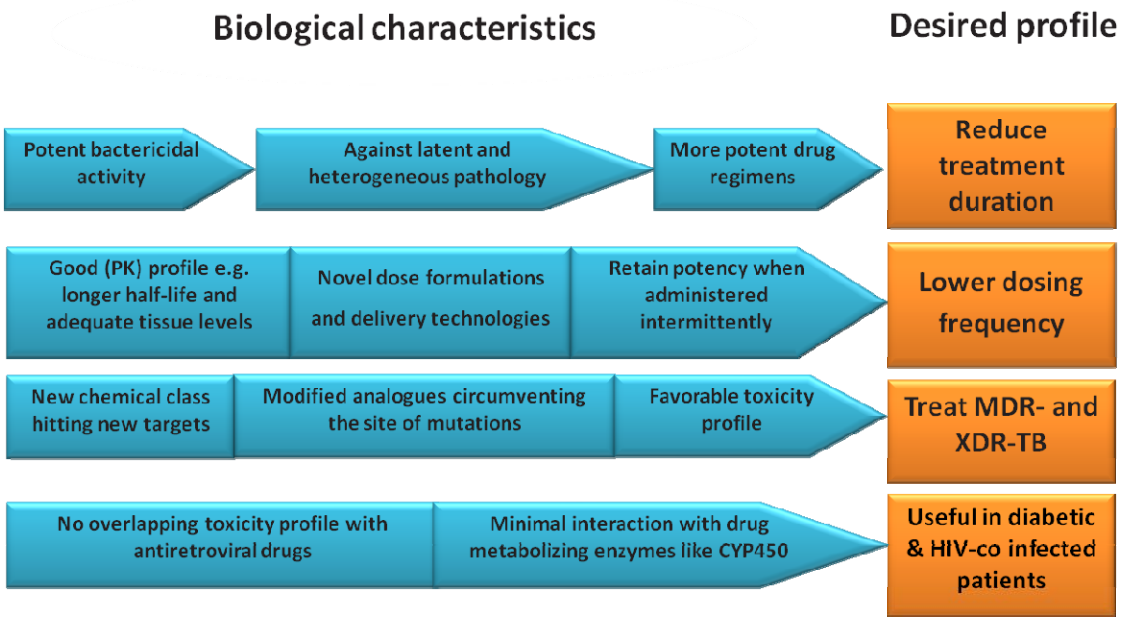

Fig. (2): Target product profile features needed in the new anti-TB drug and the biological characteristics needed to achieve each feature. (*Van den Boogaard et al., 2009*) (*Koul et al., 2011*).

1.3. Tuberculosis drug discovery pathway: approaches and critical issues:

The process by which a new anti-infective drug is introduced from the laboratory bench to the clinical use can be generally classified into two phases. The discovery, or the preclinical, phase which includes the laboratory activities up to testing the compound in relevant animal models. The second is the development phase which includes testing the compound in normal and infected human hosts (*Balganesh et al., 2004*). The phase of discovery has the following major goals:

- ***Target identification and validation:*** this field is markedly enhanced by the advanced genomic and proteomic tools and the present era of genome sequencing (*Wang et al., 2004*). Many efforts were done to identify targets which are essential for the survival and/or the persistence of the microbe e.g. L-alanine dehydrogenase (*Hutter & Singh, 1998*) and the enzymes involved in the lipid droplet metabolism like Ag85A (*Elamin et al., 2011*) (*Stehr et al., 2012*). By using comparative genomics, targets are evaluated with regard their specificity and selectivity. For more target validation, essentiality of targets under different conditions could be evaluated by whole cell or animal experiments, gene knock-outs or site directed mutagenesis

(*Raman et al., 2008*). In general, this approach had little success in the development of antibacterial agents as the essentiality of a target does not ensure its druggability.

- ***Lead identification:*** to identify compounds those inhibit the biological activity of the target molecules leading to cidal or static effect on the microbial growth *in vitro*. The two main approaches that used for lead identification are high-throughput screening, and structure based design and virtual screening.
- ***Lead optimization:*** measuring the Pharmacokinetics (PK) of compounds can provide an idea about the relationship between the *in vitro* cidal effects on the microbe and the ability to eradicate the microbe from infected animal models. Concurrently the therapeutic index, a ratio of the toxic dose to the effective dose, should be monitored for reaching an acceptable safety profile. Lead compounds are subjected to synthetic and medicinal chemistry for better quality and *in vivo* potency of the compound (*Balganesh et al., 2004*).

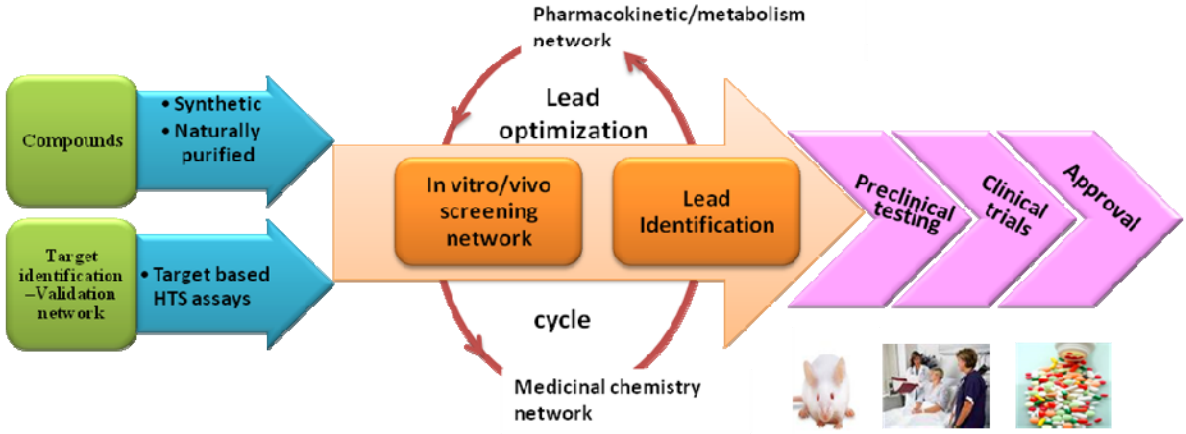

Fig. (3): Tuberculosis drug discovery pathway: Modified from (*Nwaka & Hudson, 2006*).

1.3.1. High-throughput screening:

In modern drug discovery high-throughput screening has an important role. It was used over last few years in a large scale to test the inhibitory effect of large numbers of compounds either synthesized or naturally purified (*Balganesh et al., 2004*). It has an important role in investigating the viability of small molecules as modulators of a number of anti-mycobacterial drug targets. Biochemical high-throughput screening had a major role in the finding of two clinical drug candidates, TMC207 and SQ109 (*Sacchettini et al., 2008*) High-throughput screening has two approaches that could be used individually or together:

- ***Whole cell screens (phenotypic screening):*** which target the whole cell growth. During last 10 years, it has been used to screen millions of compounds to derive 'hits' that can be used as starting points in the new drug discovery pathway. It has the advantage of providing the information about the ability of hits to kill the mycobacterium (*Nuermberger et al., 2010*). Several whole cell screens were established like AlarMar Blue redox dye assay (*Collins & Franzblau, 1997*), resazurine microtitre assay (*Palomino et al. 2002*), luciferase-reporter mycobacterial Strain (*Lee et al., 2003*) and green fluorescent protein based screening systems (*Changsen et al., 2003*) . As this kind of screening is not target or mechanism based, it has the hazard of finding compounds that have generalized toxicity (*Sacchettini et al., 2008*). As well as the lack of information on the target is considered a rate-limiting step in the ability of medicinal chemistry to modify the hits to provide good drug like qualities (*Nuermberger et al., 2010*).
- ***Cell-free target-based screens:*** which predict the inhibitory effect of different compounds on a specific target in a cell-free environment. Different assays were designed based on the action of purified drug targets (*Agren et al., 2008*) (*Bhuju, 2009*) (*Elamin et al., 2009*). In this approach it is essential to test the PK profiles of these inhibitors, as there are many examples of small molecules that have poor whole-cell potency in spite of their excellent target inhibition, most probably due their failure to permeate across the mycobacterial cell wall (*Sacchettini et al., 2008*). However, target-specific discovery programs have the advantage of accelerating the role of medicinal chemistry to provide compounds that continue to hit the desired target as well as better understanding of the mechanism of cell death (*Nuermberger et al., 2010*). Combining phenotypic and target-based screens might help to avoid the drawbacks of each.

1.3.2. Pharmacokinetic studies and drug development:

PK is the branch which is concerned with the studying of absorption, distribution, metabolism, and excretion (ADME) profile of drugs. This field offers better understanding the mechanism of action of a new potential drug candidate and at the same time helping in decreasing expensive attrition during drug development pathway.

PK studying and metabolic assessment could be considered crucial in the process of drug discovery and development and should be initiated at early stages to achieve the best PK

and pharmacodynamics (PD). It is well recognized that good *in vitro* activity cannot be extrapolated to good *in vivo* activity unless the drug has a satisfactory bioavailability and an adequate duration of action (*Jiunn & Anthony, 1997*). This means that not only the PD that control the efficacy and safety but also the PK properties (clearance, half-life, extent of protein binding and volume of distribution), the properties that determine the rate and the concentration in which the drug will reach its site of action (*Panchagnula & Thomas, 2000*). Many drug candidates were withdrawn from the development pathway due to their undesirable PK profile. In the survey done by (*Prentis, et al., 1988*), the serious PK troubles were 40 % of the causes that lead to drug attrition. So we can emphasize on the corner stone role of PK studying to guide medicinal chemistry in the drug design and to accelerate the drug development process.

1.3.2.1. Plasma protein binding:

Binding to plasma proteins, mostly to albumin and α acid glycoprotein, is profoundly affecting the PK and PD of a compound. Thus plasma protein binding (PPB) experiments are done essentially during the phase of drug discovery and development.

The importance of determining the PPB of a new potential anti-TB drug is revealed in the studies of early bactericidal activity (EBA) which needs free penetration of the substance into cavities. An obvious example, the therapeutic margin which is defined as the ratio between usual dose and dose at which EBA= 0. It was much smaller in the case of RIF than INH although their similar PK. This could be explained by the percentage of unbound part of the dose, 15% for RIF and 100% for INH, that can penetrate freely into cavities. This theory also can explain the poor results of rifapentine, 2% unbound fraction, when administrated with INH in the continuation phase in clinical trials (*Mitchison & Davies, 2008*).

The fraction of the unbound drug is a major determining factor of all PK profile of a substance as follows:

- ***Volume of distribution (V_d)*:**

It is a solid tenet that only free unbound drug can diffuse across membranes, hence protein binding can affect distribution of the drug from the vascular compartment to tissues. The relation that can be described by the following equation where (V_d) is the apparent volume of distribution, (V_p) is the volume of plasma, (V_t) is tissue volume, (F_{up}) is the unbound fraction in plasma and (F_{ut}) is the unbound fraction in tissue.

$$V_d = V_p + V_t (F_{up} / F_{ut})$$

From the previous equation we can conclude that V_d increases when F_{up} incrases and decreases when F_{ut} increases. Of course F_{ut} is playing more important role as V_t is much larger than V_p. As the measuring of F_{ut} is considered technically difficult, F_{up} is measured as a lieu of F_{ut} depending on the theory of the equilibrium of unbound unionized drug between plasma and tissues. And in this case naturally many other considerations should be taken that also govern distribution of substances across membranes as ionization, lipophilicity, active uptake and secretion and metabolism by tissues (*Jiunn & Anthony, 1997*) & (*Schmidt et al., 2010*).

- ***Clearance (CL):***

CL is defined as the volume of blood (or plasma) from which a drug is completely and irreversibly removed per unit time. Most of drugs are cleared mainly through liver and kidneys. Renal clearance (CL_{renal}) when the substance is cleared by renal filtration can be expressed by the following equation where (GFR) is the glomerular filtration rate.

$$CL_{renal} = F_{up} * GFR$$

While hepatic clearance ($CL_{hepatic}$) can be determined by the following equation where ($Q_{hepatic}$) is the liver blood flow, ($CL_{u\ int}$) is the intrinsic hepatic clearance based on unbound drug concentration.

$$CL_{hepatic} = (Q_{hepatic} * F_{up} * CL_{u\ int}) / (Q_{hepatic} + F_{up} * CL_{u\ int})$$

(*Jiunn & Anthony, 1997*) & (*Schmidt et al., 2010*).

Briefly, we can elucidate from the two previous equations that when the substance is eliminated through the glomerular filtration, PPB delays its rate of elimination. Similarly, the substance which is highly extracted by the liver, PPB decreases $CL_{hepatic}$. On the other hand, when the substance cleared by tubular excretion or its $CL_{hepatic}$ is flow dependent (low extracted substances), PPB considered as a depot that supplying the eliminating organ with the drug accelerating the rate of its CL (*Lindup & L`eorme, 1981*) & (*Beer et al., 2009*).

Finally, for antibiotics particularly, high PPB that reduces the free drug fraction reflected in diminished antimicrobial activity. Many studies showed the effect of PPB on the minimal inhibitory concentration (MIC) underlying the idea of the *in vivo* efficacy of a substance cannot only predicted from *in vitro* MIC and plasma level, but determination of the extent of PPB is a very important parameter (*Schmidt et al., 2008*).

There are numerous *in vitro* methods for the determination of PPB. Equilibrium dialysis (ED) is usually considered as the "reference method". Generally, it is easy, inexpensive and accurate. The cell of dialysis composed of two chambers separated by a semipermeable dialysis membrane, available in various molecular weight Cutoffs. (Fig. 4) shows a schematic presentation of the dialysis cell. The bound fraction can be calculated from the following equation where (C_B) is the concentration of bound drug, (C_T) is the total concentration in plasma chamber and (C_U) is the concentration in buffer chamber.

$$C_B = C_T - C_U$$

(*Beer et al., 2009*)

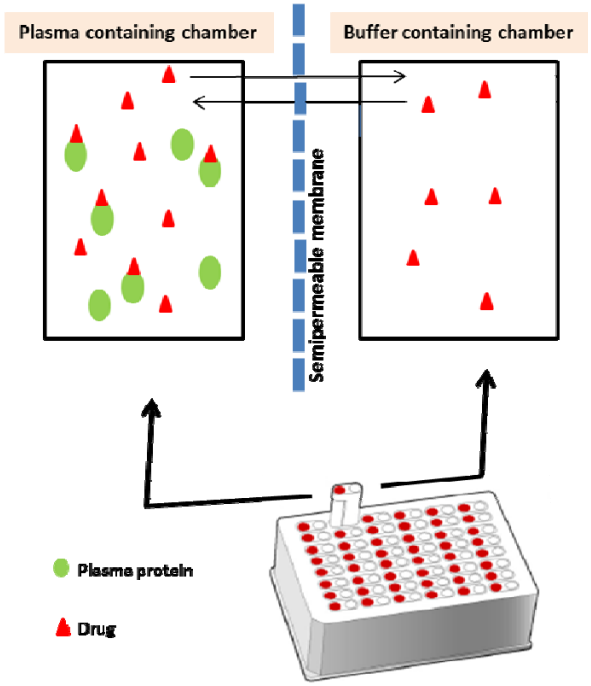

Fig. (4): Equilibrium dialysis for measuring the binding to plasma proteins.

1.3.2.2. Hepatic microsomal stability:

The hepatic microsomal stability (HMS) assay is widely used to rank substances in relation to their metabolic stability. Metabolic stability plays a major role in the success of a potential drug candidate. It is clear that the first pass metabolism by liver leads to poor bioavailability and shortens the half-life ($t_{1/2}$) of a substance. Early assessment of microsomal stability in drug discovery pathway provides the research team with valuable information about potential instability of the compounds. This is helpful to find structure–metabolic stability relationships and to modify the synthetic strategy accordingly. Typically, hepatic microsomal enzymes are used in *in vitro* microsomal stability assays for estimation of intrinsic CL caused by phase-I oxidation (*Mondal et al., 2008*) & (*Di et al., 2003*).

1.3.2.3. Pharmacokinetics/pharmacodynamics of antibiotics as preliminary indicator of *in vivo* efficacy:

In antibacterial drug discovery and with the progress of the field of anti infective pharmacology, much concern was directed to the ability to predict the efficacy of a class of compounds based on the pharmacokinetic-pharmacodynamic (PK/PD) parameters. This field integrates the composite relationship between organism susceptibility to the antibiotic, which is usually measured with the MIC, and the patient PK (*Van Bambeke et al., 2006*).

PK studies describe what the body does with the drug with regard absorption, distribution, metabolism, and elimination. And it depends on the measurement of a drug and its metabolites in an accessible biologic fluid as blood and urine. From the resulting concentration-time profile when an agent is administrated *in vivo*, we can calculate different pharmacokinetic parameters such as peak concentration (C_{max}), the serum $t_{1/2}$, CL, V_d and area under the curve (AUC) that reflects the cumulative exposure to a compound over a given time period (*Derendorf et al., 2000*).

Three main PK/PD parameters (Fig. 5) have been described to provide an indication about the antimicrobial outcomes such as bacterial eradication and/or clinical cure, as a successful outcome of an antimicrobial agent requires a specific pharmacodynamic interaction between this agent and its bacterial target. PK/PD parameters have a potential value as a guide to establish dosing regimens for new and old drugs and for new emerging pathogens and resistant organisms (*Craig, 1998*).

The first parameter, (T > MIC), is the time during which the concentration of the antibiotic remains higher than the level of the MIC. This correlation between the bactericidal effects and time is chiefly affected by the $t_{1/2}$, dosage and frequency of administration. On the other hand, (C_{max}/MIC) represents the relationship between the bactericidal effects and the concentration. It is mainly affected by the administrated dose and the volume of distribution of the substance. The third one, (AUC/MIC), combines both time and concentration effects, as it reflects the total exposure of bacteria to the antibiotic with regard time and concentration. It is directly proportional to the total amount given during certain time period and inversely proportional to the drug clearance (*Van Bambeke et al., 2006*).

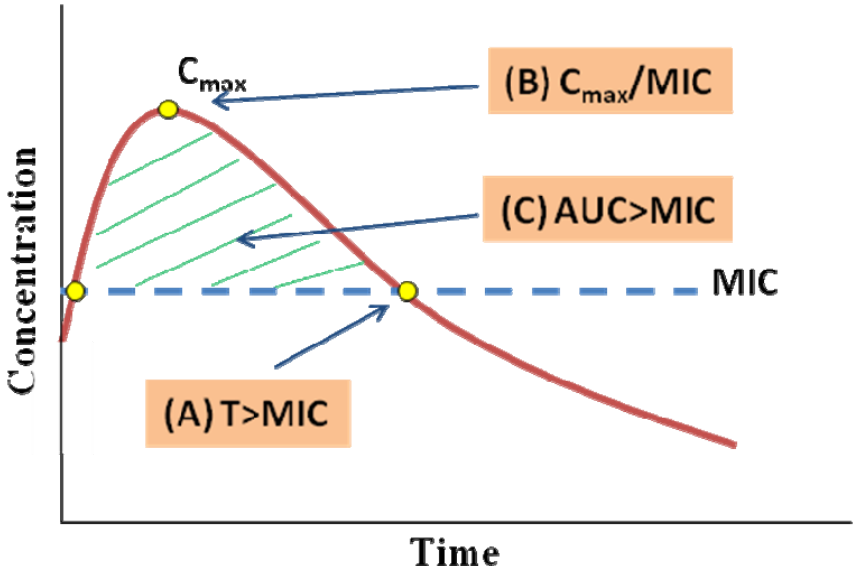

Fig. (5): The main three PK/PD parameters affecting antibiotic potency: (A) is the time (T) during which the serum concentration of a substance exceeds the minimal inhibitory concentration (MIC), **(B)** is the ratio between the peak plasma concentration (C_{max}) and the MIC, **(C)** is the ratio between the area under the concentration-time curve (AUC) for 24 hours and the MIC. (*Van Bambeke et al., 2006*) (*McKinnon & Davis, 2004*).

1.3.2.4. Lipophilicity and cell penetration:

M. tb, in comparison to other gram positive and gram negative bacteria has unique membrane architecture with high lipid content. The complex, lipid-rich envelope of *M.tb* provides the bacteria with a barrier that prevents the permeation of a broad range of therapeutic agents (*Marriner et al., 2011*). Susceptibility of *M.tb* to different antibiotics is enhanced by inhibitors of cell wall envelop synthesis (*Rastogi et al., 1990*). The special structure of mycolic acid and mycolyl-arabinogalactan found in the mycobacterial cell wall

contributes to the very poor fluidity of the inner leaflet of the cell wall (*Liu et al., 1996*). Fluoroquinolones, macrolides, rifamycins, and tetracyclines are lipophilic antibiotics. They go in the bacteria through the lipid bilayer rather than the inefficient pores of the outer leaflet. Within an antibacterial class, the more lipophilic agents have the tendency to be more effective against *M.tb* (*Brennan & Nikaido, 1995*).

Lipophilicity significantly impacts ADME/TOX profile of drugs. It is also an essential parameter in the development of quantitative structure activity relationship (QSAR) (*Kerns & Di, 2003*). Lipophilicity is measured by (Log*Pow*), the octanol–water partition coefficient, which is defined as the ratio of un-ionized drug distributed between the octanol and water phases at equilibrium. Higher Log*Pow* values entail more lipophilicity (*Leeson & Springthorpe, 2007*). Compounds that have moderate lipophilicity (Log*Pow* 1.5-3.5) show a good balance between solubility in water and permeability to cell wall. They are ideal for oral absorption in addition to low metabolic liability. On the other hand, hydrophilic compounds have good solubility, but poor permeability for gastrointestinal tract, and are more susceptible to rapid clearance by the kidney (*Kerns & Di, 2003*). Compounds with a Log*Pow* more than 5.0 are more likely to have poor absorption. Such compounds are considered non-drug-like and are commonly filtered out in the early stages of drug discovery. However, there are examples of compounds that have high Log*Pow* values and can be easily absorbed from the gastrointestinal tract. Although Entacapone and tolcapone have high Log*Pow*, they are approved drugs and have been clinically tested with satisfactory pharmacokinetic properties. Entacapone reach the C_{max} after one hour of administration. Dissolution enhancers like croscarmellose sodium are used in the formulation of entacapone to improve its solubility (*Kinnings et al., 2009*).

1.3.3 Animal models and preclinical validation:

Testing new TB drugs in animal models is extremely important as not all functions, which are essential *in vitro*, are essential *in vivo* (*Koul et al., 2011*). (Table-3) summarizes some of the current experimental animal models and their typical uses (*Marriner et al., 2011*) (*Lenaerts et al., 2008*).

Table (3): Animal models in new anti-TB drug discovery. (*Marriner et al., 2011*) (*Lenaerts et al., 2008*).

Model	Pathology	Utility	Limitations
Mice	Pulmonary pneumonia and aggregates of leukocytes, spleen, and liver, permissive for growth	Standard model for drug efficacy	limited pathology
C57BL/6 or BALB/c (usually)		- PK/PD determinations - *In vivo* toxicity/maximum tolerated dose - Early bactericidal effect assay - Standard therapy assays, regimens	
IFN-g gene knockout mouse		Rapid *in vivo* drug assay	
GM-CSF gene knockout mouse		Mouse unable to prevent disease reactivation	
'Wayne in vivo' mouse model		Mouse inoculated with nonreplicating Oxygen-deprived bacilli	
Rats	Similar to mice	Accepted PK/PD model	Little additional information than mice
Zebrafish	Necrotizing granuloma in embryo	Early granuloma formation, high throughput	Non-pharmacodynamic
Guinea pigs	Pulmonary, splenic, and liver lesions; 50% solid, 50% necrotizing granulomas	Small size with more similarity to human	Non cavitating
Rabbits	-Limited infection with Mtb strains. - Pulmonary solid and necrotizing lesions, cavities. - Extensive secondary lesions (M. bovis only)	Pathology including pulmonary, CNS system, ocular sites	Highly sensitive to GI distress from many agents
Nonhuman primates	Various presentation of lesions in multiple organs	Similar spectrum of disease and PK as in humans.	Expensive, difficult dosing.

The mouse model is considered as the most cost-effective tool. Most data from this model have the tendency to be reproduced in clinical studies (*Koul et al., 2011*). It has played a major role to predict the bactericidal and sterilizing potencies of new compounds and individual drugs, (*Rosenthal et al., 2007*) (*Andries et al., 2010*), to assess the effectiveness of

drugs in combination (*Nuermberger et al., 2006*) , the efficiency of intermittent therapy (*Dickinson & Mitchison, 1970*) and the duration of therapy needed to avoid occurrence of relapse (*Nuermberger et al., 2004*) and PK-PD parameters of different agents (*Jayaram et al., 2003*) (*Jayaram et al., 2004*). Recently, the mouse model was used to recognize bacterial targets that could modify the liability of mycobacterial persistence after INH treatment (*Dhar & McKinney, 2010*).

Mouse model does not show the marked heterogenecity of lung pathology observed in the human infection (*Flynn, 2006*).Nevertheless, the results obtained from mouse experiments are reliable on the bactericidal and sterilizing activity of existing antituberculosis drugs and going with the data from numerous clinical studies. Therefore, it is thought that the mouse model can be considered as an indicator of human relapse rates (*Nuermberger, 2008*) On the other hand, mice do not form necrotic or hypoxic granulomas which means mice do not develop the latent disease, so it is not the model of choice to test drugs under development against latent disease (*Shi et al., 2011*). Mice can be infected by a variety of routes such as intravenous, intranasal inoculation, and by aerosol exposure. One of the main features of mouse models that it is not accurately understood to what extent the route of infection affects the rate of relapse after drug withdrawal (*Koul et al., 2011*).

1.4 Pyrazinamide and rifampicin: two frontline anti-TB drugs facing the huge challenge of resistance:

Pyrazinamide and rifampicin are two frontline anti-TB drugs. It is important to point out that the combination of PZA and RIF had greatly contributed to shorten the duration of therapy. Unfortunately, the resistance to both agents is frequent representing a huge obstacle in the treatment of TB. This problem of drug resistance should be solved by intensive efforts in drug development.

An additional obstacle in front of PZA is the difficulty to test the susceptibility to PZA *in vitro*. Since the *In vitro* MIC of PZA varies markedly with pH as well as the growth enrichment agent, bovine albumin, alters the pH and seems to bind the drug (*Zhang et al., 2002*). This problem might be solved by using target based assays for diagnosis of clinical PZA-resistance.

1.4.1 Pyrazinamide

PZA, which is an analogue of nicotinamide, is one of the first line antituberculous drugs. It is bactericidal to semidormant *M.tb* that persists in acidic environments inside macrophages, so it has a remarkable role in the shortening of TB therapy from 9-12 months to 6 months and by its introduction in the antituberculous therapy the rates of relapses were obviously reduced (*Muthaiah et al., 2010*). PZA is active against the members of MTB-complex except *M. bovis*; the intrinsic resistance to PZA is a characteristic feature of this member (*Allix-Be´guec et al., 2010*).

1.4.1.1 Mechanism of action:

Despite the fact that PZA is the most sterilizing anti-TB drug, its mechanism of action is still unclear. PZA is a prodrug which is devoid of significant antibacterial activity. PZA is transformed into its active metabolite, pyrazinoic acid (POA), by the action of the *M.tb* nicotinamidase/pyrazinamidase (referred to as *PncA*), the amidase enzyme which is encoded by the *pncA* gene (*Petrella et al., 2011*).

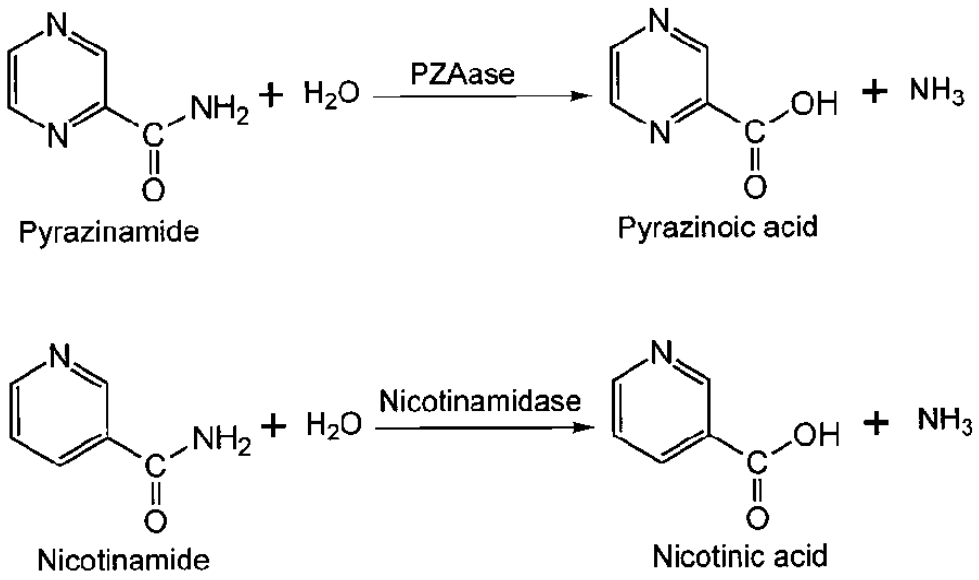

Fig. (6): Action of *PncA* enzyme on pyrazinamide and nicotinamide (*Zhang et al., 2008*).

After the formation of POA inside Mycobacterium there is no convincing evidence to explain the mechanism of action. A theory that has been developed by (*Zhang & Mitchison, 2003*) is the most predominant theory. In this theory, POA behaves as an anion that exits from the cell by passive diffusion and an inefficient efflux mechanism. In the acidic

environment POA will be protonated into the uncharged HPOA which will permeate efficiently back into the bacterial cytoplasm and in the neutral cytoplasm it will dissociate into the ionic form. Protons that enter the bacterial cell with HPOA could eventually acidify the cytoplasm with subsequent inhibition of the vital enzymes. In addition, HPOA could de-energise the membrane with disruption of the membrane function. With this theory and by applying the Henderson-Hasselbach equation to the weak acid POA (pKa 2.9) we can explain the differences in MIC of PZA at different pH. In neutral pH the majority of POA will be in the charged anion form which cannot enter cells easily (*Salfinger & Heifets, 1988*) (*Jureen, 2008*). This also explains the greater activity of PZA against old non-replicating bacilli in which the passive uptake would remain unchanged while the active efflux mechanism is down-regulated (*Zhang & Mitchison, 2003*).

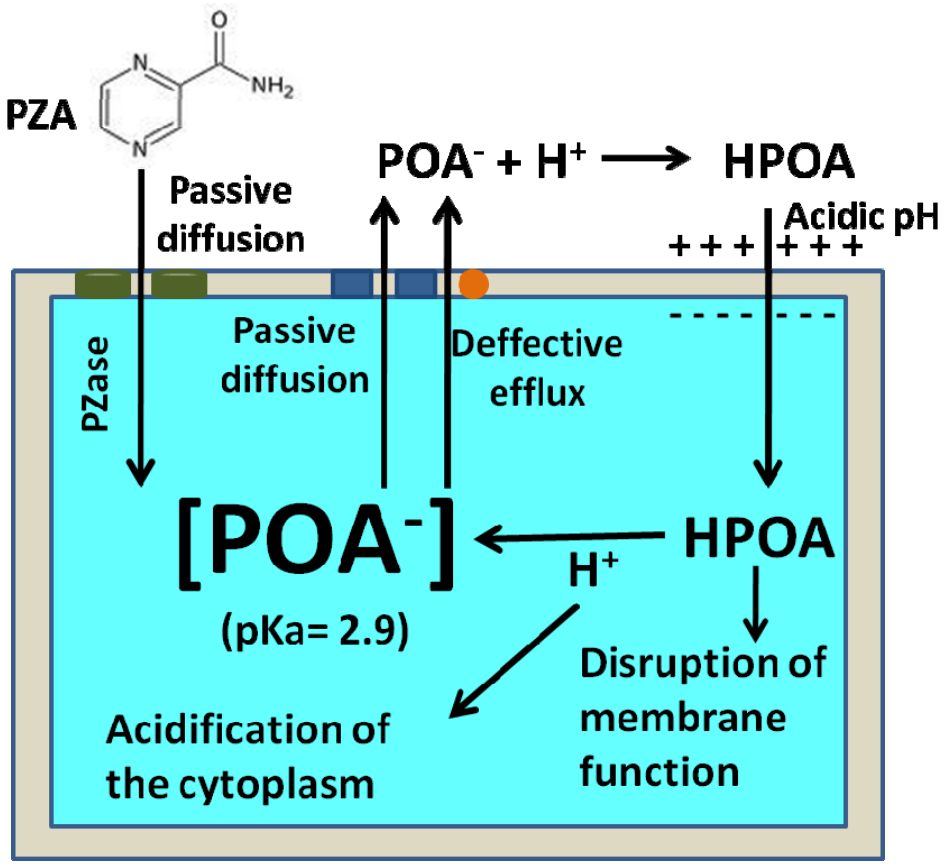

Fig. (7): Mode of action of Pyrazinamide. PZA: pyrazinamide; POA: pyrazinoic acid; HPOA: protonated POA. (*Zhang & Mitchison, 2003*).

This theory is supported by the results of (*Zhang et al. 1999*) that showed that the efflux blocker reserpin increased the accumulation of POA in *M.tb*. Also reserpin enhanced the susceptibility of *M.tb* to PZA not POA in the results achieved by (*Zhang et al., 2002*).There is another theory which is based on that PZA inhibits fatty acid synthetase I (FASI). (*Zimhony et al., 2000*) using the PZA analogue 5-Cl-PZA and *M. smegmatis* showed inhibition of FASI. However, in PZA-resistant *M.tb* strains, no mutations in FASI have been found.This theory needs to be further investigated as it seems as 5-Cl-PZA and PZA/POA may have different drug targets (*Zhang & Mitchison, 2003*) (*Jureen, 2008*).

1.4.1.2. Use in clinical treatment of TB:

PZA when was introduced for the 1st time into clinical treatment of TB in 1952, it was found to improve cough and the initial febrile reactions (*Cordice et al., 1953*). Clinical studies-evaluating the action of anti-TB drugs in short course chemotherapy- revealed the high sterilizing activity of RIF and PZA and their synergism in reducing the proportion of positive 2-month cultures and the rates of relapses after treatment (*Mitchison, 1985*). Further studies showed that the sterilizing effect of PZA decreased after the 1st 2 months of therapy (*East and Central African/British Medical Research Council, 1986*) (*Hong Kong Chest Service/British Medical Research Council, 1991*), this could be due to the inflammation that leads to an acid environment in the lesions is usually decreased after 2 months (*Zhang & Mitchison, 2003*). PZA helped to shorten the therapy from 12 to 6 months when was combined with RIF (*Singh et al., 2006*).

Current recommended treatment regimens depend on the combination of INH, with RIF and PZA. After the initial high bactericidal activity of INH, RIF and PZA act as the main sterilizing drugs which eliminate residual, persisting bacilli. Continuation with PZA after the first 2 months is usually not recommended, in spite of its minor role in preventing late failures (*Zhang & Mitchison, 2003*).

The combination of PZA with aminoglycosides as streptomycin can be useful in retreatment. Aminoglycosides are more active in an alkaline or neutral pH than at acid pH. Such combination would be active against all bacilli regardless the pH of the micro-environment. Treatment regimen with a combination of PZA, streptomycin and para amino salicylic acid was found to be successful in 94% of patients (*The East African and British Medical Research Counsels, 1971*).

Using PZA in the short-course studies was not highly hepatotoxic in comparison to the earlier studies in which large doses were used and hepatitis was frequent(*Girling, 1978*). The most frequent side effect of PZA is arthritic symptoms due to accumulation of uric acid. Intermittent administration (e.g., three times per week) could solve this problem (*Ellard & Haslam, 1976*).

1.4.1.3 Mechanism of pyrazinamide resistance:

The lack of nicotinamidase/Pyrazinamidase activity due to mutation in the encoding gene *pncA* seems to be the cause of resistance in the majority of PZA-resistant strains. These strains are cross resistant to nicotinamide but not to other antituberculous drugs (*Zhang & Mitchison, 2003*). The transformation of *pncA* gene into the inherently PZA-resistant *M. bovis* BCG and PZA-resistant *M.tuberculosis H37Rv* retain PZA-susceptibility to theses strains (*Scorpio & Zhang, 1996*). The mutations of *pncA* gene are characterized by a very high diversity, not like mutations in other drug resistance genes, which has no clear explanation. This could be explained that pyrazinamidase (PZase) is a non-essential enzyme and all types of mutations in the *pncA* gene are tolerated without affecting the full virulence of the strain. On the other hand no mutations in *pncA* gene or its promoter region were found in a small group of PZA-resistant strains which was PZase-negative, suggesting mutations in an unknown *pncA* regulatory gene. Another rare PZA-resistant group was found to be PZase-positive with no *pncA* mutations, indicating a possible alternative mechanism of PZA resistance (*Cheng et al., 2000*). *M. smegmatis* and *M. avium* are naturally resistant to PZA due to POA active efflux mechanism not due to the lack of PZase activity (*Sun & Zhang, 1999*).

As the PZA-resistant *M. tb* is still susceptible to POA, a lot of efforts were directed to develop POA precursors that could circumvent the mutations in *pncA* gene and activated by other enzymes like estrase. Increasing lipophilicity of POA by converting POA into esters was found to increase the anti-tuberculosis activity *in vitro* (*Cynamon et al., 1992*) (*Yamamoto et al., 1995*). The main disadvantage of these compounds is their instability in Serum. (*Simões et al., 2009*) showed that longer side chain of POA esters can improve serum stability.

1.4.2 Rifampicin:

Prokaryotic DNA-dependent RNA polymerase (RNAP) is a multi-subunit enzyme responsible for transcription in bacteria. It is an attractive target for development of antibacterial agents as it is crucial for bacterial growth and survival, and shows features that make it different from mammalian RNAP. At present, the rifamycins are the only group of RNAP inhibitors (RNAPIs) that have been approved for clinical use (*Chopra, 2007*).

RIF is the most important rifamycin in the treatment of tuberculosis. Other rifamycins of importance are, rifapentine, rifabutin, rifalazil, and rifamycin T9 (*Aristoff et al., 2010*). Some of them have higher anti-tuberculous activity than RIF (*Sánchez et al., 2011*). The action of rifamycins is not limited against *M. tb* but also against gram positive bacteria and they are used in the treatment of leprosy (*Bujnowski et al., 2003*). RIF is a first line anti-TB medication and it is a key component of the initial anti-TB regimen. It is most efficient in inhibiting actively replicating bacteria. It is not useful only in treating active TB, but also in inhibiting latent bacteria; however it is not recommended to be used alone due to high rate of resistance (*Campbell et al., 2001*) (*Chao & Rubin, 2010*).

1.4.2.1 Mechanism of rifampicin action and resistance:

The mycobacterial RNAP consists of five subunits. The core enzyme is formed of α, α2, β, and β' subunits. The ω subunit only binds when the polymerisation is initiated and falls off when the elongation starts. RIF binds to β subunit however, the core can be still assembled to the DNA and the first phosphdiester bonds can be formed RIF blocks further formation of transcripts after three or four base pairs and RNA elongation is inhibited (*Artsimovitch &Vassylyev, 2006*). More than 96% of RIF-resistant clinical isolates of *M. tb* were found to have mutations in the 81-bp core region of *rpoB* gene encoding the β subunit. (*Musser, 1995*) (*Valim et al., 2000*). These mutations can circumvent RIF binding through steric hinder or reduced affinity; also the inhibitory signal of the drug can be distorted through allosteric modulation (*Artsimovitch &Vassylyev, 2006*).

Not all mutations within the 81 bp region display the same level of resistance, mutations in codon 526 or codon 531which represent 65-85% of mutations result in high-level resistance to RIF with MIC >32μg/ml. However, alterations in codons 511, 516, 518, and 522 result in strains that have low-level resistance to RIF and rifapentin but remain susceptible to

two other rifamycins, rifabutin and rifalazyn (*Moghazeh et al., 1996*) (*Ohno, et al., 1996*). Rare mutations associated with RIF-resistance have also been found in the amino-terminal region of *rpoB* (*Heep et al., 2000*)

Approximately 90% of RIF-resistant isolates are also resistant to isoniazid, so RIF-resistance could be considered a useful surrogate marker for multidrug resistance and indicating the urgent need to the second line drugs (*Yuen et al., 1999*) (*Watterson et al., 1998*).

1.4.2.2 Progress in the development of new RNAP inhibitors:

One of the main requirements in any developing RNAPI is to have potential novel target sites which are distinct from the RIF-binding site (*Chopra et al., 2002*). Any novel drug candidate designed to replace RIF, it is essential to show activity against RIF-resistant mutants (*Weissman & Müller, 2010*).

Many natural products RNAPI have been discovered. These inhibitors include the ripostatins (*Irschik et al. 1995*), corallopyronins (*Irschik et al., 1985*), myxopyronins (*Kohl et al., 1983*), zwittermicins (*Stabb & Handelsman, 1998*), and the pyrrothines, thiolutin (*Khachatourians &Tipper, 1974*) and holomycin (*Oliva et al., 2001*).

(*O'Neill et al., 2000*) concluded that thiolutin, holomycin, corallopyronin A, and ripostatin A likely interact with sites of RNAP distinct from rifampicin. They did not observe cross-resistance with genetically defined rifampicin resistance alleles in Staphylococcus aureus and these compounds. The absence of pharmacophoric similarity between these compounds and RIF supports also this hypothesis. On the other hand *rpoB* mutants were cross resistant to sorangicin A. Also the results of (*Römmele et al., 1990*) and (*Xu et al., 2005*) showed the cross resistance between rifampicin and sorangicin suggesting that sorangicin A binding site is closely related to that of RIF inspite of the difference in their chemical structure.

Using a combination of genetic, biochemical and structural approaches, (*Mukhopadhyay et al. 2008*) showed that myxopyronin interacts with the RNAP "switch region," the hinge that mediates opening and closing of the RNAP active center cleft. They showed that myxopyronin prevents RNAP to interact with promoter DNA. They proposed

that myxopyronin inhibits the initiation of transcription by "jamming the hinge" as it prevents opening of the RNAP active-center cleft to permit entry of DNA. The authers provided experimental evidence that the structurally related α-pyrone antibiotic corallopyronin and the structurally unrelated macrocyclic-lactone antibiotic ripostatin inhibit RNAP through the same target and same mechanism. This explained the absence of cross resistance between these substances and rifamycins, as the residues involved in the interaction are not related to the rifamycins-binding site.

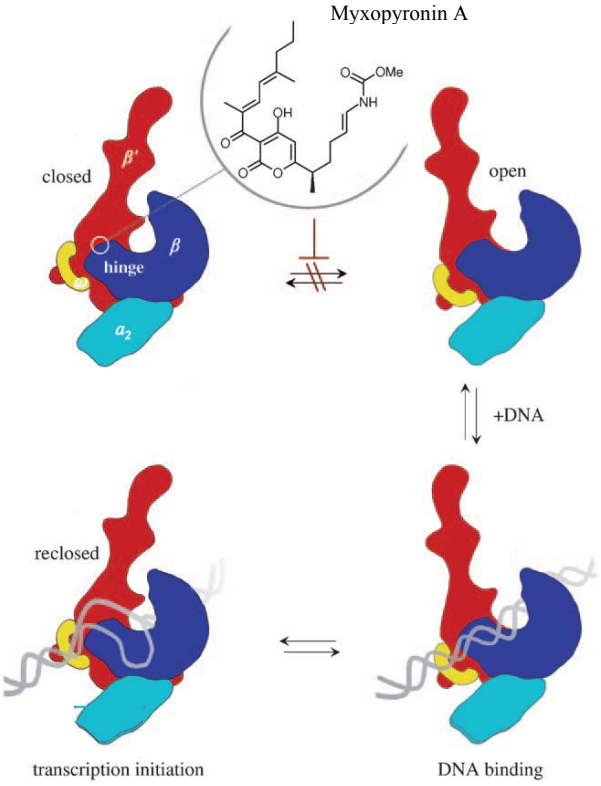

Fig. (8): Structure and function of bacterial RNAP. The crab-claw-like RNAP can open and close by a 30° rotation of the larger ß' subunit (clamp) around the switch region (hinge). Myxopyronin A blocks transcription initiation by jamming the hinge (*Haebich &Von Nussbaum, 2009*).

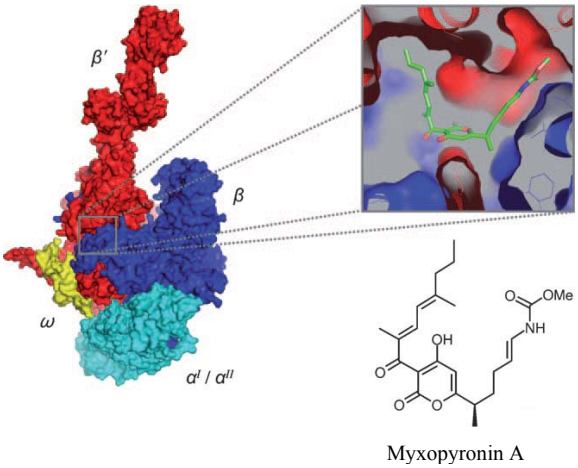

Fig. (9): X-ray crystal structure of myxopyronin A buried in the switch region of bacterial RNAP (*Haebich &Von Nussbaum, 2009*).

With regard the physiochemical and pharmacokinetic properties, myxopyronin and corallopyronin exhibit insufficient physiochemical properties, and they have high serum protein binding which reduces their active free part in blood. However the RNAP switch

region is a very attractive drug target, these substances need to be further developed to improve their physiochemical and pharmacokinetic properties to meet the requirements of the drug (*Haebich &Von Nussbaum, 2009*).

1.4.2.3 RNAP assay as a tool:

RNAP assay can be used as a screening tool to predict the inhibitory effect of different substances on RNAP. Historically, there are some assays that used to quantify the activity of RNAP. The utilizing radioisotopically tagged ribonucleotides, as prescribed by (*Daniel et al., 1975*) (*McClure, 1980*) (*Wu et al., 1997*), has the disadvantages of high reagent cost, high disposal cost of isotopically tagged materials, short shelf life of isotopes and strict monitoring of the laboratory area where isotopes are used. On the other hand, using chemically modified nucleotides like fluorescent derivative of nucleotide (*Bertrand-Burggraf et al., 1984*) (*Kozlov et al., 2005*) (*Bhat et al., 2006*) or other derivative of nucleotide (*Vassiliou et al., 2000*) may not be as good substrate as the natural nucleotides. (*Kuhlman et al., 2004*) used the florescent RiboGreen dye to detect RNA as an end product of transcription. RiboGreen is enhanced by both DNA and RNA, so Dnase digestion and ultrafiltration steps should be added to remove the DNA template. For these reasons, (*Bhuju, 2009*) developed a non radioactive assay in which the normal nucleotides were utilized. The assay based on measuring the pyrophosphate (PPi) that released as an end product of transcription. It depends on converting PPi using ATP sulfurylase into ATP that could be measured by luciferin-Luciferase system.

2. Motivation and objectives:

Tuberculosis (TB) drug resistance is increasing worldwide with the recent emergence of totally drug resistant TB which does not respond to any of the commercial drugs. This is emphasizing on the inevitable need to accelerate the anti-TB drug discovery and development pathway.

Pyrazinamide (PZA) and rifampicin (RIF) are two important frontline anti-TB drugs. RIF is the most potent sterilizing agent against log phase or semi-dormant bacteria, it works through the inhibition of the microbial RNA polymerase (RNAP). PZA is one of the most important drugs for anti-TB short course chemotherapy. It could be considered the only drug which is bactericidal to dormant *mycobacterium tuberculosis* (*M. tb*), its activity increases in acidic environment and under the anaerobic conditions, the conditions similar to the environment inside macrophages and in necrotic caseous lesions. PZA and RIF when combined together they helped to shorten the duration of therapy from 12 to 6 months. The widespread of the resistance to these front line drugs underscores the necessity of developing alternative agents. These facts highlight the importance of finding PZA analogues that can evade the mutations in *pncA* gene and RNAP inhibitors that can substitute RIF. This work is an approach to characterize possible anti-tuberculous agents aimed at generating the essential pharmacological database with regard their efficacy, toxicity and PK/PD profile *in vitro* and *in vivo*. The objectives of the thesis could be summarized in the following points:

- Evaluation of the *in vitro* activity of different compounds using two cell-free target-based screens namely the RNAP and pyrazinamidase (PZase) assays. And to use the PZase assay to characterize the role of *pncA* gene in PZA resistance.
- Evaluation of the *in vitro* inhibitory profile of PZA analogues, different RNAP inhibitors and a library of compounds against *M. tb* using whole cell screens.
- Measurement of the *in vitro* cellular toxicity of different compounds.
- Measurement of the acute toxicity of selected compounds in mice.
- Evaluation the *in vivo* pharmacokinetic profile of selected substances, calculating their pharmacokinetic/pharmacodynamic PK/PD parameters and combining these results with the *in vitro* PK testing.

3. Materials and methods:

Experimental design:

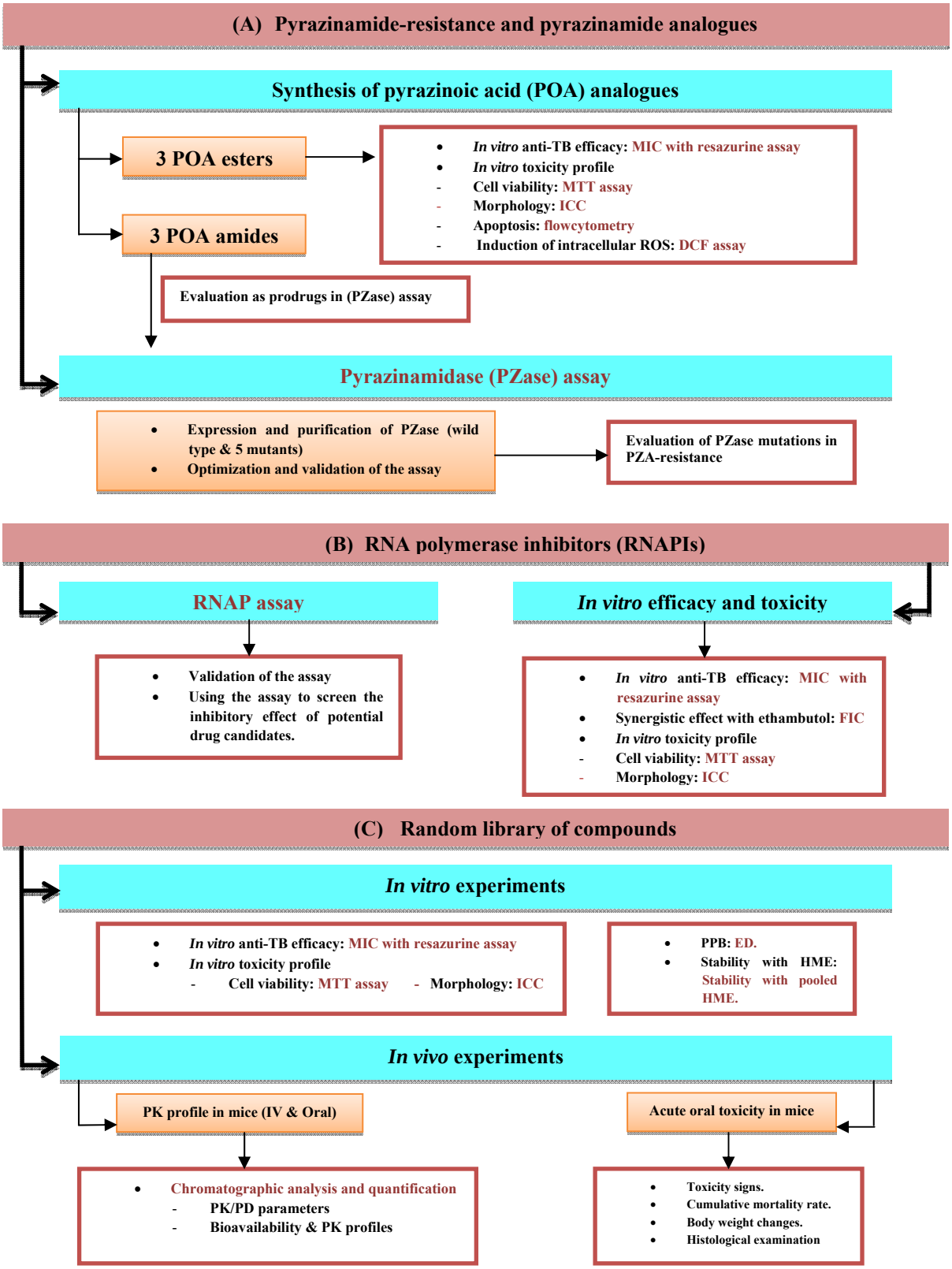

Fig. (10): Flowchart outlining overall design of experiments undertaken in the thesis: Words in red color represent the methods used.

In order to fulfil the objectives of the thesis, the work was divided into three parts as presented in the experimental design (Fig.10). The part that was concerned with the pyrazinamide (PZA) resistance and PZA analogues was successfully completed in the Helmholtz Centre for Infection Research (HZI), Braunschweig, Germany.

With regard the work with the RNA polymerase (RNAP) inhibitors, the test substances were kindly provided by Lionex GmbH, Braunschweig, Germany. The RNAP assay was done in HZI. While testing their *in vitro* efficacy and toxicity was started in HZI and continued in Lionex.

3.1 Synthesis of pyrzinoic acid analogues:

Three pyrazinoic acid (POA) amides, hexadecylpyrazinamide, tetradecylpyrazinamide, dodecylpyrazinamide, were synthesized following the protocol described in (*Ley& Priour, 2002*). And three POA esters, hexadecylpyrazinoate, tetradecylpyrazinoate, dodecylpyrazinoate, were synthesized according to the literature (*Nishimura et al., 2009*). The scheme of synthesis and the structure of the compounds are shown in figures (11) and (12).

3.1.1 Materials and reactions:

Chemical reagents for the synthesis of compounds were purchased from Sigma (Germany) and used without further purification. Reactions were carried out under argon (99.996%) to maintain dry conditions.

3.1.1.1 Pyrazinoic acid amides:

A solution of (1.2 mmol) the desired amine, (1-hexadecylamine: 290 mg), (1-tetradecylamine: 270 mg) or (1-dodecylamine: 223 mg.), was prepared in (5 ml) dichloromethane. Then (425 µl, 1.27 mmol) methanolic 3N HCl was added. 1 ml toluene was added and then the excess toluene and dichloromethane were evaporated twice to obtain the hydrochloric salt of the amine. Pyrazinoic acid (100 mg, 0.8 mmol), 1-(3-dimethylaminopropyl)-3-ethylcarbodiimide hydrochloride (EDC), (235 mg, 1.2 mmol), N,N-diisopropylethylamine (DIPEA), (200µl, 1.2 mmol) and 1-hydroxybenzotriazole (HOBt), (162 mg, 1.2 mmol) were added to the reaction at 0°C. The reaction mixture was stirred for 3 h at room temperature, then diluted with dichloromethane, washed with brine, dried over

sodium sulfate, filtered and concentrated. Dichloromethane was evaporated completely and the reaction products were dissolved in diethyl ether and filtered.

3.1.1.2 Pyrazinoic acid esters:

A mixture of pyrazinoic acid (200 mg, 1.6 mmol), and triphenylphosphine (PPh_3) (420 mg, 1.6 mmol) and 0.8 mmol of the desired alcohol, (1-hexadecanol: 190mg), (1-tetradecanol: 172mg) or (1-dodecanol: 224 µl) was dissolved in 5ml tetrahydrofuran (THF). A solution of diethyl azodicarboxylate (DEAD), (325µl, 1.6 mmol) in 2.5 ml (THF) was added to the reaction over 15 minutes at 0°C, then the whole reaction was stirred for 2 hours at room temperature. The reaction mixture was diluted with ethyl acetate, and was washed with brine, dried over sodium sulfate, filtered, and concentrated.

3.1.2 Chromatography

3.1.2.1 Thin layer chromatography (TLC):

Silica gel 60 F_{254} sheets, 0.2 mm (Merck, Germany) were used for TLC analysis. The solvent system used for TLC was a mixture of hexane:ethyl acetate (4:1). TLC was visualized by UV irradiation or stained with Potassium permanganate.

3.1.2.2 Column Chromatography (CC):

Silica gel 60 (0.063-0.200 mm) (Merck, Germany) was used for column chromatography. The solvent system applied for the Silica gel column was a mixture of hexane: ethyl acetate (5:1) as eluent.

Each compound was dried under high vacuum and the yield was determined. ^{1}HNMR spectra were recorded at 400MHz, and ^{13}CNMR spectra at 100 MHz on a Bruker AM 300 spectrometer. Chemical shifts are reported in δ (ppm), expressed relative to the solvent signal at 7.25 ppm ($CDCl_3$, ^{1}HNMR) and at 75.5 ppm ($CDCl_3$, ^{13}CNMR). Coupling constants (J) are given in Hz. HPLC-HRMS data were recorded on a Maxis UHR spectrometer (Bruker Daltonics); ionization: ESI, positive mode; scan range: m/z 50-1600; rate 1 Hz; external calibration using sodium formate clusters; column 50 x 2.1 mm, Acquity UPLC BEH C-18, 1.7 µm (Bruker); temperature 40 ^{o}C; eluent A: H_2O/CH_3CN 95:5, 0.1% HCOOH, eluent B: CH_3CN/H_2O 95:5, 0.1% HCOOH, gradient: 5% B for 0.5 min, then to 100% B in 19.5 min; flow: 0.6 mL/min.

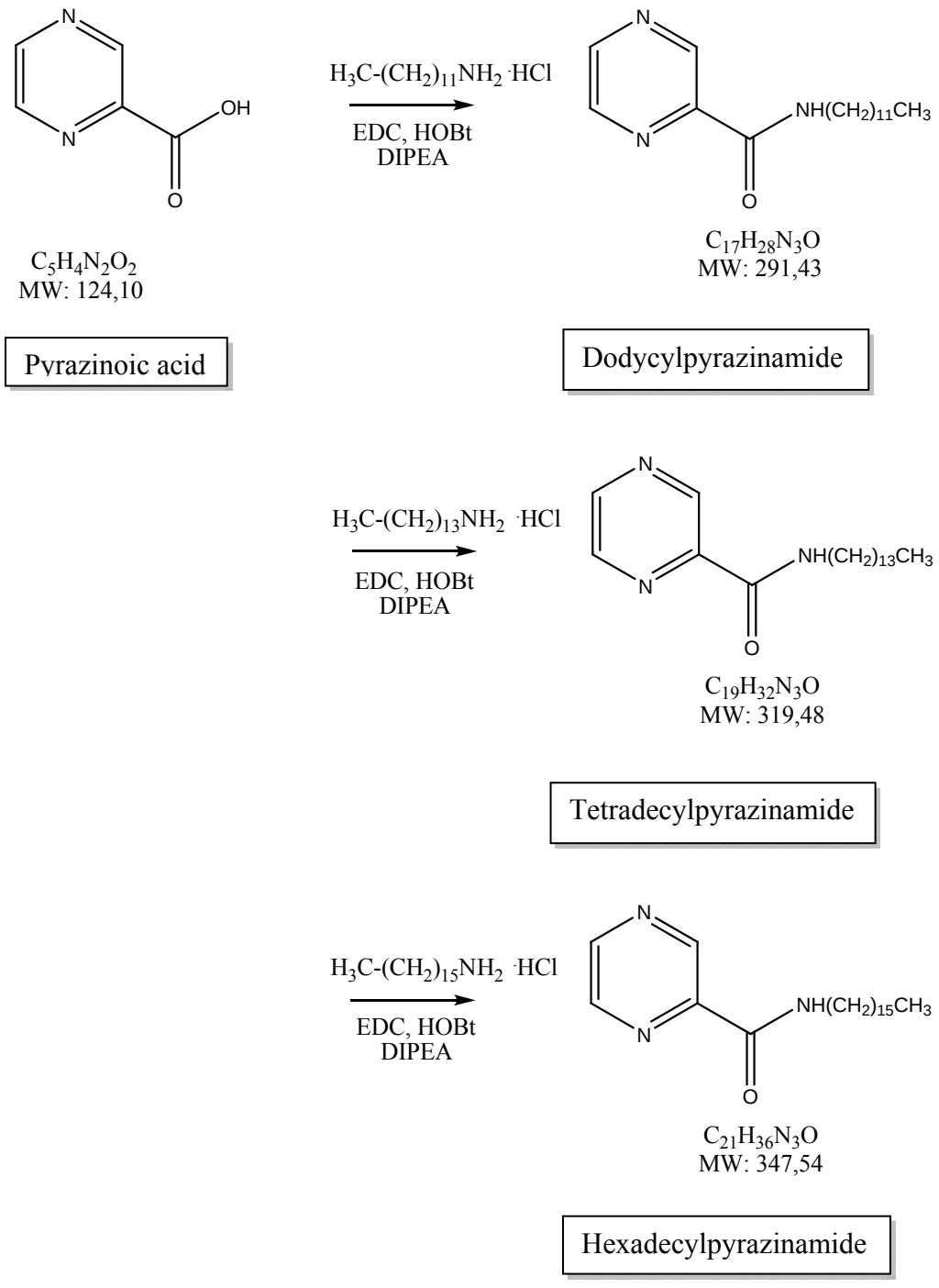

Fig (11): Scheme of synthesis of amides of pyrazionic acid: DIPEA: N,N-diisopropylethylamine; **HOBt:** 1-hydroxybenzotriazole; **EDC:** 1-(3 dimethylaminopropyl)-3-ethylcarbodiimide hydrochloride.

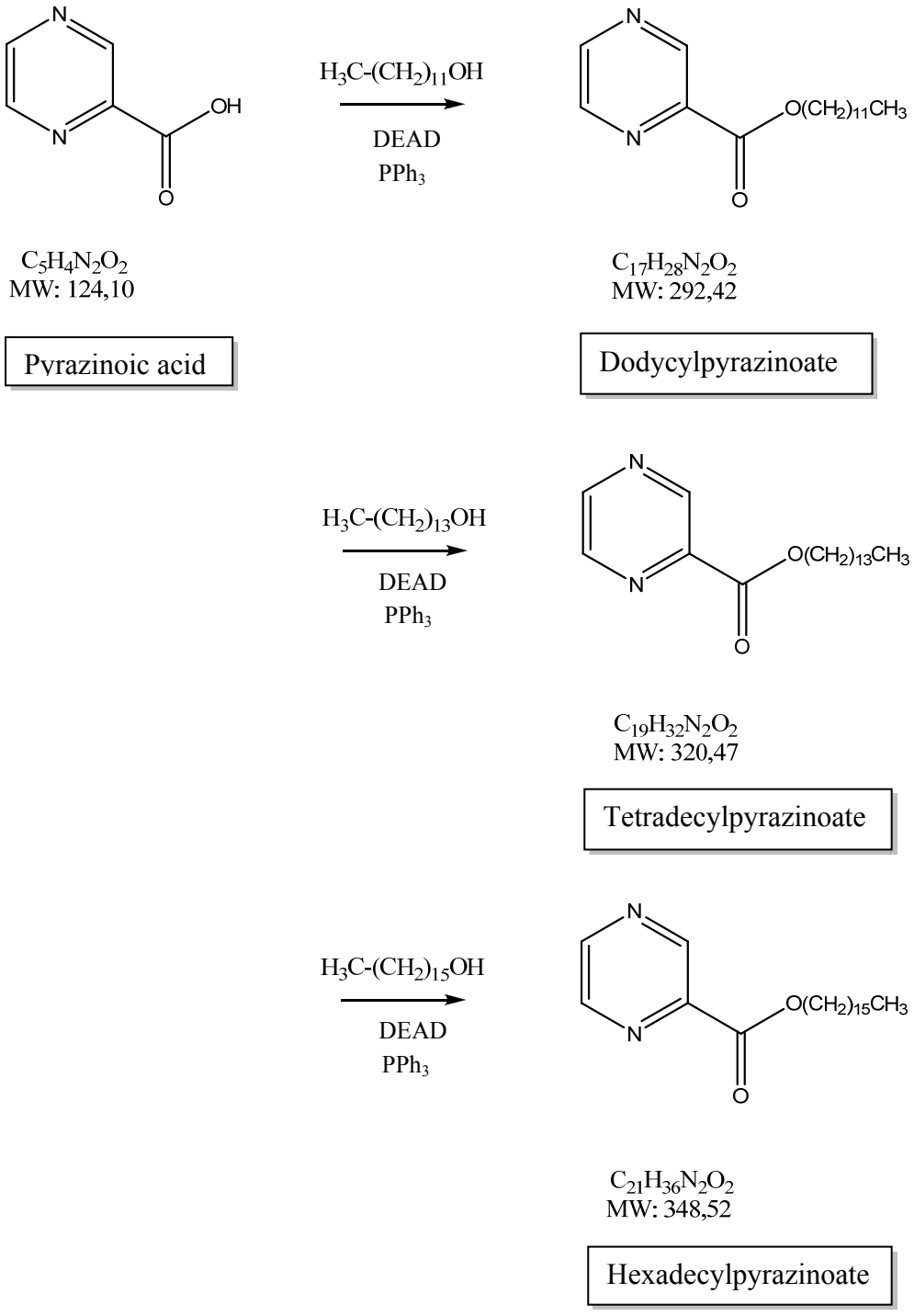

Fig (12): Scheme of synthesis of pyrazionic acid esters: DEAD: diethyl azodicarboxylate ; **PPh_3:** triphenylphosphine.

3.2 Expression and purification of pyrazinamidase wild type and its mutants:

Mycobacterial 6x His- tagged PZase (Wild type and five mutants from clinical PZA-resistant strains which were cloned in *E.coli* BL21 were expressed and purified. The glycerol stocks of different clones were kindly obtained from Dr. Sabin Bhuju who had constructed these clones during his Ph.D. work in the group of Prof. Dr. Mahavir Singh, Helmholtz centre for infection research, Braunschweig, Germany. It is known that, the small His-tag has a negligible effect on the protein structure and function. Protein expression and purification were done through different steps as follows:

3.2.1 Auto-induction:

It was done according to the proprietary protocol from Lionex GmbH, Braunschweig, Germany. 3 ml from overnight culture (160 rpm, 37°C) of *E.coli* BL21 in LB media supplemented with 50 µg/ml kanamycin was spread in Qtray (Genetix) containing 200 ml APS medium with the same antibiotic to form a lawn culture, and the plates were incubated at 18°C for 3-4 days. The composition of the LB and APS media are shown in the following tables.

Table (4): Composition of LB medium.

Tryptone (BD)	10.0 g
Yeast Extract (BD)	5.0 g
NaCl	10.0 g

Distilled water was added up to 1 L and pH was adjusted to 7.4

Table (5): Composition of APS medium.

Difco Select APS Super Broth	49.1 g
Glyerol (87%)	5 ml
Distilled water was added up to 1 L and pH was checked between 6.8-7.5	
Agar	15 g

3.2.2 Preparation of cell lysate:

The following steps were performed in cold conditions or instead in ice. Cells from APS plates were collected using cell scrapper, suspended in saline and then centrifuged for 1 hour at 4000 rpm. Cell pellet was resuspended in an appropriate volume (5 ml for each gram cell mass) of 20 mM Tris-HCl buffer, pH 8.0. Cell lysis was carried out by the mechanical ultrasonicator (Braun Biotech international GmbH). Maximally 20 ml was sonicated at a time for 3 x 2.5 min. with 30 sec. interval. Finally, cell lysate was separated from cell debris by centrifugation at 18,000 rpm for 15 min.

3.2.3 Fast protein liquid chromatography (FPLC) :

For all chromatographic processes, ÄKTA purifier system (GE-Healthcare) or Pharmacia LKB system (Pharmacia), were used. All buffers were filtered through 0.2 μm membrane filter (Sartorius) and degassed under a negative pressure before use. In the case of affinity chromatography (Ni-NTA) and ion exchange, the used column was washed with 2 times column volume from the eluting buffer to remove any old bound proteins. Before loading the sample, the used column was first equilibrated with at least 2 times column volume of 20 mM Tris-HCl buffer or 50 mM Tris-HCl buffer in the case of ion exchange.

- ***Immobilized metal affinity chromatography (IMAC):*** The purification was performed using Ni-NTA Superflow resin (Qiagen). This technique works by allowing the histidine tagged protein to be retained by the immobilized nickel in the column. Elution of the retained proteins was done with linear gradient of a buffer containing 500 mM Imidazole as a competitive molecule.
- ***Ion exchange chromatography (Mono Q):*** In which proteins are separated according to their net charge for a high resolution separation. Proteins were eluted by increasing the ionic strength of the mobile phase with a linear gradient of 50 mM Tris-HCl, 500 mM NaCl pH 7.8.
- ***Desalting and buffer exchange:*** desalting was done in Hi Trap Desalting 5x5 ml column (Amersham Bioscience) Packed with Sephadex™ G-25, a gel filtration product that separates molecules on the basis of size. In a single step, the sample is desalted, exchanged into a new buffer and low molecular weight materials such as unwanted salts are removed. 20 mM Tris HCl buffer was used for the buffer exchange.

- ***Gel filtration on a Superdex 200:*** Gel filtration with Superdex (Amersham Biosciences) provides the buffer exchange and separation of protein according to the size.

3.2.4 SDS polyacrylamide gel electrophoresis (SDS-PAGE):

To check the purity of the separated proteins, SDS-PAGE gel was carried out according to (*Laemmli, 1970*) by separating the denatured proteins according to the size in an electrical field. Equal volume of 2X loading buffer (with 1/10 volume DTT) was added to the protein sample and incubated at 95°C for 10 min for protein denaturation. PageRuler™ Protein Ladder (Fermentas) was run simultaneously to define the molecular mass of the separated proteins. At the beginning of electrophoresis, a potential difference of 60 V was applied till the proteins accumulate in the stacking gel. Afterwards the potential difference was increased to 120 V.

The gel was then stained in coomassie blue solution containing 0.1% coomassie blue, 10% acetic, 40% ethanol and 50% de-ionized water. The gel in the stain was heated in microwave for 1-2 minutes until it just started to boil then was shacked at room temperature for 15 min. to fix the stain. To remove the excess background, the gel was destained in 10% ethanol.

3.2.5 Protein concentration measurement:

Bradford method (*Bradford, 1976*) was used to measure the protein concentration using the Coomassie Plus™ Protein Assay Reagent (Pierce) and bovine serum albumin (BSA) with known concentrations as a standard. 5 µl of protein samples and from each standard were mixed with 200 µl Protein Assay Reagent then incubated at room temperature for 5 minutes in 96 well microplate (Greiner). The absorbance was measured at OD_{595} with MRXTC Revelation (Dynex) using Revelation v4.25 (Dynex). Revelation v4.25 (Dynex) was used to generate calibration curve with BSA standards and to calculate the protein concentration of the samples.

3.2.6 Protein concentration:

Vivaspin 6 (Sartorius) was used for the concentration of small amounts of proteins. For larger volume of protein, 3K PALL concentrator with stirrer was alternatively used. Pressure up to 2.5 bar with nitrogen was applied with stirring at 4°C till suitable volume was achieved.

3.3 Cell free PZase assay:

3.3.1 Principle of the assay:

As shown in (Fig. 13), the assay depends on the ability of the POA to interact with ammonium ferrous sulphate $(NH_4)_2Fe(SO_4)_2$ and to produce red-orange complex (*Allen et al., 1953*). The optical density of the resulting compound is correlating to the amount of the liberated POA.

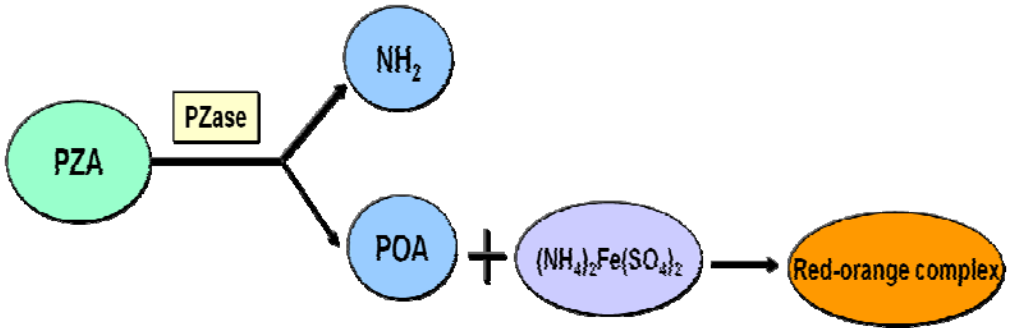

Fig. (13): Schematic Diagram showing the principle of PZase assay (*Bhuju, 2009*).

3.3.2 Procedure:

The cell free PZase assay was optimized as follows to screen the PZA and the synthesized amides with the wild type of *PncA* and its mutants. The Enzymatic assay of *PncA* was done in volume of 200µl of 100 mM Glycine buffer pH 6.2 with 0-8 mM PZA, 0.875 µMol (4.4 µM) *M. tuberculosis PncA*, the amount of the enzymes was increased 5 times for mutants with almost no activity. The reaction was carried out in thermocycler at 37°C for 5 minutes then the enzyme was denaturated at 100°C for 5 miutes. Then 25 µl of ammonium ferrous sulphate 100 mM was added. After 10 minutes of incubation at room temperature 200 µl were transferred to 96 well plate (Greiner). The absorbance was measured at OD_{450} with MRXTC Revelation (Dynex).

3.3.3 Quantification and kinetic calculation:

A standard curve was done using different concentrations of POA correlating the absorbance of the red-orange complex with the concentration of the POA. The rates of the reactions were calculated (µM/min) and plotted versus substrate concentrations and kinetic constants were obtained by fitting the experimental data to the appropriate rate equations by

nonlinear regression ($Y = (V_{max} * X)/ (K_m + X)$, where X is substrate concentration; Y, the enzyme velocity; (V_{max}), the maximum enzyme velocity; (K_m), the Michaelis-Menten constant. The turnover number K_{cat} was calculated by dividing V_{max} over E_t where E_t is the concentration of the enzyme. The kinetic data were calculated and plotted using GraphPad Prism 5.0.

3.4 RNAP assay:

3.4.1 Principle of the assay:

The assay was done as described by (*Bhuju, 2009*) with few modifications. The assay depends on measuring the activity of RNA polymerase (RNAP) through quantification of the amount of released pyrophosphate (PPi) as an end product of transcription. PPi is transformed by ATP sylfurylase into ATP that could be measured using the Luciferin-Luciferase system. To lower the background of the reaction, apyrase is used to degrade the remaining nucleotides after the RNAP reaction before converting PPi into ATP (Fig. 14).

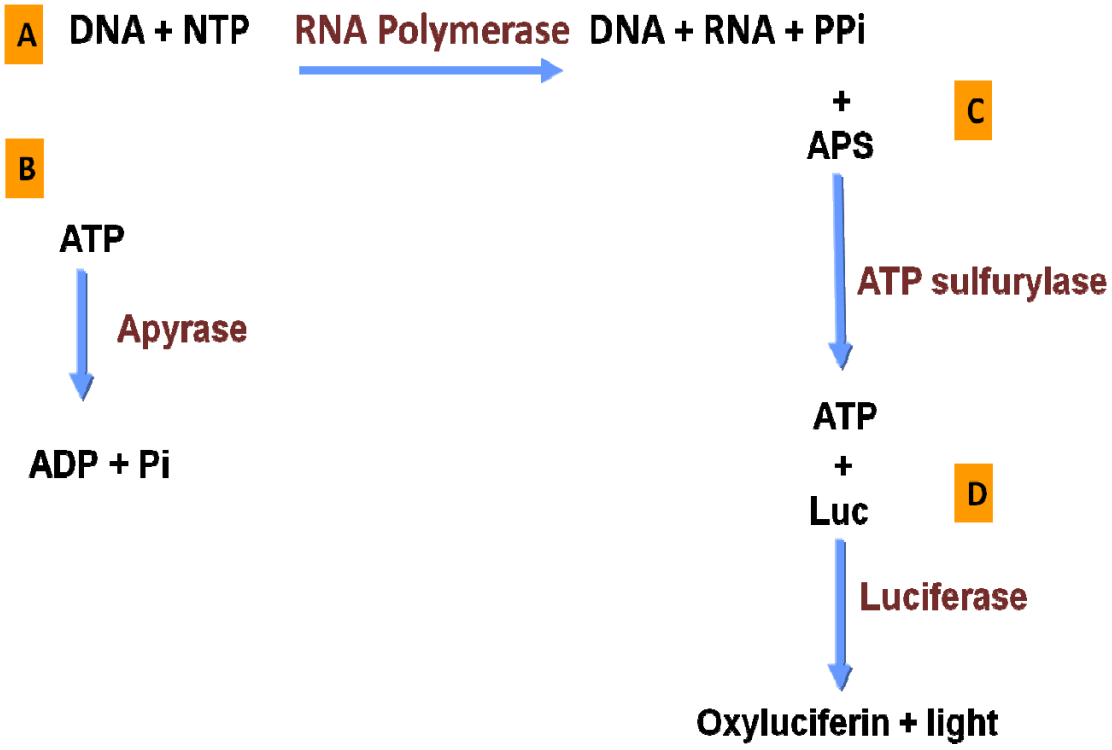

Fig. (14): Schematic presentation of the RNAP assay. A, B, C and D represent the sequential steps of the assay**.** NTP: Nucleotides (ATP, UTP, GTP& CTP), PPi: Pyrophosphate, APS: adenosine 5´ phosphosulfate, Luc: Luciferin. **(***Bhuju, 2009***).**

3.4.2 Chemicals used for the assay:

Table (6): Chemicals used for RNAP assay:

Substance	Company
Adenosine 5′-phosphosulfate sodium salt	(Sigma Aldrich)
Apyrase	(NEB)
ATP Determination Kit	(Biaffin GmbH)
ATP Sulfurylase	(NEB)
CTP, 100mM Solution	(Fermentas)
GTP, 100mM Solution	(Fermentas)
UTP, 100mM Solution	(Fermentas)
ATP, 100mM Solution	(Fermentas)
Manganese Chloride tetrahydrate	(Sigma Aldrich)
E. coli RNAP core enzyme	(Biozym)
Sodium Pyrophosphate Decahydrate	(Sigma Aldrich)
Rifampicin	(Sigma Aldrich)
Test compounds	(Lionex)

3.4.3 DNA preparation for the assay:

pUC18 was purified using Maxi prep according to manufacturer's instruction. A colony of *E. coli* Top 10F′ with pUC18 was cultivated in 100 ml LB medium supplemented with 100 µg/ml ampicillin. After centrifugation at 6000 x g for 15 min at 4°C,the pellet was homogenously resuspended in 10 ml Buffer P1 (Resuspension buffer). Then10 ml Buffer P2 (Lysis buffer) was added and mixed by vigorously inverting 4-6 times. The mixture was left to be incubated at room temperature for 5 min to lyse the cells. QIAfilter cartridge was prepared by screwing the cap onto the outlet nozzle of the QIAfilter Maxi cartridge. After the incubation period, 19 ml of chilled Buffer P3 (Neutralization buffer) was added and mixed by vigorously inverting 4-6 times in order to neutralize the effect of lysis. And to clear the bacterial lysate, it was poured into the barrel of the QIAfilter cartridge and left at room temperature for 10 min. The cap from the QIAfilter cartridge outlet nozzle was removed and carefully inserted into the QIAfilter Maxi cartridge and the cell lysate was filtered. Buffer ER (2.5 ml) was added to the filtrate. Mixing was carried out by inverting the tube for 10 times and the mixture was incubated on ice for 30 min. equilibration of Qiagen-tip 500 was done by

adding 10 ml of Buffer QBT and leaving the column to empty by gravity flow. The filtered lysate was applied to the QIAGEN-tip to allow the plasmid to bind to the resin. Unnecessary contaminants were removed by washing the QIAGEN-tip with 30 ml of Buffer QC (Wash buffer). Elution of bound DNA was done with 15 ml of Buffer QF (Elution buffer). The eluted DNA was precipitated by adding 10.5 ml of isopropanol. After centrifugation at 15,000 x g for 30 min at 4°C, the supernatant was decanted. The DNA pellet was washed with 5 ml of 70%ethanol and the supernatant was decanted after centrifugation at 15,000 x g for 10 min. The pellet was air-dried and the DNA was redissolved in 500 µl distilled water.

The size of the plasmid was determined by analysis on 1% or agarose gel. Agarose was dissolved in 1x TAE buffer. DNA was loaded with 6-fold loading buffer (Fermentas) onto the gel using 1 x TAE as running buffer. The electrophoresis was performed at 80 - 100 Volts for 30-45 minutes. The agarose gel was stained in a GelStar Nucleic Acid Stain (Lonza Verviers) in 1x TAE for 10 min. DNA was visualized using Dark Reader transilluminator (Clare Research) and Photography of the agarose gel was done under UV light with Fluor-S MultiImager (Bio-Rad). The DNA concentration was measured using Qubit quantification fluorometer and Quant-iT reagents (Invitrogen) and finally, the concentration was adjusted to 250µg/ml.

Table (7): Composition of 50X TAE buffer.

Tris-Base	242 g
Glacial acetic acid	57.1 ml
0.5 M EDTA (pH 8.0)	100 ml
Water up to	1000 ml

3.4.4 Procedure of the assay:

1) ATP alone was measured with the Luciferin-Luciferase system as the first standard method (using ATP 1nm, 10nm, 100nm, 1µM, 10µM solutions).
2) The ability of ATP Sulfurylase to utilize PPi and convert it into ATP was confirmed by using PPi as a substrate: The positive reaction contained 10 µM of PPi, 5 µM adenosine-5´ phosphosulfate, 30 mU ATP Sulfurylase. The positive reaction was repeated with the presence of RIF 10 µg/ml and in the negative reaction, PPi was

excluded. The reaction was run in a thermocycler for 10 min at 30°C. Then denaturation of the enzyme was performed at 85°C for 10 min. lastly net ATP produced during the whole reaction was measured using ATP kit.

3) The whole assay was performed as follows (all incubation and denaturating steps were carried in a thermocycler :

- The RNAP reaction mixture contained 2U of *E. coli* RNAP core enzyme, 500 ng pUC18 plasmid DNA in 10 mM MgCl2, 1.5 mM MnCl2, 0.1 mM EDTA, 50 mM NaCl, 20 mM Hepes, pH 8.0 and 25 µM of each NTPs (ATP, UTP, GTP and CTP). The DNA was excluded in the negative reaction and the positive control is repeated with the presence of RIF 10 µg/ml. The mixture then incubated for 30 minutes at 37°C for RNAP to synthesize RNA. This results in at least 90% maximal RNA synthesis (*Kuhlman et al. 2004*).
- 50 mU of apyrase was added to degrade the residual NTPs present in the reaction mixture. The reaction was carried out for 15 min at 30°C. Then denaturating of the enzyme was done for 10 min at 85°C.
- (APS) adenosine-5′-phosphosulfate (15 µM) and ATP Sulfurylase (30 mU) were added to transform PPi into ATP. This step was carried out for 15 min at 30°C.
- A final denaturating of the enzymes present in the whole reaction was performed at 85°C for 10 min.
- Finally, the amount of ATP produced during the whole reaction was evaluated with ATP kit (Biaffin GmbH). ATP catalyzes the conversion of luciferin into oxyluciferin with production of visible light.
- Luminance was measured with POLARstar OPTIMA (BMG Labtech) in half area white plates (Costar). The relative light unit detected from a reaction mixture corresponds to the amount of ATP present in the reaction mixture, which reflects the amount of PPi produced during the polymerization reaction of RNAP.

4) The whole assay was repeated with the presence of different concentrations of the test compounds.

3.5 Minimal inhibitory concentration (MIC):

The minimal inhibitory concentrations (MICs) of the substances were determined using resazurin microtiter assay (REMA) as described by Palomino (*Palomino et al., 2002*) in 96 well microplate. Mycobacterial strains were kindly provided by Lionex GmbH, Braunschweig, Germany. Resazurin is a blue dye, itself nonfluorescent until it is reduced to the pink colored and highly red fluorescent resorufin by living cells. Resazurin sodium salt powders (Sigma) were prepared at 0.01% (wt/vol) in distilled water and filter sterilized. It was stored at 4°C and used within 1 week. The assay was performed in 7H9 medium (BD) supplemented with 10% ADC enrichment medium (Fluka), 0.2% glycerol (Roth), 0.02% Tween-80 (Sigma).

Two-fold serial dilutions of the tested compounds were prepared in 96 well plates in 7H9 medium with volume 100µl. When the bacteria reached early exponential phase (OD_{550} =0.3), it was sonicated in ice bath for 30 sec and then diluted 1:20, and 100 µl was used as an inoculum. Growth controls containing no antibiotic and sterility controls without inoculation were also included. The plates were covered, sealed, and incubated at 37°C in the normal atmosphere. After 7 days, 30 µl of resazurin solution was added to each well and the plates were further incubated overnight at 37°C. The change of color was assessed; a change from blue to pink indicated reduction of resazurin and thus bacterial growth. The MIC is defined as the lowest substance concentration that prevents this color change. Dose-response curves were drawn by measuring the florescence in black plates with excitation at 560nm and emission at 590nm.

To determine the effect of protein binding on the *in vitro* MIC, the test was performed in medium that contains 50% fetal bovine serum (FBS).

3.6 Assessment of *in vitro* cellular toxicity profile:

Cell lines and media:

Cell lines were kindly provided by Dr. Florence Sasse, Helmholtz Center for Infection Research, Braunschweig, Germany. L-929 and J-774A.1 cells were also provided by Lionex GmbH, Braunschweig, Germany. Cells were grown at 37°C and 10% CO_2 in the following media:

- L-929 cells (mouse connective tissue fibroblast), J-774A.1 (mouse monocytes-macrophages), HEPA 1-6 cells (mouse hepatoma), KB-3-1 (human cervix

carcinoma): Dulbecco's modified Eagle's medium (DMEM), Lonza

- PtK2 cells (rat kangaroo kidney epithelial cells): Minimum Essential Medium (MEM) medium, supplemented with 1 % non-essential amino acids and 1 % glutamax, Invitrogen.
- U-937 (human histiocytic lymphoma): Roswell Park Memorial Institute medium (RPIM 1640), Invitrogen
- HUVEC cells (human umbilical vein endothelial cells): endothelial basal medium (EBM-2), (Lonza) supplemented with endothelial growth medium 2 (EGM-2) kit (FCS, hydrocortisone, hFGF-B, VEGF, R3-IGF-1, ascorbic acid, hEGF, GA-1000, heparin)

All media were supplemented with 10 % fetal calf serum except for HUVEC cells it was 5% (Lonza or Gibco).

Table (8): Apparatus & materials used for cell culture

Item	Details
Incubator	CO_2-Auto-Zero, Thermo Scientific
Microscope	Axiovert 35, Zeiss, Germany
Hemocytometer	Neubauer improved, Assistent Germany
Multi-plate reader	Wallac, 1420 Victor Multilabel Counter
Vortex	Heidolph, REAX 1 R, Germany
Digital multichannel Pipette	Matrix Technologies Corp, Thermo Scientific
FacScan	BD LSR II
Flourescent Microscope	Zeiss, Germany
96 well plates	Falcon, Becton Dickinson, USA
Scraper	Nalge nunc international, nunc, USA
Resevoir	Carl Roth, Germany
4-well plates	Nalge nunc international, nunc, USA
Round cover slips	Thermoscientific
Trypsin	Invitrogen
0.25 % trypsin/EDTA	Invitrogen
Earle's balanced salt solution	Gibco

3.6.1 *In vitro* toxicity testing:

The effects of the tested compounds on cell proliferation and the acute toxic effects were assayed *in vitro* on different mammalian cell lines. The metabolic activity was measured by means of (MTT) cell survival colorimetric assay. MTT (3-[4,5-dimethylthiazol-2-yl]-2,5-diphenyl tetrazolium bromide) is a yellow dye that was used to measure the metabolic activity of cells which are capable of reducing it by dehydrogenases to a violet formazan product.

Solutions:

- **Phosphate buffered saline (PBS):**

PBS solution (pH = 7.45) was prepared by dissolving one PBS tablet (Gibco) in 500 ml distilled water.

- **Acidified isopropanol:**

0.4 ml of concentrated HCl was added to 100 ml isopropanol.

- **(MTT) dye:**

1 g of MTT (98%, Sigma Aldrich) powder was dissolved in 200 ml of PBS and used directly without dilution. It was stored below 4°C, in the dark and was used within two weeks.

Steps:

A) Effect on proliferation:

60 µl of serial dilutions of the test compounds were added to 120 µl aliquots of a cell suspension (50,000 cells/ml) in 96-well microplates then incubated 5 days at 37°C and 10% CO_2. 20 µl MTT dye were added to a final concentration of 0.5 mg/ml. After 2 h the precipitate of formazan crystals was centrifuged, and the supernatant discarded. The precipitate was washed two times with 100 µl PBS and dissolved in 100 µl of the acidified propanol. The plates were stirred for 20 minutes on a microtitre plate shaker. The resulting colour was measured at 590 nm using a multi-plate reader.

B) Acute toxic effect:

When a substance showed an anti-proliferative effect, the acute toxic effect was evaluated as follows.120 µl aliquots of a cell suspension (100,000-200,000 cells/ml) in 96-well microplates were incubated at 37°C and 10% CO_2 and allowed to grow for two days to stop the cell propagation. Then 60 µl of serial dilutions of the test compounds were added

and incubated for further 24h. After 24h incubation at 37°C and 10% CO_2 the MTT assay was performed as described before.

All investigations were carried out in two parallel experiments. Results of cytotoxicity assays were expressed as the percentage of cellular viability. The IC_{50} values were determined as the concentrations of tested compounds, at which cell samples developed 50% of the absorbance of untreated control cells as estimated from the dose-response curves (Sigma Aldrich protocols) (Shaaban, 2010).

3.6.2 Immunocytochemistry (ICC):

The effects of substances on the phenotypical changes of cell shape and adhesion were investigated by the technique of immunocytochemistry (ICC). ICC is a technique used to assess the presence of a specific protein or antigen in cultured cells by using a specific primary antibody, which binds to this protein. And by using a florescent labeled secondary antibody, cells can be visualized under microscope. By this method we can visualize different structures in the cell as the endoplasmic reticulum (ER), microtubules and actin stress fibers. And by staining normal controls of untreated cells we can predict the morphological changes that could be produced by treatment with different substances (*Immunocytochemistry Methods, Techniques & Protocols*). Actin filaments, microtubules and the ER were investigated upon treatment of the potoroo cells (PtK2) cells with/without test compounds.

Reagents:

- Ice cold MeOH/acetone (1:1)
- Paraformaldehyde, Sigma aldrich: 3.7 % in PBS
- PBS
- Triton X-100, Sigma aldrich: 0.1 % in PBS
- Anti-fade solution with DAPI, (Invitrogen)
- Primary and secondary antibodies

Procedure:

PtK2 cells were grown on cover slips in 4-well plates. semi-confluent cells were treated with test compounds and the plates were incubated over the night. According to the type of the antibody that will be used, the cells were fixed either with cold methanol /acetone for 10 min or with 3.7% paraformaldehyde for 10 min followed with Triton X-100 (0.1%) for 5 min. Then the cells were washed with PBS and the primary antibody was added and incubated for

45 min and washed with PBS. Secondary antibody was then added to the cells and incubated for additional 45 min. After washing with PBS, Cover slips were mounted in anti-fade mounting medium with DAPI. Images were taken with a CCD camera attached to a flourescence microscope. The following antibodies were used:

- endoplasmic reticulum (*after MeOH/acetone fixation*)
  - Primary antibody: anti GRP-94, thermoscientific
  - Secondary antibody : Alexaflour goat anti-rat 488, Invitrogen

- tubulin (*after MeOH/acetone fixation*)
  - Primary antibody: α-tubulin, (Sigma)
  - Secondary antibody: Alexaflour 488 anti-mouse, (Invitrogen)

- *Actin; (after formalin-triton X-100 fixation)*
  - Phalloidin Ph594, (Molecular probe)

3.6.3 Induction of apoptosis (Double-labeling assay with annexin-V and PI):

Apoptosis were assessed by flow cytometric analysis of U937 cells treated for 12 h with test compounds using the FITC Annexin V Apoptosis Detection Kit II (BD Pharmingen). Annexin V has a high affinity for the membrane phospholipid phosphatidylserine (PS). In the early stages of apoptosis, PS is translocated from the inner to the outer leaflet of the cell membrane due to loss of membrane symmetry. Propidium Iodide (PI) is used to differentiate viable from nonviable cells as it cannot pass through the membrane of viable cells (BD Bioscience data sheets).

Assay procedure:

U937 cells (10^6/experiment) were treated with different concentrations of test compounds. After 12 hours incubation, they were suspended in 1 ml binding buffer. 100 µl of the cell suspension were stained with a mixture of 5 µl FITC Annexin V and 5 µl PI. After 15 min of incubation in dark, 400µl of binding buffer was added and the samples were analyzed after further 30 min by FacScan.

3.6.4 Dichlorofluorescein assay (DCF):

DCF assay was used as a general indicator of intracellular reactive oxygen species (ROS) formation. The DCF assay is sensitive to H_2O_2, $ONOO^-$ and lipid hydroperoxides. It is also used to predict the production of $O_2^{\cdot-}$ which is transformed rapidly into H_2O_2. 2`,7`-dichlorodihydrofluorescein diacetate (DCFH-DA) is a cell-permeable non-fluorescent probe. It is de-esterified intracellularly into non-fluorescent 2`,7`-dichlorodihydrofluorescein

(DCFH). The later turns to highly fluorescent 2′,7′-dichlorofluorescein upon oxidation (Fig. 15).(*Karlsson et al., 2010*) (*Xu & Lu, 2010*).

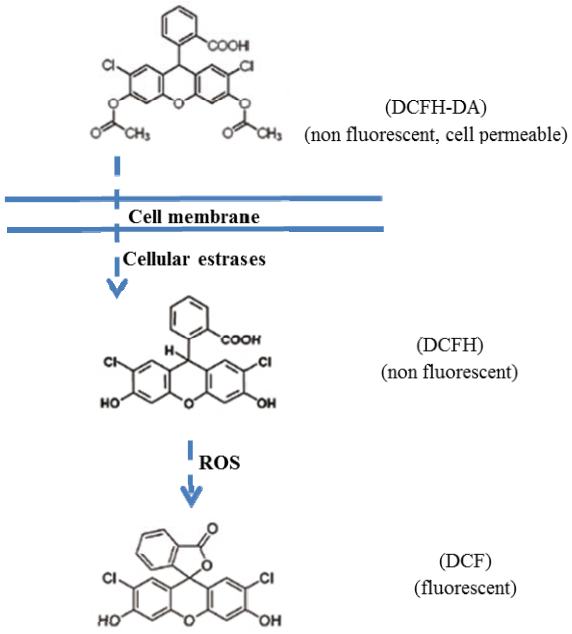

Fig (15): Detection of ROS with the DCFH-DA probe: DCFH-DA is cleaved by intracellular esterases to DCFH and oxidized by ROS to the highly fluorescent molecule DCF.

Assay procedure

30 mM DCFH-DA stock solution was prepared by dissolving 2′,7′-dichlorodihydrofluorescein diacetate (50 mg, 97%, Sigma Aldrich) in 3.4 ml DMSO.

HEPA 1.6 were seeded in a black-walled 96-well plate at a density of 10^5 cells per well in DMEM medium supplemented with 10% fetal bovine serum. Cells were treated with different concentrations of the test compounds for 1 hour. Then 20 µl of 10 µM DCFH-DA was added to each well and the plates were incubated in dark for 30 minutes.The intensity of fluorescence was measured immediately by a spectrofluorophotometer at excitation and emission wavelengths 485±20 nm and 528±20 nm respectively. Results were expressed as arbitrary units of fluorescence (Au) per 10^5 cells (Shaaban, 2010).

3.7 *In vitro* pharmacokinetics:

3.7.1 Hepatic microsomal stability and 1st pass effect:

Pooled mouse microsomes (protein concentration, 20 mg/mL) were purchased from XenoTech (Lenexa, KS). NADPH was purchased from Sigma. Compound stock solution was

prepared in DMSO. The final concentration of DMSO in the reaction was 0.2% (v/v). The stability of LX079 in microsomes was determined after their incubation at 1 μM with mouse liver microsomes (0.5 mg/mL) in 50 mM potassium phosphate buffer (pH 7.4) at 37 °C. The total incubation volume was 100 μL. The reaction mixture was prewarmed at 37 °C for 5 min before adding NADPH (1.0 mM). Reactions were quenched at 0, 5, 10, 15, 20, 30 min by adding acetonitrile (300 μL). For control experiments, NADPH was omitted from these incubations. The samples were filtered using miniuniprep filter PTFE 0.2 μM (Whatman) and then analyzed with UHPLC/MS. The hepatic intrinsic clearance was estimated by scaling up the *in vitro* $t_{1/2}$.

3.7.2 Equilibrium dialysis for plasma protein binding:

The rapid equilibrium dialysis device (RED) was purchased from thermoscientific with cutoff-mass of dialysis membrane 8,000 daltons. Pooled mice plasma was prepared by K_3EDTA and by centrifugation for 10,000 for 2 min. The substance was prepared at a concentration of 1μM and 2 μM in plasma and the organic content was kept below 1%. 300μl plasma was dialyzed against 500 μl PBS at 37°C for 4 hours. The dialysis device was sealed properly and vortexed 500 rpm on a plate vibrator for achieving equilibrium. Nonspecific binding to the membrane was excluded by running control experiments with buffer in the both chambers. At the end of dialysis 100 μl of plasma and buffer was collected and precipitated with 300μl acetonitrile. The samples were filtered using miniuniprep filter PTFE 0.2 μM (Whatman) and then analyzed with UHPLC/MS.

For determination of the degree of binding to hepatic microsomal enzymes, 2μM of the substance was prepared in pooled hepatic microsomes diluted to 1mg/ml in PBS and then 100μl of pooled hepatic microsomes was dialyzed against 300μl PBS.

3.8 *In vivo* studies:

All animal procedures were approved and supervised by the Animal Care Committee of the Germans Trias i Pujol University Hospital and by the Department of Environment of the Catalan Government (approval number 4095). Mice were weighed and checked according to the protocols and observation data sheets that were requested. Animals were followed for weight loss, apparent good health (bristled hair and wounded skin) and behaviour (signs of aggressiveness or isolation).

3.8.1 Animals:

Young adult (6-8 weeks old) female C57/BL6 mice, 20 mice for acute oral toxicity testing and 81 mice for pkarmacokinetic experiment were used. The animals were nulliparous and non-pregnant weighing 20 ±1.5 g each. They were maintained in their cages provided with a standard laboratory rodent diet and unlimited supply of drinking water and were allowed to acclimatize to the laboratory conditions for seven days before starting the experiments. The temperature in the experimental animal room was kept at 22°C ± 3°C and the relative humidity was 50 ± 20 %. Lighting was artificial with the sequence 12 hours light and 12 hours dark.

3.8.2 Substance formulation for *in vivo* model:

Doses were prepared in 5% DMSO in sterile water for oral dosing through oral gavage at a dose volume of 0.3 ml, and in 5% DMSO in PBS, pH 7.4 for IV bolus injection via tail vein at a dose volume 0.1 ml.

3.8.3 Testing of acute oral toxicity in mice:

The oral acute toxicity study was carried out using 20 mice that were randomly distributed into one control group and 3 treated groups, containing five animals per group. The control group received the vehicle while each treated group received the substance at doses 62.5, 125 or 250 mg/kg as a single oral dose. The animals were observed continuously for the first 4 h and then daily for the following 14 days, to observe any death or changes in general behavior and other physiological activities. Animals were weighted at the time of dosing then after 1 week and at the end of the experiment. Animals were observed for morbidity conditions, pain, skin, fur, respiratory distress, allergic reactions, eyes, salivation, diarrhea, behavior (hypo-hyper reactivity), tremors, convulsions, ataxia, lethargy or coma. At the end of the experiment mice were sacrificed and the internal organs were observed for the presence of any gross necropsy, the histopathology was done for the liver, spleen, lungs and kidneys in the control and highest dose groups. The cumulative mortality rate was calculated using Reed–Muench method (*Reed &Muench, 1938*).

3.8.4 *In vivo* pharmacokinetics:

For studying the PK profile of the LX079, 81 mice were used each received single dose either oral or IV. The animals were divided into one IV group (27 mice), 2 oral groups

(24 mice each), control IV group (3 mice) and control oral group (3 mice). The IV group and one oral group were dosed with 12.5 mg/kg and the other oral group was dosed with 25 mg/kg, while the control groups received the vehicle. All blood samples were collected at 15 and 30 min and 1, 2, 4, 6, 8, and 24 h after oral dosing, and at 5, 15, and 30 min and 1, 2, 4, 6, 8, and 24 h following intravenous administration. The blood was collected from the control groups at 24 h. Mice were euthanized with isoflurane and a 0.3 mL aliquot of blood was collected via terminal bleed from three mice at each time point. Blood samples were collected in heparin as anticoagulant and plasma was harvested by centrifugation at 10,000 rpm for 2 minutes. Plasma samples were kept at -80 °C until analysis.

3.9 UHPLC/MS analysis:

For quantification, calibration standards for LX079 were prepared in normal mice plasma by two-fold serial dilutions. After protein precipitation and filtration as described above, the parent substance was quantified in the samples using LC/MS in the cooperation with Knauer GmbH, Germany.

The LC-MS analysis was performed using PLATINblue UHPLC-MSQ system (Knauer, Germany). Reversed phase liquid chromatography separations during LC-MS were carried out by using BlueShell 80-2.6 C18, 100 x 2 mm ID column connected to the UHPLC system. The LC separation was performed using a binary gradient consisted of a mixture of 0.1% formic acid in water (solvent A) and 0.1% formic acid in acetonitrile (solvent B). The gradient (at flow rate of 0.6 ml/min) was programmed as follows: 0 - 2 min (40 % B), 2 - 2.2 min (40 - 100 % B) and 2.2 - 3 min (100 % B). The column temperature was 35°C and the injection volume was 5 µl. A full scan in the range of 20 – 1000 m/z was performed to find the mass of the target compound. The highest signal was reached for m/z = 490 and it was chosen for quantification. The electrospray ionization (ESI) was conducted in the positive ionization mode with needle voltage 4 KV and cone voltage 75 V. The capillary temperature was 500°C.

3.10 Pharmacokinetic analysis:

The area under the 24 hours plasma concentration-time curve (AUC) was calculated using the linear trapezoidal rule. Following IV bolus administration, half-life ($t_{1/2}$) and plasma clearance (CL) were calculated using the following equations where K is the elimination rate constant of the one phase decay (*Shahab et al, 2010*).

$$t_{1/2} = 0.693 / K$$

$$CL = Dose / AUC$$

Following oral dosing, absolute bioavailability (*F*) was calculated from the following equation where (AUC_{PO}) and (AUC_{IV}) are the areas under the 24 hours plasma concentration-time curves following oral and IV administration respectively (*Shahab et al, 2010*).

$$F = (AUC_{PO} / AUC_{IV}) * (dose_{IV} / dose_{PO})$$

The *in vitro* stability with the hepatic microsomal enzymes was calculated as follows:

$$\text{Stability (\%)} = 100 \times \text{Conc. at 30 min} / \text{Conc. at 0 min}$$

The *In vitro* $t_{1/2}$ was calculated from the following equation, where K is the elimination rate constant obtained from the slope of disappearance kinetics (in the form of relative remaining concentration of the parent substance versus time).

$$t_{1/2} = 0.693 / K$$

The *In vitro* clearance ($CL_{int, inc}$) was calculated from the equation:

$$CL_{int, inc} = k * (V/M) / F_{ub}$$

Where V is the volume of incubation, M is the amount of microsomes in the incubation and F_{ub} is the unbound fraction. F_{ub} was calculated from the results of the equilibrium dialysis as follows:

$$F_{ub} = \text{Conc. in buffer side} / \text{Conc. in side of microsomes}$$

The hepatic intrinsic clearance CL_{int} from microsomal incubation in turn was calculated as:

$$CL_{int} = CL_{int,inc} * MPPGL * \text{weight of liver}$$

Where MPPGL is the scaling factor for microsomal protein per gram of liver (*Davies & Morris, 1993*) (*Nassar et al., 2009*) (*Houston, 1994*) (*Naritomi et al., 2001*) (*www.admescope.com*) (*www.cyprotex.com*).

4. Results

4.1 Pyrazinamide resistance and pyrazinamide analogues:

4.1.1 Synthesis of pyrazinoic acid analogues:

4.1.1.1 Pyrazinoic acid amides:

Three pyrazinoic acid (POA) amides, N-dodecylpyrazinamide, N-tetradecylpyrazinamide, N-hexadecylpyrazinamide, were synthesized to be evaluated in the pyrazinamidase assay and to be compared with pyrazinamide. The three amides were synthesized following the method described by (*Ley & Priour, 2002*). In this synthesis we succeeded to obtain good to excellent yields of the desired amides (47-97%) in comparison to the yield (less than 55%) obtained in the method used by (*Simões, et al. 2009*) when they synthesized the same pyrazinoic acid amides.

N-Dodecylpyrazinamide:

White solid; TLC hexane:ethyl acetate (4:1), r_t 0.13; yield 46.8%; 1H NMR (400 MHz, $CDCl_3$) δ 0,89 (3H, t, *J* = 6.6 Hz), 1.23–1.45 (18H, m), 1.60–1.70 (2H, m), 3.50 (2H, m), 7.83 (1H, ^{s}broad), 8.54 (1H, dd, *J* = 2.4, 1.2 Hz), 8.76 (1H, d, *J* = 2.4 Hz), 9.43 (1H, d, *J* = 1.2 Hz); ^{13}C NMR (100 MHz, $CDCl_3$) δ 14.14, 22.70, 26.98, 29.31, 29.35, 29.54, 29.58, 29.59, 29.64, 29.65, 31.92, 39.51, 142.46, 144.43, 144.62, 147.15, 162.85; MS $+H^+$, 301.4.

N-Tetradecylpyrazinamide:

White solid; yield 96%; TLC hexane:ethyl acetate (4:1), r_t 0.13; 1H NMR (400MHz, $CDCl_3$) δ 0.89 (3H, t, *J* = 6.6 Hz), 1.24–1.46 (22H, m), 1.60–1.70 (2H, m), 3.50 (2H, m), 7.83 (1H, ^{s}broad), 8.34 (1H, s), 8.76 (1H, s), 9.43 (1H, s); ^{13}C NMR (100 MHz, $CDCl_3$) δ 14.14, 22.70, 26.98, 29.31, 29.35, 29.37, 29.54, 29.58, 29.60, 29.66, 29.68, 29.69, 31.93, 39.51, 142.46, 144.43, 144.62, 147.15, 162.85; MS $+H^+$, 329.48.

N-Hexadecylpyrazinamide:

White solid; yield 96.8%; TLC hexane:ethyl acetate (4:1), r_t 0.13; 1H NMR (400 MHz, $CDCl_3$) δ 0.90 (3H, t, *J* = 6.8 Hz), 1.23–1.47 (26H, m), 1.67 (2H, m), 3.50 (2H, m), 7.83 (1H, ^{s}broad), 8.54 (1H, dd, *J* = 2.4, *J* = 1.2 Hz), 8.77 (1H, d, *J* = 2.4 Hz), 9.44 (1H, d, *J* = 1.2 Hz); ^{13}C NMR (100 MHz, $CDCl_3$) δ 14.15, 22.71, 26.98, 29.32, 29.38, 29.55, 29.58, 29.61, 29.66, 29.67, 29.68, 29.69, 29.70, 31.94, 39.52, 142.47, 144.44, 144.62, 147.16, 162.92; MS $+H^+$, 357.54.

4.1.1.2 Pyrazinoic acid esters:

Three POA esters, dodecylpyrazinoate, tetradecylpyrazinoate, hexadecylpyrazinoate, were synthesized. The aim was to evaluate the possibility if these esters could be an alternative to pyrazinamide (PZA) in a trial to circumvent the mutation in *PncA*, the most common cause of PZA resistance. The three esters were synthesized by Mitsunobu reaction described in (*Nishimura et al., 2009*). The three esters were synthesized by reactions of POA with the corresponding alcohols in the presence of diethyl azodicarboxylate (DEAD) and triphenylphosphine (PPh_3) in tetrahydrofuran (THF). By this method and with the results of (*Nishimura et al., 2009*), the reaction proceeded completely by adding a solution of (DEAD) in (THF) slowly at 0°C to the mixture of the alcohol, pyrazinoic acid, and (PPh_3) in (THF) before leaving the reaction to proceed at room temperature. In this synthesis we succeeded to obtain excellent yield of the desired esters (100%) in comparison to the yield (less than 50%) obtained in the method used by (*Simões et al. 2009*) when they synthesized the same pyrazinoic acid esters.

***Dodecylpyrazinoate*:**

Waxy white solid; TLC hexane:ethyl acetate (4:1), r_t 0.22; yield 100%; 1H NMR (400 MHz,$CDCl_3$) δ −0.81 (3H, t, *J* = 6.6 Hz), 1.22–1.40 (16H, m), 1.45 (2H, m), 1.84 (2H, m), 4.45 (2H, t, *J* = 6.4 Hz) 8.75 (1H, dd, *J* = 2.4, 1.2 Hz), 8.78 (1H, d, *J* = 2.4 Hz) 9.32 (1H, d, *J* = 1.2 Hz); ^{13}C NMR (100 MHz, $CDCl_3$) δ 14.11, 22.67, 25.87, 28.60, 29.23, 29.33, 29.48, 29.55, 29.61, 29.62, 31.90, 66.53, 163.98, 143.66, 144.45, 146.26, 147.55; MS $+H^+$, 302.42.

Tetradecylpyrazinoate:

Waxy white solid; TLC hexane:ethyl acetate (4:1), r_t 0.24; yield 100%; 1H NMR (400 MHz,$CDCl_3$) δ 0.81 (3H, t, *J* = 6.6 Hz), 1.14–1.32 (20H, m), 1.37 (2H, m), 1.76 (2H, m), 4.38 (2H, t, *J* = 7.0 Hz) 8.67 (1H, dd, *J* = 2.4,1.2 Hz), 8.70(1H, d, *J* = 2.4 Hz), 9.25(1H, d, *J* = 1.2 Hz); ^{13}C NMR (100 MHz, $CDCl_3$) δ 14.13, 22.69, 25.88, 28.61, 29.24, 29.36, 29.50, 29.56, 29.64, 29.65, 29.66, 29.68, 31.92, 66.55, 164.00, 143.66, 144.45, 146.26, 147.55; MS $+H^+$, 330.47.

Hexadecylpyrazinoate:

Waxy white solid; TLC hexane:ethyl acetate (4:1), r_t 0.25; yield 100%; 1H NMR (400 MHz, $CDCl_3$) δ 0.88 (3H, t, *J* = 6.6 Hz), 1.21–1.40 (24H, m), 1.45 (2H, m,), 1.83 (2H, m),

4.45 (2H, t, J = 6.8 Hz,) 8.75 (1H, dd, J = 2.4, 1.2 Hz), 8.77 (1H, d, J = 2.4 Hz), 9.32 (1H, d, J = 1.2 Hz); ^{13}C NMR (100 MHz, $CDCl_3$) δ 14.12, 22.69, 25.88, 28.60, 29.24, 29.36, 29.49, 29.55, 29.56, 29.63, 29.66, 29.68, 29.69, 31.92, 33.00, 66.54, 163.98, 143.66, 144.45, 146.26, 147.55; MS $+H^+$, 358.52.

4.1.2 Pyrazinamidase (PZase) assay and evaluation of *in vitro* activation of pyrazinamide and different analogues:

In an attempt to evaluate the role of *PncA* gene mutation in mycobacterial PZA-resistance, and in a trial to use the cell free PZase assay to assess the *in vitro* activation of PZA and its analogues into the active form POA, the following steps were done:

4.1.2.1Expression and purification of PZase wild type and its mutants:

Histidine tagged mycobacterial PZase (wild type) was expressed in *E. coli* BL21 in APS medium and purified with different steps of protein chromatography from Ni-NTA to Q-Sepharose ion exchange chromatography and finally with sephadex-200 size exclusion chromatography . The molecular weight and the purity of the purified enzyme were assessed in SDS-PAGE as shown in (Fig. 16).

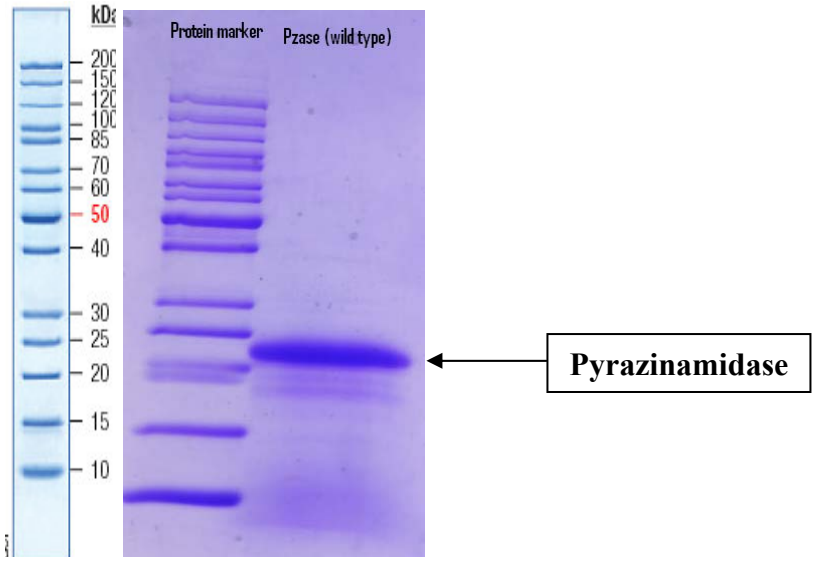

Fig (16): SDS-PAGE of *Mycobacterium tuberculosis* pyrazinamidase (wild type) after the different steps of protein purification: The molecular weight of the enzyme ranges between 20-25 KDa.

Similarly, 5 mutants of pyrazinamidase were purified using the affinity chromatography Ni-NTA. The amino acid substitution in the different mutants was

characterized using the free online GENTLE software (table-9). The fractions collected from each mutant for the buffer exchange are shown in (Fig.17).

Table (9): Types of mutation in pyrazinamidase gene from clinical PZA-resistant strains.

Mutant number	Type of mutation	Amino acid change
Mut-1	*MtPncA* T515C	*Leu172Pro*
Mut- 2	*MtPncA* A188G	*Asp63Gly*
Mut- 3	*MtPncA* C475G	*Leu159Val*
Mut- 4	*MtPncA* A287G	*Lys96Arg*
Mut- 5	*MtPncA* T350C	*Leu117Pro*

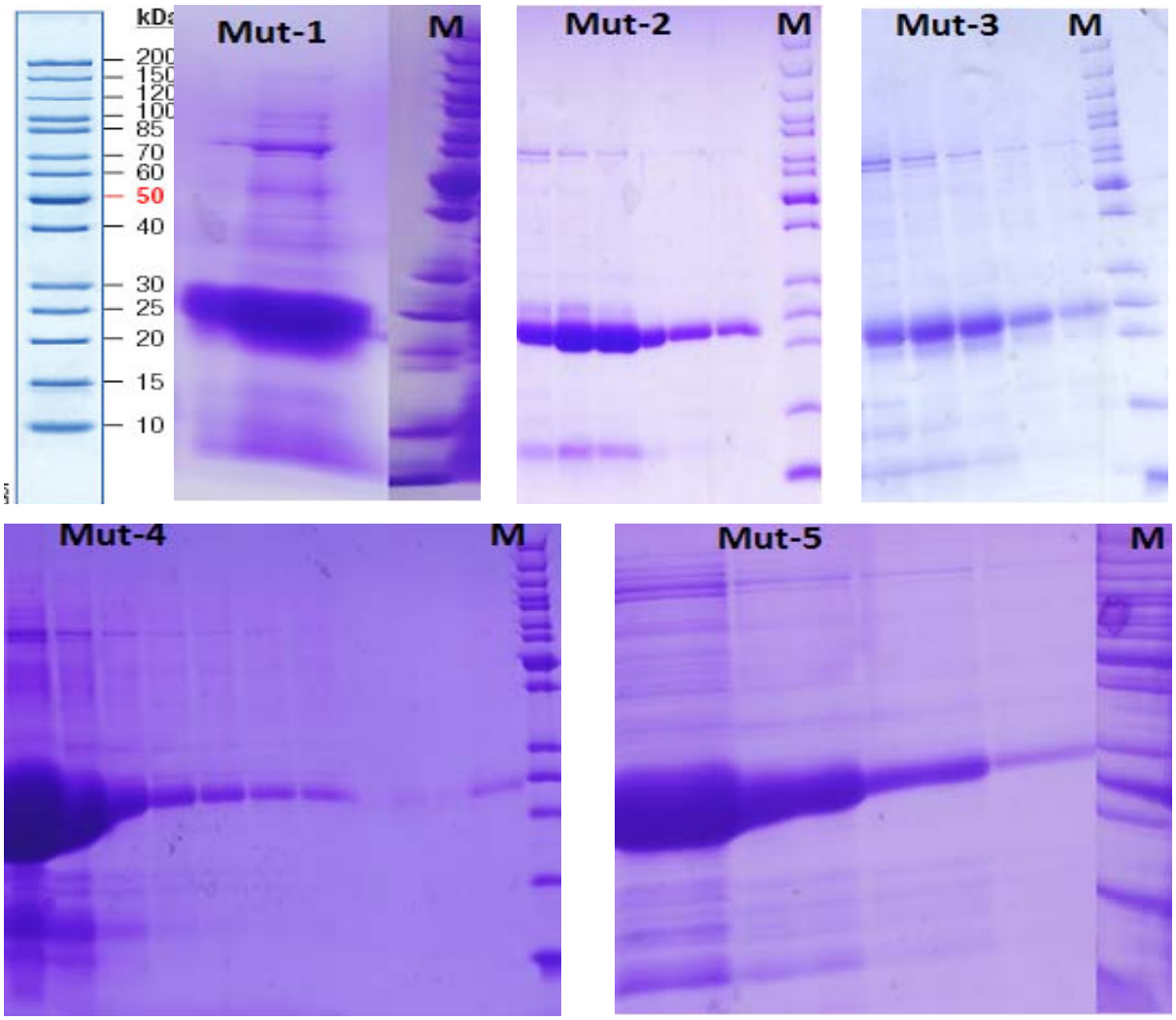

Fig (17): SDS-PAGE of 5 mutants of *Mycobacterium tuberculosis* pyrazinamidase. The figure shows the fractions collected after Ni-NTA chromatography for desalting and buffer exchange. **M**: protein marker**.**

4.1.2.2 Pyrazinamidase (PZase) assay:

For quantification, standard curve was done first using different concentrations of POA alone with ammonium ferrous sulphate to correlate the absorbance at OD_{450} with the concentration of POA as shown in (Fig. 18). The cell free PZase assay was optimized to evaluate the PZA and its analogues as prodrugs that liberate the active form POA with the action of *PncA*.The characterization of the activity of the PZase and its mutants with PZA and its analogues was done by measuring the absorbance of the colored complex formed from the liberated POA and the ammonium ferrous sulphate at 450 nm. The rate of reactions was calculated (µM/min) and these rates were applied to Graphpad prism v5.0 for kinetic parameters calculation.

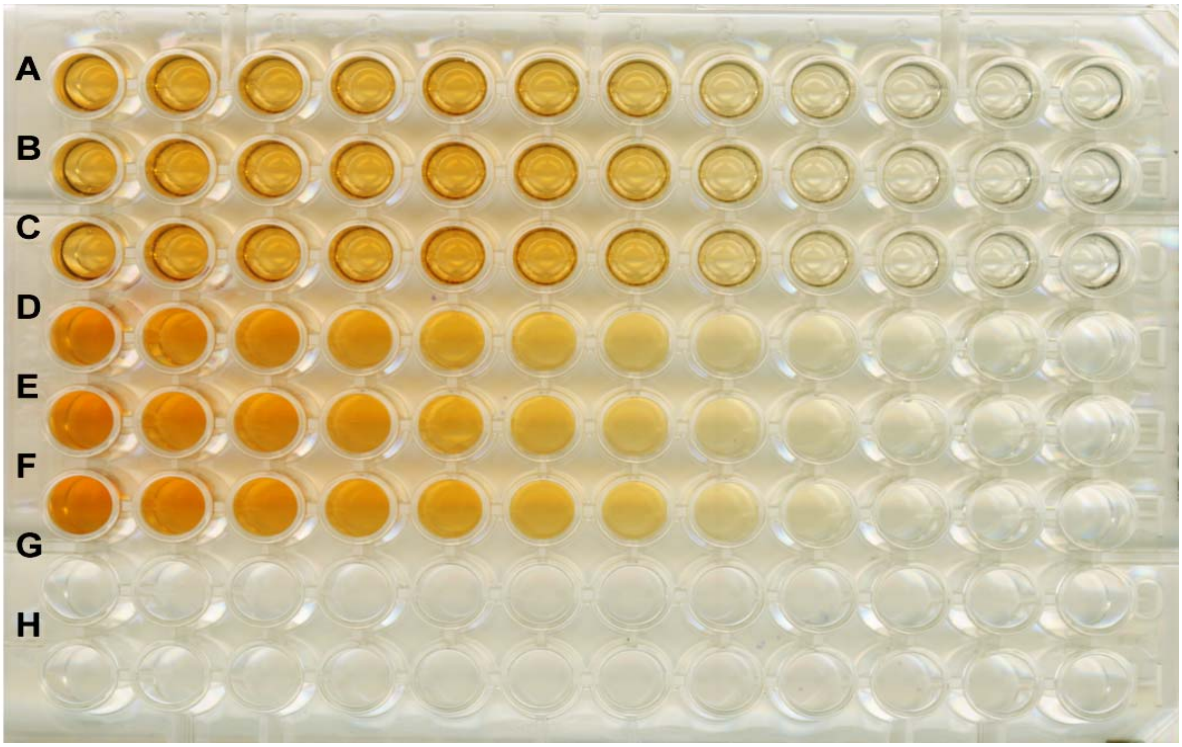

Fig (18): pyrazinamidase assay in a 96 well plate: A, B& C show effect of increasing concentrations of PZA with the wild type of *PncA*. D, E& F show the control reactions with the product only POA without enzyme for the purpose of quantitation.

4.1.2.2.1Evaluation of PZA as a substrate for mycobacterial *PncA*:

The following figure and table are showing the kinetic of the wild type *PncA* with PZA. The calculated K_m value with PZA was 1,271 mM. This high value shows a low specificity to PZA as a substrate.

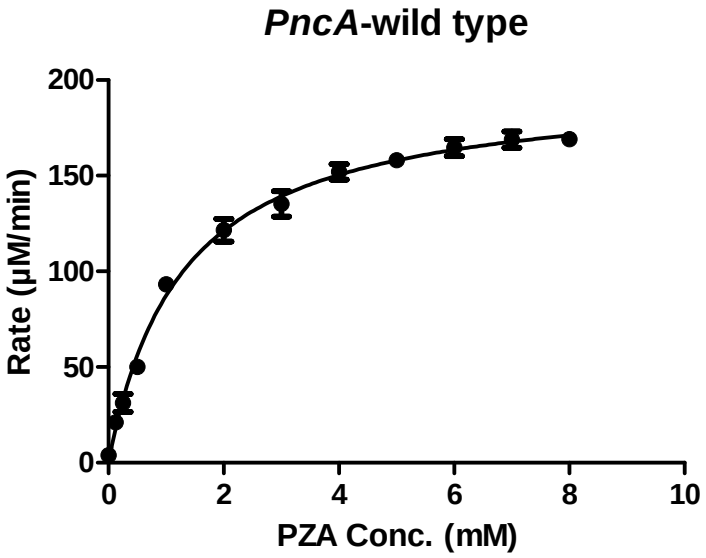

Fig (19): Michaelis-Menten plot of the wild type of *PncA*: The rate of the reaction (µM/min) is plotted against the concentration of PZA (mM)

Table (10): Kinetic parameters of the wild type of *PncA* with PZA.

Michaelis-Menten	
Best-fit values	
V_{max}	198,2
K_m	1,271
Std. Error	
V_{max}	2,636
K_m	0,06183
95% Confidence Intervals	
V_{max}	192.8 to 203.6
K_m	1.146 to 1.397
Goodness of Fit	
Degrees of Freedom	34
R^2	0,9944
Absolute Sum of Squares	739,9

4.1.2.2.2 Role of *PncA* mutation in clinical PZA-resistance:

For evaluation of the role of *PncA* mutations in the PZA-resistance, the rate of reactions carried by *PncA* mutants were evaluated and compared with the wild type as presented in (Fig.20). The K_{cat} was calculated for the wild type and the mutants. The K_{cat} is the turnover number which represents the number of times each enzyme site can convert the prodrug to its active form per unit time. Reactions with 1 mM of PZA were used for the calculation of the specific activity of the each enzyme (U/mg), where the unit (U) is the

amount of the enzyme that produces 1 micromole of POA per minute. The results were summarized in (table-11).

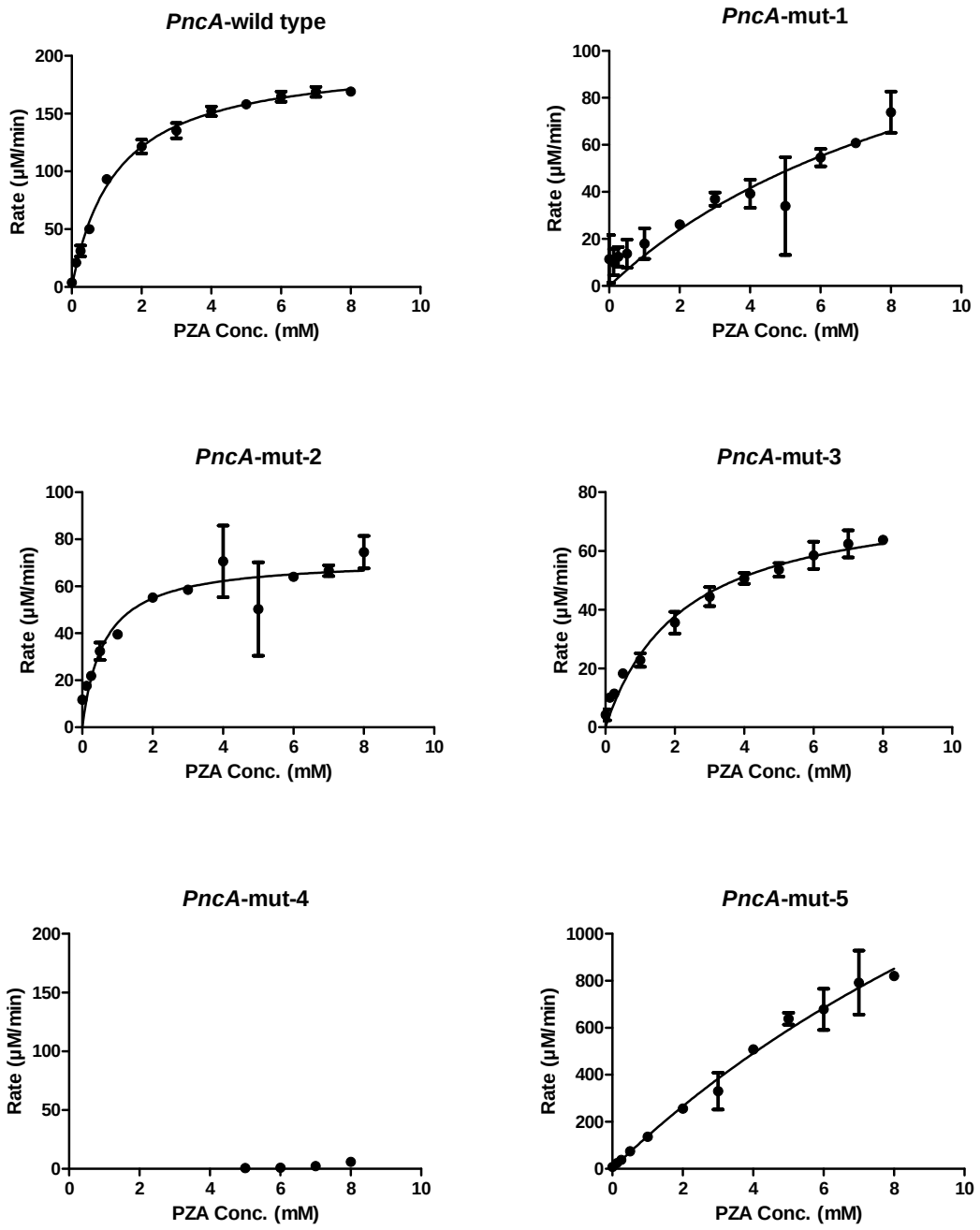

Fig (20): Comparison between the wild type of *PncA* and the 5 mutants using the pyrazinamidase assay: PZA was evaluated as a substrate at different concentrations which were plotted against the rates of reactions (µM/min). 5 times higher of the enzyme concentration was used with *PncA*-mut-1 and *PncA*-mut-4 due to their low activity. All mutants showed lower activity than the wild type and even complete inactivity as *PncA*-mut-4 except *PncA*-mut-5 that showed higher activity.

Table (11): K_{cat} and the specific activity of different enzymes with PZA.

	K_{cat}	Specific activity (*U/mg)
***PncA*-Wild type**	45.04 ± 0.6	5.91 ± 0.12
***PncA*-mut-1**	7.2 ± 3.31	0.23 ± 0.08
***PncA*-mut-2**	16.3 ± 0.92	2.54 ± 0.6
***PncA*-mut-3**	18.17 ± 0.88	1.47 ± 0.15
***PncA*-mut-4**	NM	NM
***PncA*-mut-5**	725.1± 226	8.75 ± 0.45

The data are presented as the mean ± standard deviation
NM: Non-measurable.
* One unit of pyrazinamidase was defined as the amount of enzyme required to produce 1 µmol of POA per minute.

The results revealed that not all *PncA* mutants were inactive. *PncA*-mut-2 and *PncA*-mut-3 retained some activity; however they transform PZA into POA at slower rates than that of the wild type. Even *PncA*-mut-5 had higher activity than the wild type. On the other hand PncA-mut-4 was completely inactive.

4.1.2.2.3 Evaluation of the synthesized POA amides as prodrugs:

In order to evaluate the synthesized amides as prodrugs and their ability to liberate POA, the *PncA* reactions were carried with 1mM of PZA and different analogues to compare the rate of reaction with each substance. The three synthesized analogues were considered as very poor prodrugs since they almost could not be transformed to the active form with the *PncA* as shown in (Fig. 21). The synthesized analogues were also screened with the purified mutants and no activity was observed (the results are not shown).

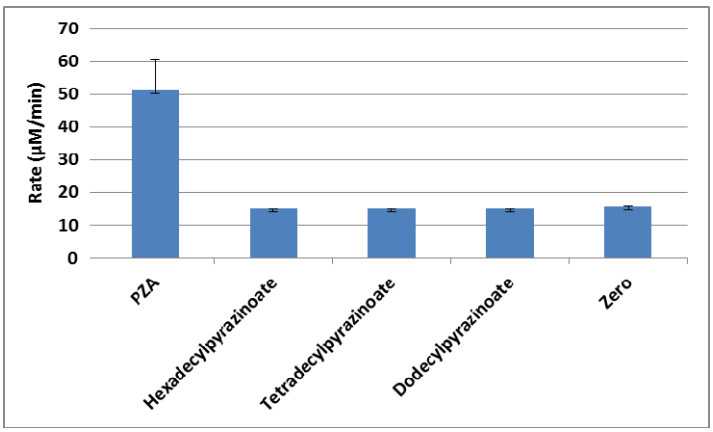

Fig (21): Screening of different analogues with pyrazinamidase assay: The three synthesized amides were considered as very poor prodrugs.

4.1.3 Pyrazinoic acid esters as an alternative to pyrazinamide, *in vitro* efficacy and toxicity:

4.1.3.1 *In vitro* activity:

Resazurin microtiter assay (REMA) was used to determine the minimal inhibitory cocentrations (MICs) of POA esters against the inherently PZA resistant strain, *M. bovis* BCG. The percentage of bacterial viability in comparison to untreated controls correlates with the reduction of resazurin to the red florescent resorufin. And the resulting change in color from blue to pink was detected and quantified by measuring the degree of fluorescence.

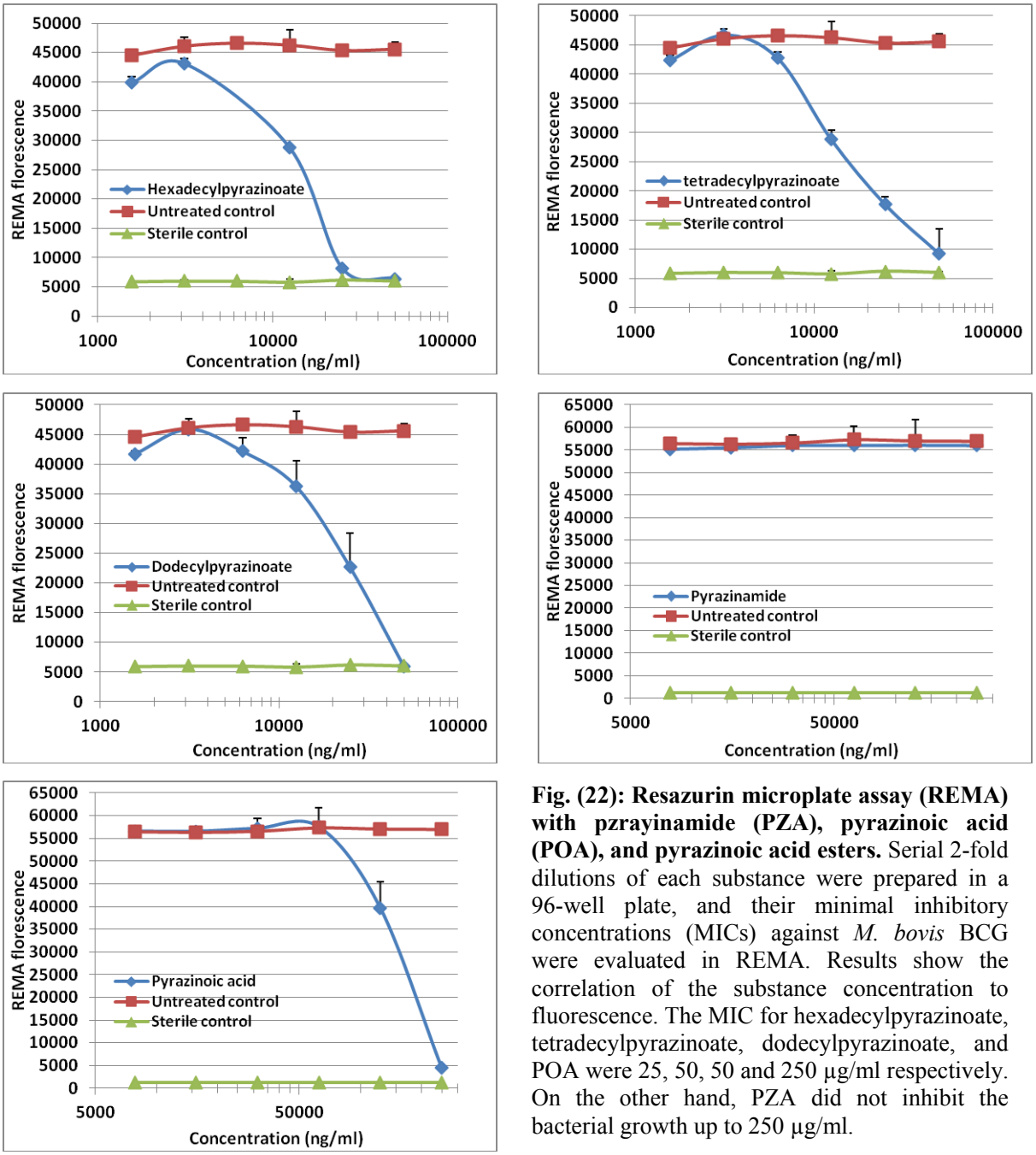

Fig. (22): Resazurin microplate assay (REMA) with pzrayinamide (PZA), pyrazinoic acid (POA), and pyrazinoic acid esters. Serial 2-fold dilutions of each substance were prepared in a 96-well plate, and their minimal inhibitory concentrations (MICs) against *M. bovis* BCG were evaluated in REMA. Results show the correlation of the substance concentration to fluorescence. The MIC for hexadecylpyrazinoate, tetradecylpyrazinoate, dodecylpyrazinoate, and POA were 25, 50, 50 and 250 µg/ml respectively. On the other hand, PZA did not inhibit the bacterial growth up to 250 µg/ml.

(Fig. 22) shows the inhibitory effect of POA esters in comparison to PZA and its active form pyrazinoic acid against *M. bovis* BCG**.**The MIC was defined as the concentration of the substance that inhibited more than 90% of bacterial growth. The percentage of growth inhibition was calculated as follows:

Percentage of growth inhibition (%) = [1- (REMA florescence of a compound - REMA florescence of the sterile control) / (REMA florescence of the untreated control - REMA florescence of the sterile control)] * 100

The MICs of hexadecylpyrazinoate, tetradecylpyrazinoate, dodecylpyrazinoate, and POA against *M. bovis* BCG were 25, 50, 50 and 250 µg/ml respectively. While, PZA did not inhibit the bacterial growth up to 250 µg/ml. The MICs of the three esters against against *M. tuberculosis* H37Rv were evaluated in REMA, and the MIC was defined as the lowest concentration that prevented the transformation of the color from blue to pink (Table-12).

4.1.3.2 *In vitro* toxicity profile:

4.1.3.2.1 Effect on cell viability and selectivity index (SI):

Cytotoxicity of the different three POA esters was measured by using the 3-(4, 5-dimethylthiazol-2-yl)-2,5-diphenyltetrazolium bromide (MTT) reduction assay on mouse connective tissue fibroblast L929 cells. The IC_{50} value, the dose inhibiting the 50% of cell viability, after 24 h and 5 days was calculated based on dose–response relationships. The ratio between IC_{50} and MIC against *M. tuberculosis* H37Rv was used to calculate the selectivity index (SI) of each compound as an estimate of the therapeutic window (Table-12).

Table (12): Minimal inhibitory concentration (MIC), IC_{50}, selectivity index (SI) of pyrazinoic acid esters:

	(MIC) against *M. tuberculosis* H37Rv (µg/ml)	**IC_{50} (µg/ml) in MTT with L929 cell line**		**SI (IC_{50}/MIC)**	
		5 days	**1 day**	**5 days**	**1 day**
Hexadecylpyrazinoate	25	7	25	0.28	1
Tetradecylpyrazinoate	25	20	>100	0.8	>4
Dodecylpyrazinoate	50	20	>100	0.4	>2

The 3 POA esters were inhibiting the L929 cell proliferation as shown in the results of MTT assay after 5 days, however tetradecylpyrazinoate and dodecylpyrazinoate did not show acute toxic effect against the same cell line at all doses used in MTT assay after 1 day. The anti-proliferative effect of the three POA esters was further screened with different cell lines. The HUVEC cell line was tested as an example for primary cell lines, as well as the J774 a.1 cell line to be comparable with the results of (*Simões et al. 2009*). (table-13) shows the calculated IC_{50} from the dose response curve in addition to the log_p value which reflects the degree of the lipophilicity of the compounds. The results showed that the higher lipophilicity was associated with higher toxicity (lower IC_{50}). In addition, the highest toxicity was noticed against the HUVEC cell line.

Table (13): Lipophilicity and anti-proliferative effect of POA esters:

	MIC (µM)	***Logp****	**IC_{50} (µM)**				
			HUVEC	**KB 3.1**	**Ptk2**	**J774 a1**	**HEPA 1.6**
Hexadecylpyrazinoate	70	5.85	7.8	26.6	22.4	55.9	42
Tetradecylpyrazinoate	75.9	5.46	21.2	62.2	75.9	63.7	57.7
Dodecylpyrazinoate	165.9	4.55	21.6	99.5	69.7	92.9	99.5

* (*Simões et al. 2009*)

4.1.3.2.2 Effect on cell morphology:

Phenotypical changes in the nucleus and alpha tubulin and actin stress fibres were monitored in potoroo cells (PtK2) treated with 20 µg/ml of different compounds. And the endoplasmic reticulum was stained after the treatment with 10 and 20 µg/ml of each compound. The 3 compounds at concentration 20 µg/ml induced stress of the endoplasmic reticulum that was revealed by the appearance of the stress vacuoles in comparison to the untreated cells. On the other hand cells showed normal appearance of the stress fibres and microtubules.

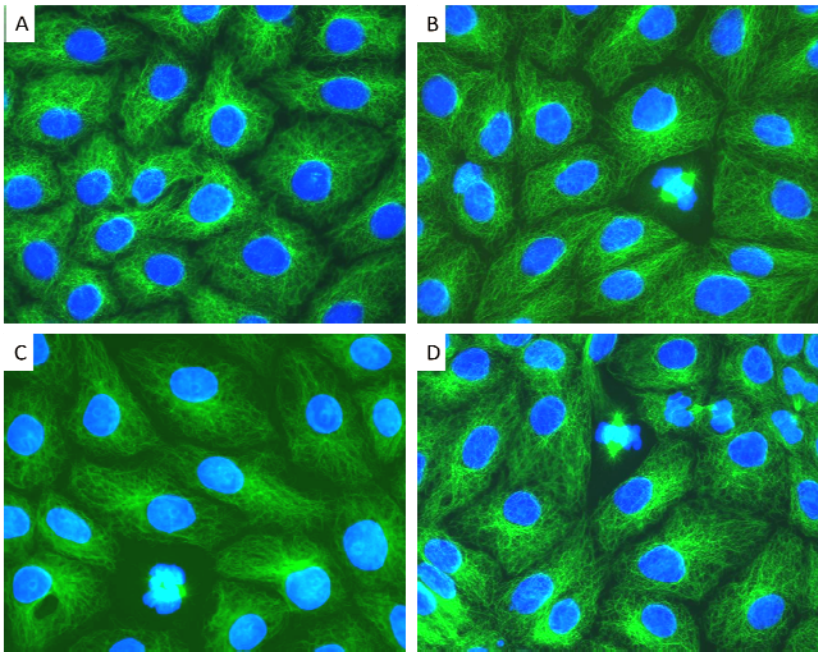

Fig (23): Immunoflorescent staining of alpha tubulin. A: Control of untreated cells, **B**: Hexadecylpyrazinoate, **C**: Tetradecylpyrazinoate, **D**: Dodecylpyrazinoate. PtK2 cells were incubated with 20 µg/ml of different compounds for 18 hours. In comparison with control cells, Treated cells show normal appearance of the microtubules.

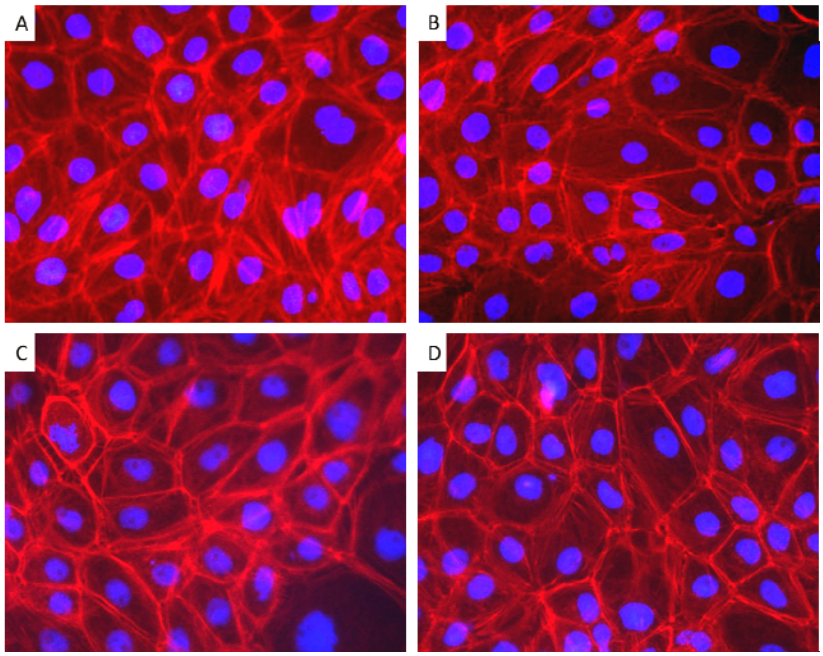

Fig (24): Immunoflorescent staining of actin: A: Control of untreated cells, **B**: Hexadecylpyrazinoate, **C**: Tetradecylpyrazinoate, **D**: Dodecylpyrazinoate. PtK2 cells were incubated with 20 µg/ml of different compounds for 18 hours. In comparison with control cells, Treated cells show normal appearance of the actin stress fibres.

Fig(25)-a

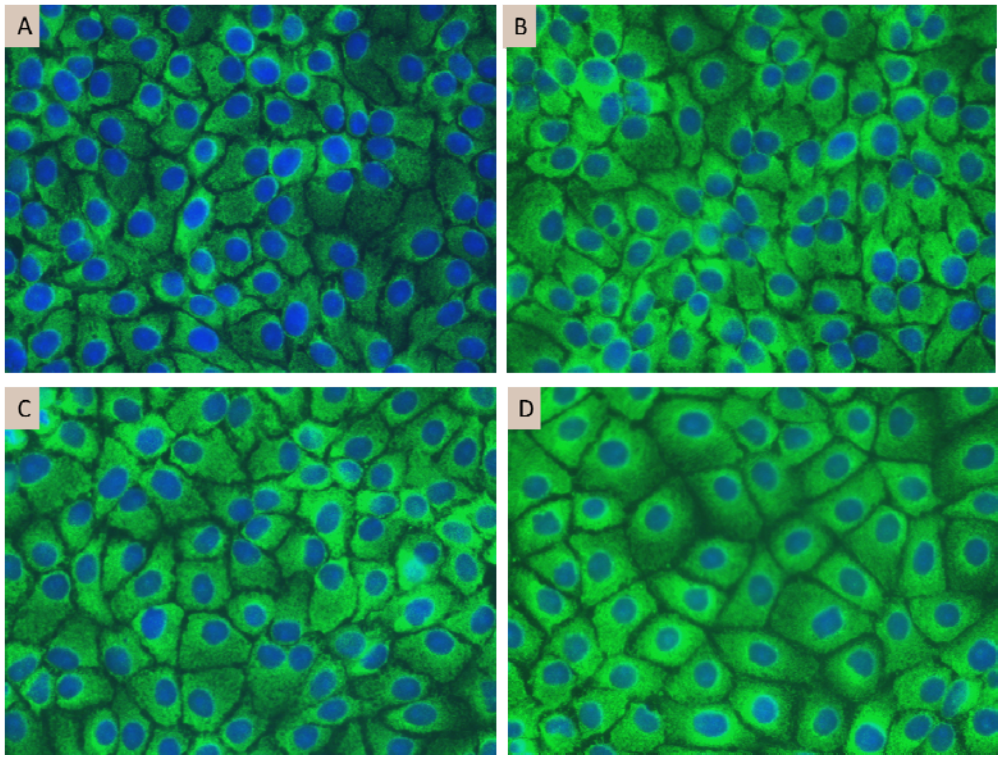

Fig(25)-b

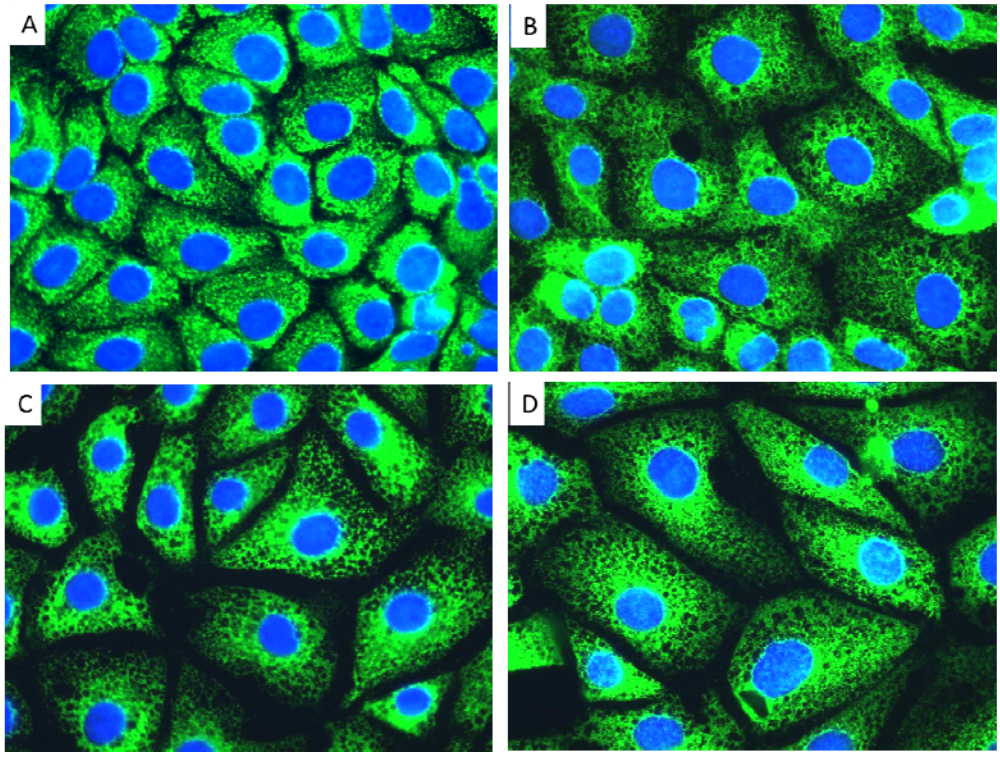

Fig (25): Immunoflorescent staining of endoplasmic reticulum: A: Control of untreated cells, B: Hexadecylpyrazinoate, C: Tetradecylpyrazinoate, D: Dodecylpyrazinoate. PtK2 cells were incubated with 10µg/ml (a) and 20 µg/ml (b) of different compounds for 18 hours. In comparison with control cells, Treated cells at Conc. 20 µg/ml show vacuoles in the endoplasmic reticulum. While at Conc. 10 µg/ml, cells show normal morphological appearance.

4.1.3.2.3 Induction of apoptosis:

Human macrophage cells U937 were treated with the IC_{90} of the POA esters (35µg/ml) for 12 hours. At this concentration hexadecylpyrazinoate, tetradecylpyrazinoate, dodecylpyrazinoate induced late apoptosis in 60.1, 85, and 98.4% of treated cells in comparison to 12.8 % in the untreated control.

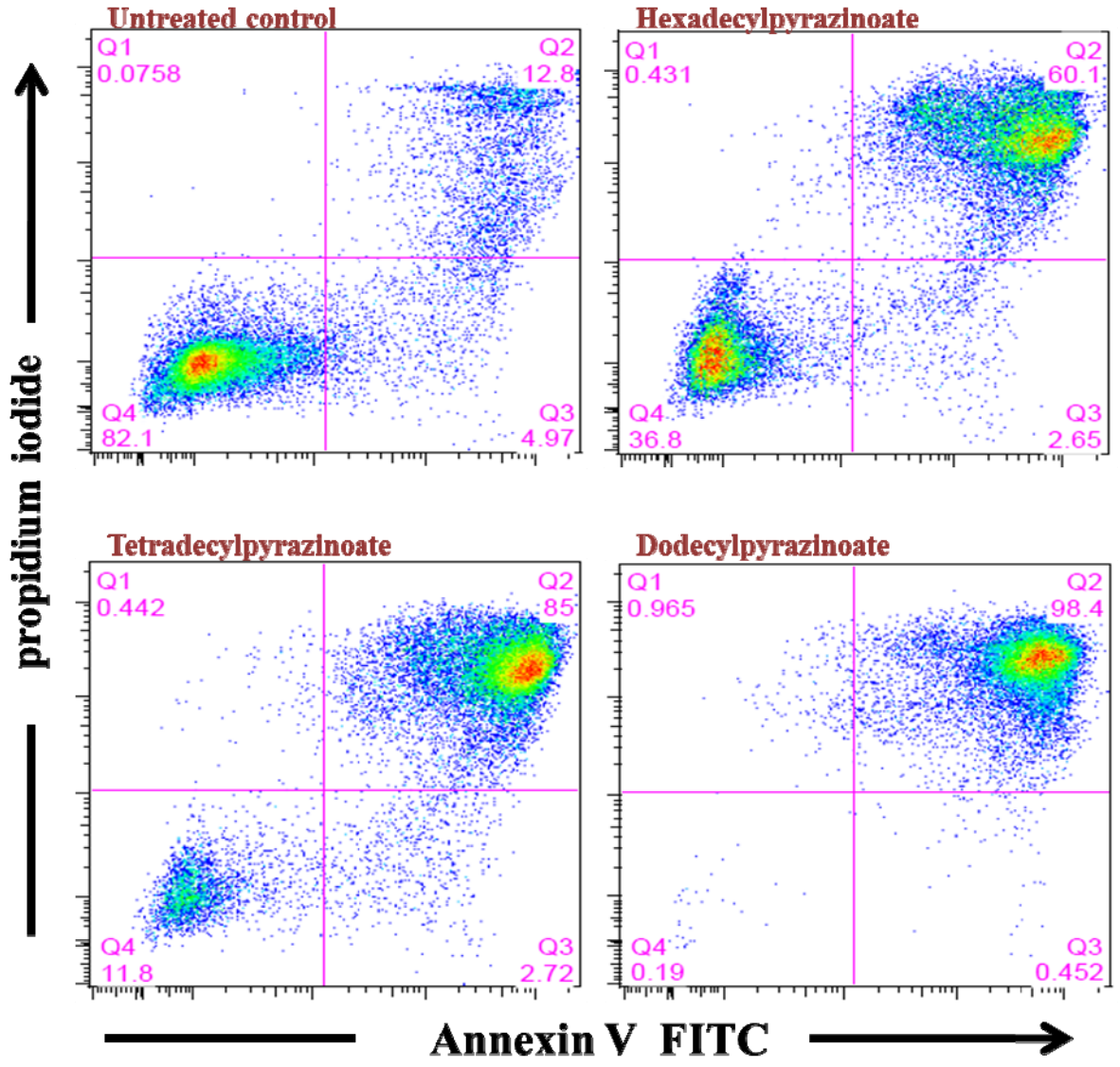

Figure (26). Flow cytometric analysis of apoptosis:
U937 cells were treated with 35 µg/ml of the test compounds for 12 h, and stained with FITC Annexin V and propidium iodide (PI). Q4 contains the percentage of viable cells (stained neither with PI nor with FITC Annexin V); Q2 shows the percentage of late apoptotic cells (stained with both PI and FITC Annexin V), and Q3 the percentage of early apoptotic cells (stained with FITC Annexin V only).

4.1.3.2.4 Induction of reactive oxygen species:

As the induction of reactive oxygen species (ROS) is one of the common causes of the ER stress, the DCF assay was used to evaluate the induction of ROS by the three esters. The DCF assay was carried out after 1 hour of treating HEPA 1.6 cell line with different concentrations of the compounds and a control experiment with H_2O_2 was included. In comparison to the control experiment, the POA esters were found to have no role to induce the intracellular ROS levels.

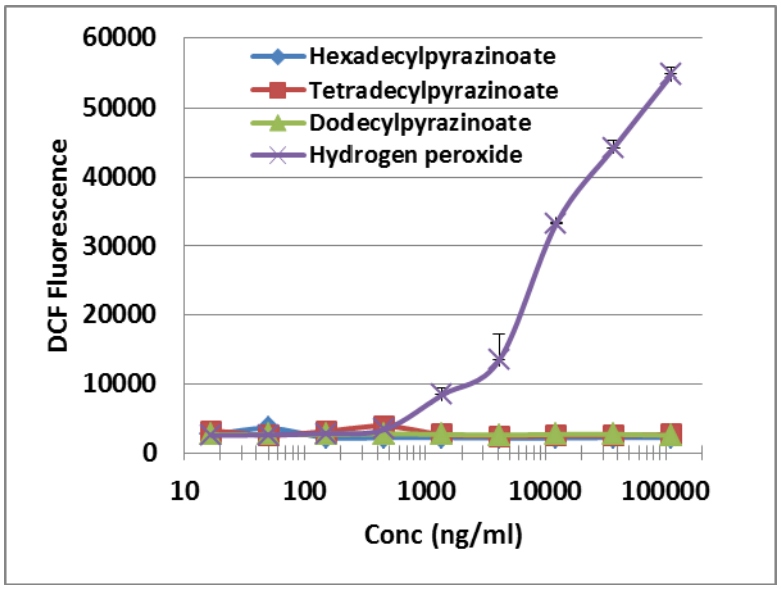

Fig (27): Evaluation of induction of reactive oxygen species (ROS) in HEPA 1.6 cell line after 1 hour treatment with different concentrations of pyrazinoic acid esters using the DCF assay: in comparison to the control experiment that was treated with H_2O_2, the 3 pyrazinoic acid esters did not induce the intracellular ROS levels.

As revealed from the previous results, the three POA esters were found to have very narrow therapeutic window as revealed from their SI. They induced ER stress in Ptk2 cells at a concentration lower than their *in vitro* MICs. By testing the antiproliferative effect of the three compounds with different cell lines, it was noticed that their IC_{50} values were in reverse order of their lipophilicity. In addition the three esters had a lower IC_{50} against HUVEC cell line than other cell lines.

4.2 RNAP inhibitors:

4.2.1 *In vitro* screening of different substances with RNAP assay.

4.2.1.1 Validity of the assay:

As a preparatory step of the assay, different concentrations of ATP alone were measured with the Luciferin-Luciferase system (Fig. 28). Then the ability of ATP sulfurylase enzyme to utilize pyrophosphate (ppi) and to produce ATP was confirmed by measuring the liberated ATP from the reaction using the Luciferin-Luciferase system (Fig. 29).

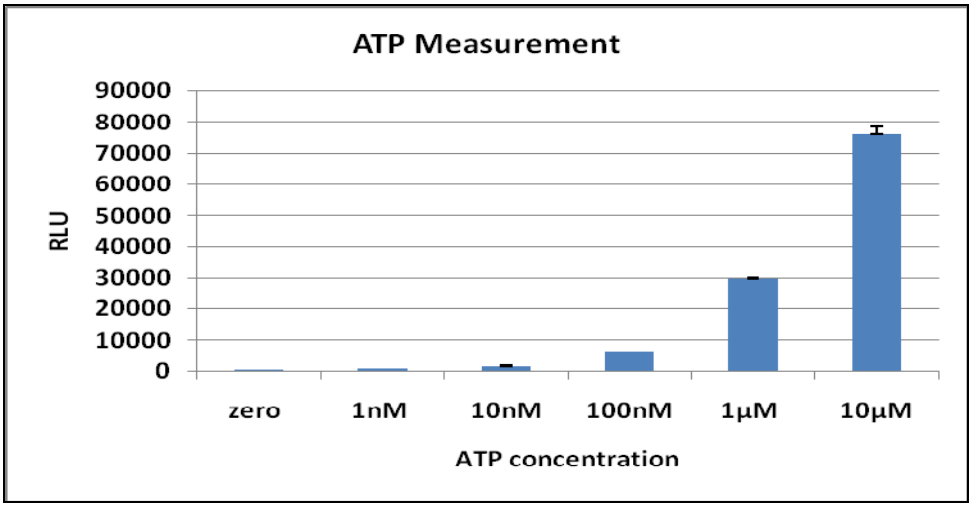

Fig. (28): Test of Luciferin-Luciferase system: The relative light unit (RLU) was measured with different concentrations of ATP (1 nM to 10 µM) with Luciferin-Luciferase System.

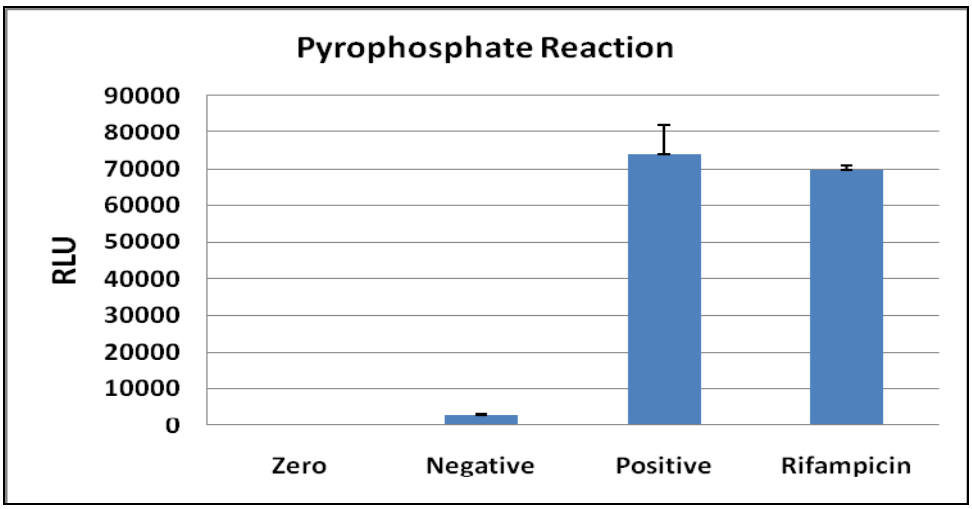

Fig. (29): Pyrophosphate reaction to test the ability of ATP Sulfurylase to convert PPi into ATP: In the positive reaction, PPi was used as a substrate for ATP sulfurylase. ATP that produced from the reaction was then tested with Luciferin-Luciferase system and RLU values were measured. Rifampicin: rifampicin was added to the positive reaction, Negative: PPi was excluded and Zero: was the blank value.

Then the whole reaction was carried out starting by the reaction of RNAP followed by the sequential steps of the assay as described previously in the section of the materials and methods. In parallel the assay was performed with the presence of rifampicin (RIF) as an inhibitor of RNAP (Fig. 30).

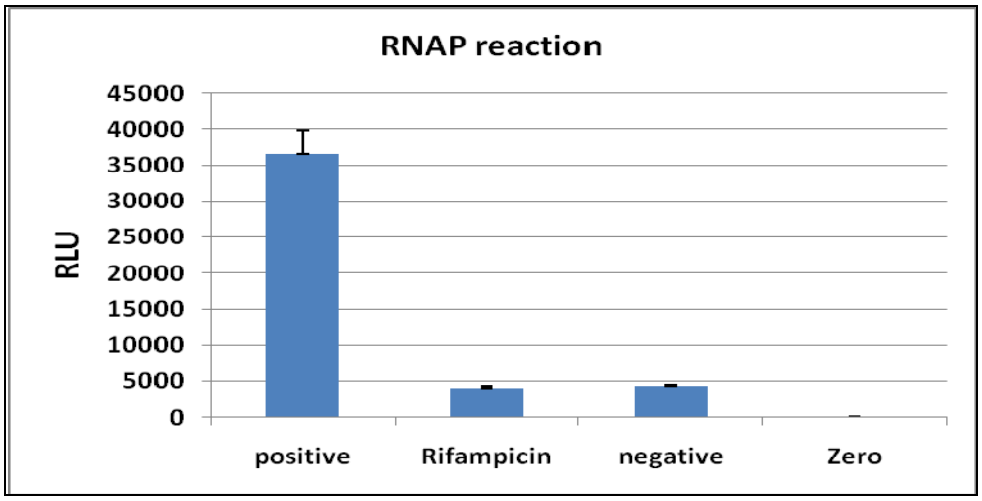

Fig (30): RNA polymerase reaction. Positive reaction contains all reactants necessary for RNAP Assay. Rifampicin contained rifampicin with the positive reaction, as an inhibitor of RNAP. Negative reaction did not have DNA necessary for the transcription of RNAP and Zero was the blank well.

4.2.1.2 Screening potential drug candidates using the RNAP assay:

The inhibitory effect of different substances and LX cocktails was evaluated in the RNAP assay (Fig. 31). Almost all cocktails inhibited the RNAP in a dose related manner. On the other hand the OCI substances, intermediates in the synthesis of corallopyronin, showed no inhibitory effect.

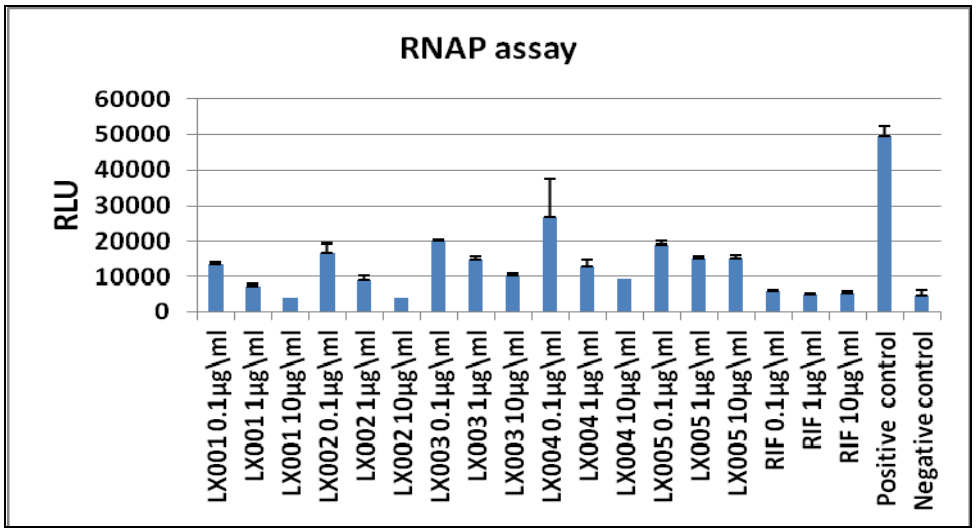

Fig. (31): Continued.

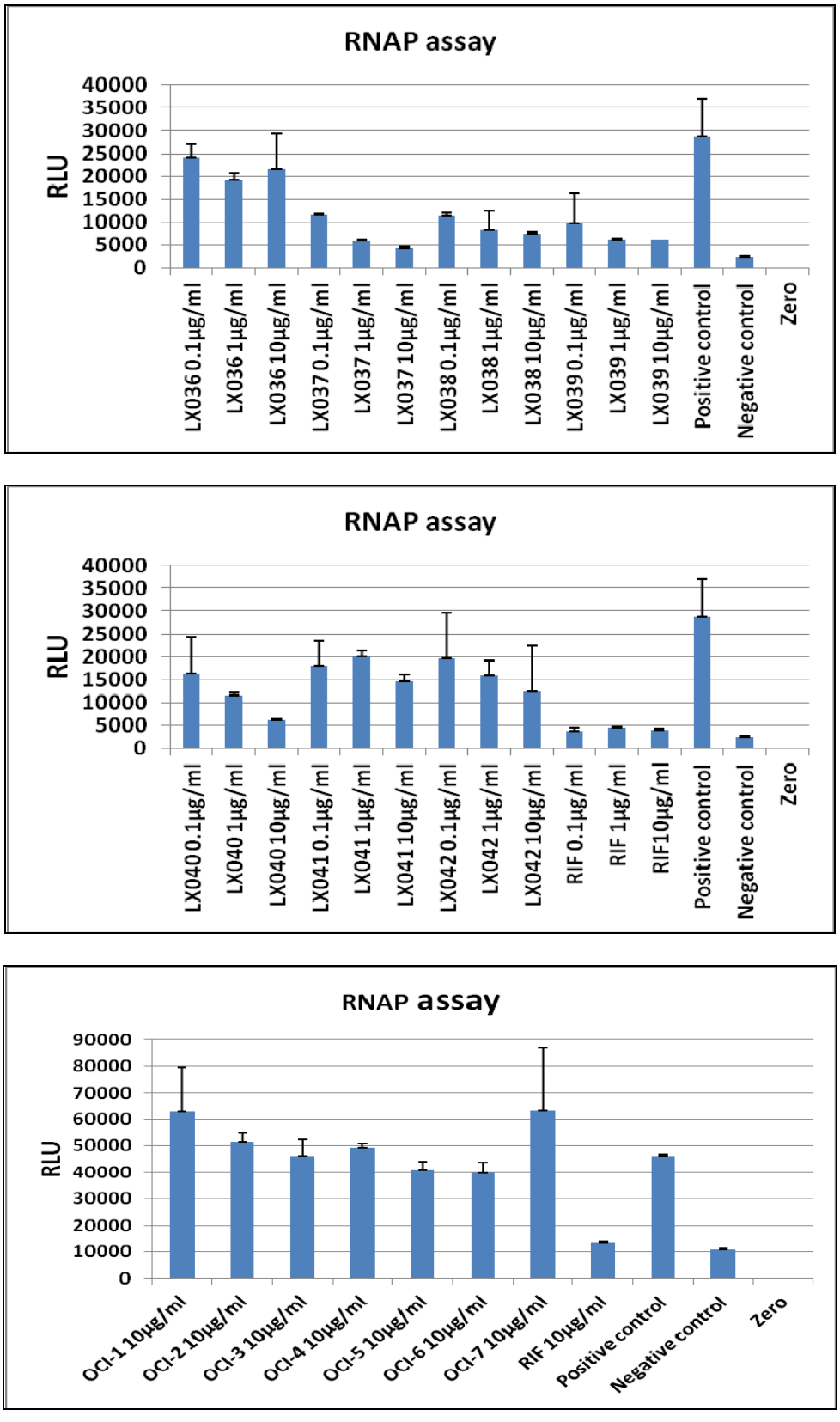

Fig. (31): Screening of different substances in RNAP assay: RNAP assay was used to predict the inhibitory effect of different substances at different concentrations along with positive control that contained all constituents of the reaction, negative control in which RNAP was excluded and rifampicin (RIF) as a control of RNAP inhibition. The Y-axis represents the RLU and at the X-axis the substances are shown.

4.2.2 Evaluating the *in vitro* inhibitory profile and cellular toxicity of RNAP inhibitors (RNAPIs).

4.2.2.1 Synergistic effect between RNAP inhibitors and ethambutol:

The MICs for the individual RNAPI, corallopyronin, ripostatin and myxopyronin against *M. tuberculosis* H37Rv were evaluated in REMA as described above. Ethambutol is a commercially available anti-TB drug which functions through inhibiting the cell wall. And to evaluate the synergistic effect of the three RNAPI with ethambutol, the test was repeated using 7H9 medium containing sub-MIC of ethambutol to calculate the fractional inhibitory concentration (FIC). The synergism was considered when FIC is less than 1. The SI was calculated by dividing the IC_{50} obtained from the MTT assay over the *in vitro* MIC of each individual substance as shown in the following table.

Table (14) Synergistic effect between the RNAP inhibitors and ethambutol:

	MIC (µg/ml) against *M. tuberculosis* H37Rv		***In vitro* toxicity with L929 cell line**	
	Individual substance	**With medium containing ethambutol [b]**	**IC_{50} (µg/ml) [a]**	**SI**
Myxopyronin	6.25	3.125	>100	>16
Corallopyronin	12.5	12.5	25	2
Ripostatin	no inhibition up to 25 µg/ml	no inhibition up to 25 µg/ml	>100	
Ethambutol	1.6		>100	>62.5

[a] MTT assay after 5 days.
[b] Ethambutol at Conc. 0.3 µg/ml

Myxopyronin did not inhibit L929 cell proliferation at all tested concentrations with SI more than 16. On the other hand corallopyronin exhibited low SI and ripostatin did not inhibit the growth of *M. tuberculosis* H37Rv up to concentration of 25 µg/ml.The results showed the synergistic effect between myxopyronin and ethambutol. The calculated FIC was less than 1.

FIC = MIC ethambutol in combination/MIC ethambutol alone + MIC myxopyronin in combination/MIC myxopyronin alone = 0.3/1.6 + 3.125/6.25= 0.64 (FIC less than 1 means synergism)

4.2.2.2Minimal inhibitory concentration of different combinations:

REMA was used to determine the MICs of different combinations of myxopyronin and ethambutol against *M. bovis* BCG (Fig 32).

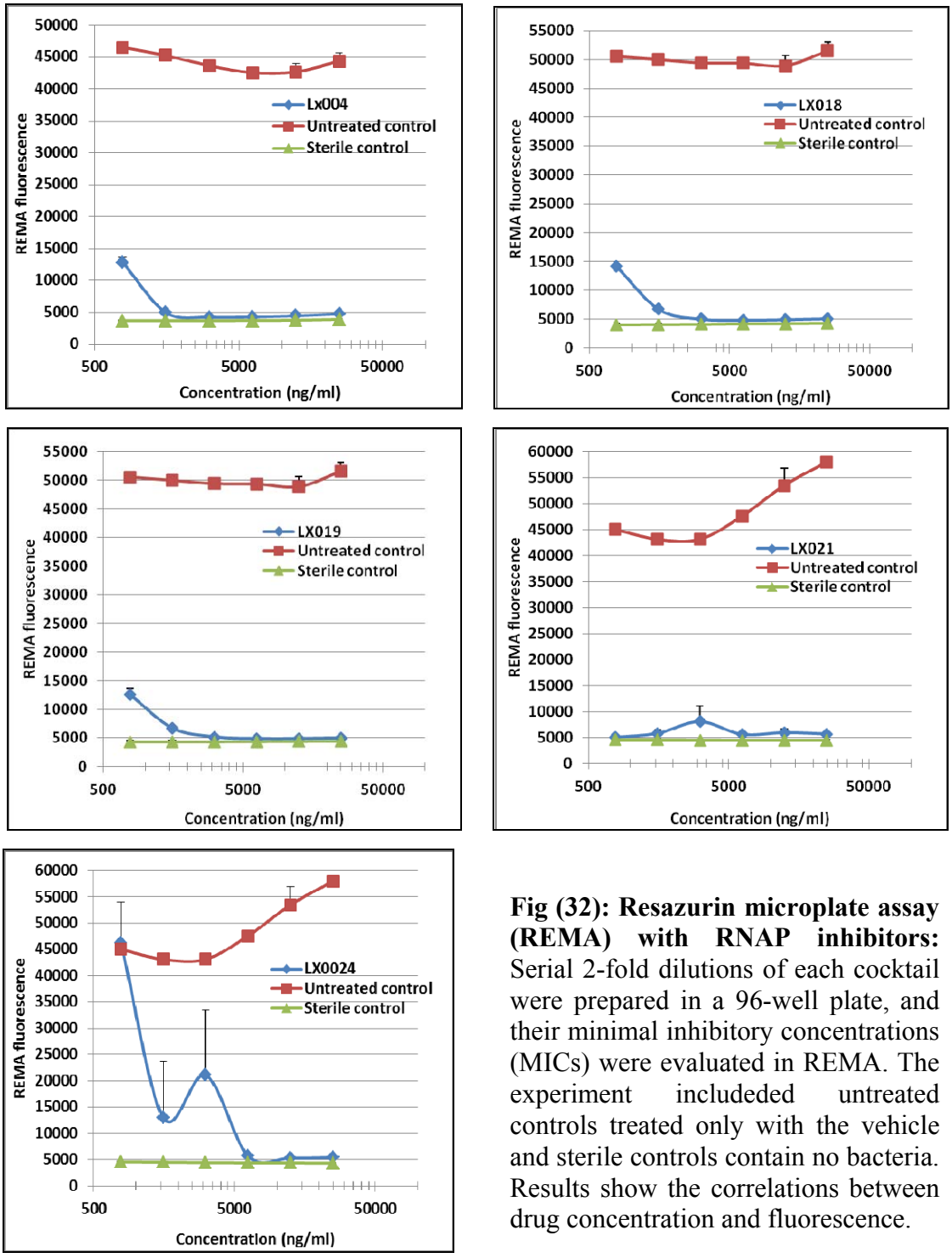

Fig (32): Resazurin microplate assay (REMA) with RNAP inhibitors: Serial 2-fold dilutions of each cocktail were prepared in a 96-well plate, and their minimal inhibitory concentrations (MICs) were evaluated in REMA. The experiment includeded untreated controls treated only with the vehicle and sterile controls contain no bacteria. Results show the correlations between drug concentration and fluorescence.

4.2.2.3 Effect on cell viability and selectivity index:

As the different combinations inhibited the mycobacterium at low concentrations, they were further tested in MTT assay with L929 to determine the effect on cell viability and to calculate the selectivity index as shown in (table-15).

Table (15) Minimal inhibitory concentration (MIC), IC_{50} and selectivity index (SI) of different cocktails:

	MIC (µg/ml)[a]	IC_{50} (µg/ml) after 5 days [b]	SI ([c]IC_{50}/MIC)
LX004	1.5	35	23.3
LX018	1.5	>100	> 66.7
LX019	1.5	>100	> 66.7
LX021	<0.8	>100	>125
LX024	6.5	>100	> 15.4

[a] MIC was calculated as the dose that inhibited more than 90 % of *M. bovis* BCG growth in REMA . [b] in MTT assy with L929 cell line. [c] IC_{50} after 5 days.

The IC_{50} and MIC data, as described before, were used to calculate the SI as an estimate of the therapeutic window. All combinations did not inhibit cell proliferation at all tested concentrations except LX004. The combinations between myxopyronin and ethambutol inhibited the bacterial growth at lower concentrations at the same time they showed high SI even LX004 it has also wide safety margin.

4.2.2.4 Effect on cell morphology:

Phenotypical changes in the nucleus, endoplasmic reticulum (Fig. 33), microtubules (Fig. 34) and actin stress fibres (see appendix) were monitored in potoroo cells (PtK2) treated with 20 µg/ml of the individual substances.

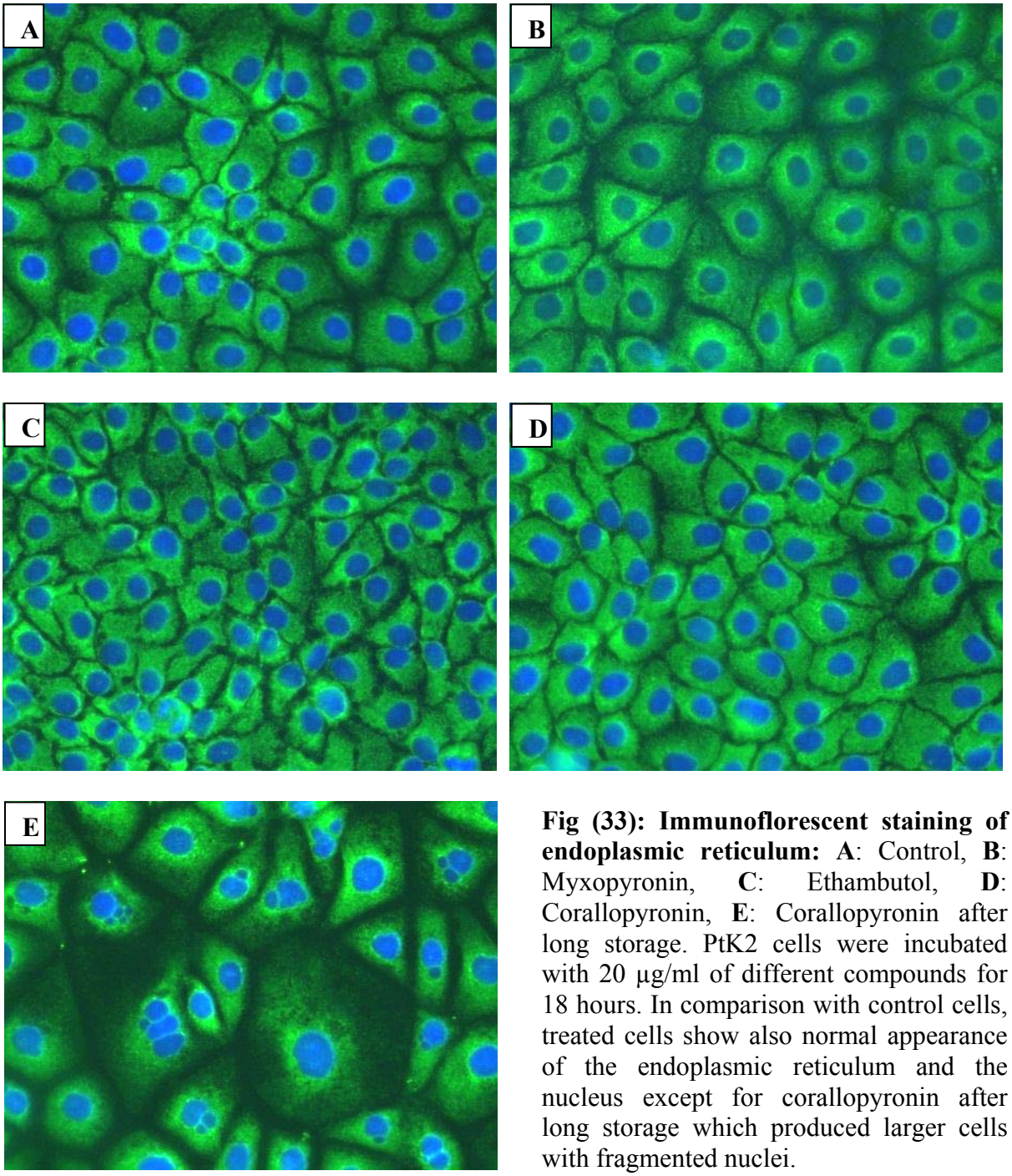

Fig (33): Immunoflorescent staining of endoplasmic reticulum: A: Control, **B**: Myxopyronin, **C**: Ethambutol, **D**: Corallopyronin, **E**: Corallopyronin after long storage. PtK2 cells were incubated with 20 µg/ml of different compounds for 18 hours. In comparison with control cells, treated cells show also normal appearance of the endoplasmic reticulum and the nucleus except for corallopyronin after long storage which produced larger cells with fragmented nuclei.

Myxopyronin and ethambutol had no effect on the cell morphology. It was noticed that corallopyronin upon long storage it produced fragmentation of the nucleus. And as revealed from the staining of the microtubules, it induced abnormal mitotic spindles.

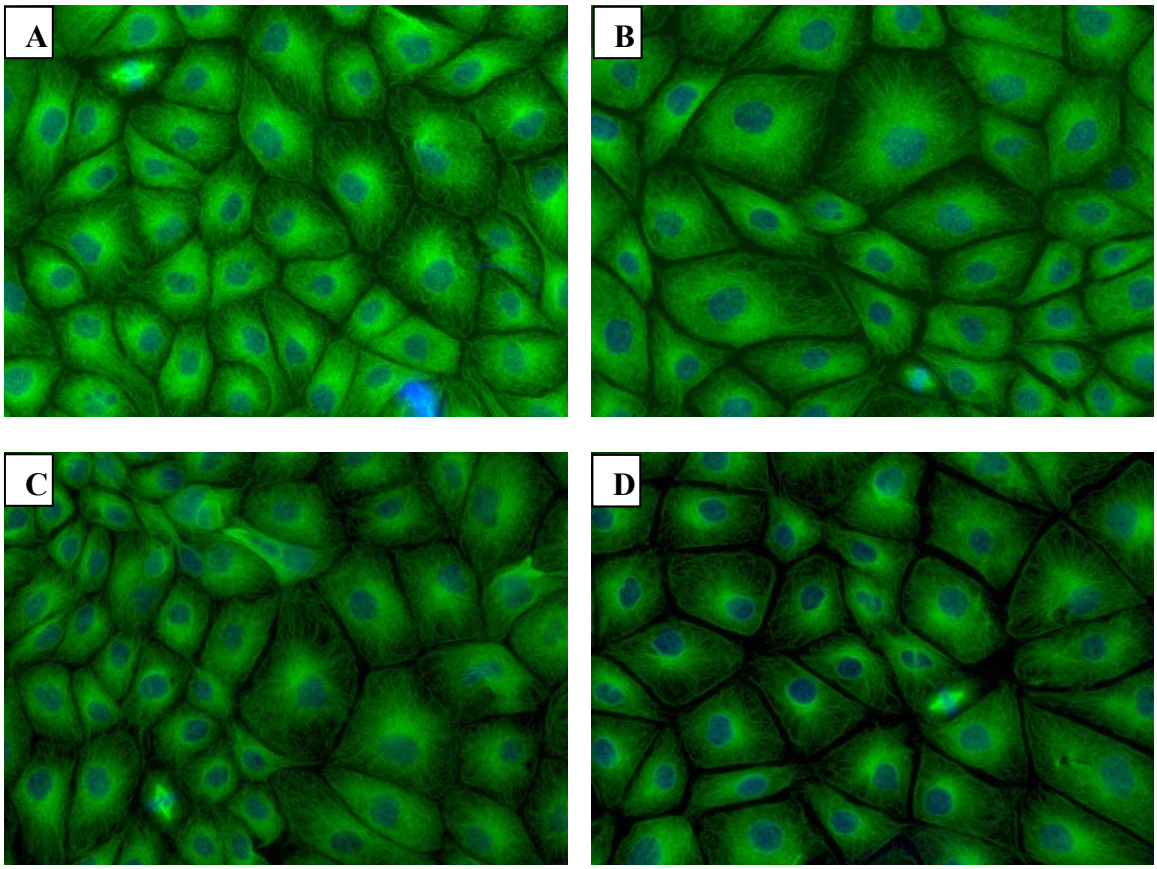

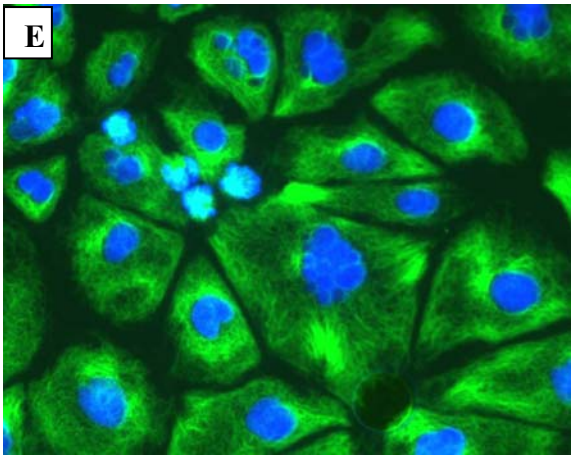

Fig (34): Immunoflorescent staining of microtubules: **A**: Control, **B**: Myxopyronin, **C**: Ethambutol, **D**: Corallopyronin, **E**: Corallopyronin after long storage. PtK2 cells were incubated with 20 µg/ml of different compounds for 18 hours. In comparison with control cells, treated cells show also normal appearance of the microtubules and the nucleus except for corallopyronin after long storage which produced abnormal mitotic spindles and multinucleated cells.

Furthermore the diferent combinations between myxopyronin and ethambutol were also evaluated with regard their effect on cell morphology. All combinations did not produce any abnormality of the cellular structures, nuclus, endoplasmic reticulum, microtubules and stress fibres (see appendix).

4.2.2.5 Effect of protein binding on *in vitro* MIC:

Binding to proteins in plasma is a very important factor that can influence the *in vivo* antimicrobial activity. For this reason, the MICs of Myxopyronin, ethambutol and their

combination in LX004 and LX018 against *M. bovis* BCG were investigated using resazurin assay in 100 % medium and with the presence of 50 % fetal bovine serum (FBS).

Table (16): Effect of protein binding on *in vitro* MIC.

	MIC in 100% medium	**With medium containing 50 % FBS**
Myxopyronin	6.25	no inhibition up to 25 µg/ml
Ethambutol	2.5	2.5
LX004	1.5	1.5
LX018	1.5	3.125

It was noticed that myxopyronin did not inhibit the growth of *M. bovis* BCG in the presence of 50% FBS with concentration 4 times higher than its MIC in 100 % medium. On the other hand, the MICs of the LX004, LX018 and ethambutol were not affected by the addition of the FBS. These two combinations retained FIC below than 1 even with the presence of FBS.

In between the three RNAPIs, myxopyronin, ripostatin and corallopyronin, we found that myxopyromin seems to be very attractive for further testing. Beside that it showed a satisfactory SI, it exhibited synergism with the cell wall inhibitor, ethambutol. The results showed that the high binding of myxopyronin to proteins might be compensated with this synergistic effect *in vitro*.

4.3 Random library of compounds:

4.3.1 *In vitro* screening of a random library of compounds:

4.3.1.1 Primary screening: Evaluating the *in vitro* antituberculous activity:

A library of about 480 compounds was screened against *M. tuberculosis* H37Rv using REMA. In between the 480 compounds, 5 compounds had low or submicromolar MIC (Table-16).

4.3.1.2 Secondry screening: Evaluating the *in vitro* toxicity profile against mammalian cells.

Subsequently, the *in vitro* cytotoxicity and SI of the 5 compounds were assessed using the MTT assay with L929 cell line after 1 and 5 days. The MIC, IC_{50} and the SI of the 5 compounds are listed in (Table-16).

4.3.1.2.1 Effect on cell viability and selectivity index:

In between the 5 compounds the, LX077 and LX079 had the most promising results. When the SI was calculated by the IC_{50} obtained after 5 days incubation with the substances, their SI were exceeding 10. And their SI when calculated from IC_{50} from the acute toxic effect experiment, their SI were 30.6 and 65.3 respectively.

Table (16) Minimal inhibitory concentration (MIC), IC_{50} and selectivity index (SI) of the selected compounds:

	(MIC) against *M. tuberculosis* H37Rv(µg/ml)	IC_{50} (µg/ml) in MTT with L929 cell line		SI (IC_{50}/MIC)	
		5 days	1 day	5 days	1 day
LX076	0.32	0.6	6.8	1.88	21.3
LX077	0.15	2	9.8	13.3	65.3
LX078	0.07	0.07	7.2	1	103
LX079	0.18	2.2	5.5	12.2	30.6
LX080	0.19	0.1	1.29	0.53	6.8

4.3.1.2.2 Effect on cell morphology:

Ptk2 cell lines were treated with 5µg/ml of different compounds then the immunoflorecent staining for the ER was carried out. The effect of the different compounds is shown in (Fig. 35). Cells that were treated with LX079 showed normal appearance. LX076 and LX077 produced the appearance of the ER stress. At the same concentration, the other two compounds induced death of the most of cells.

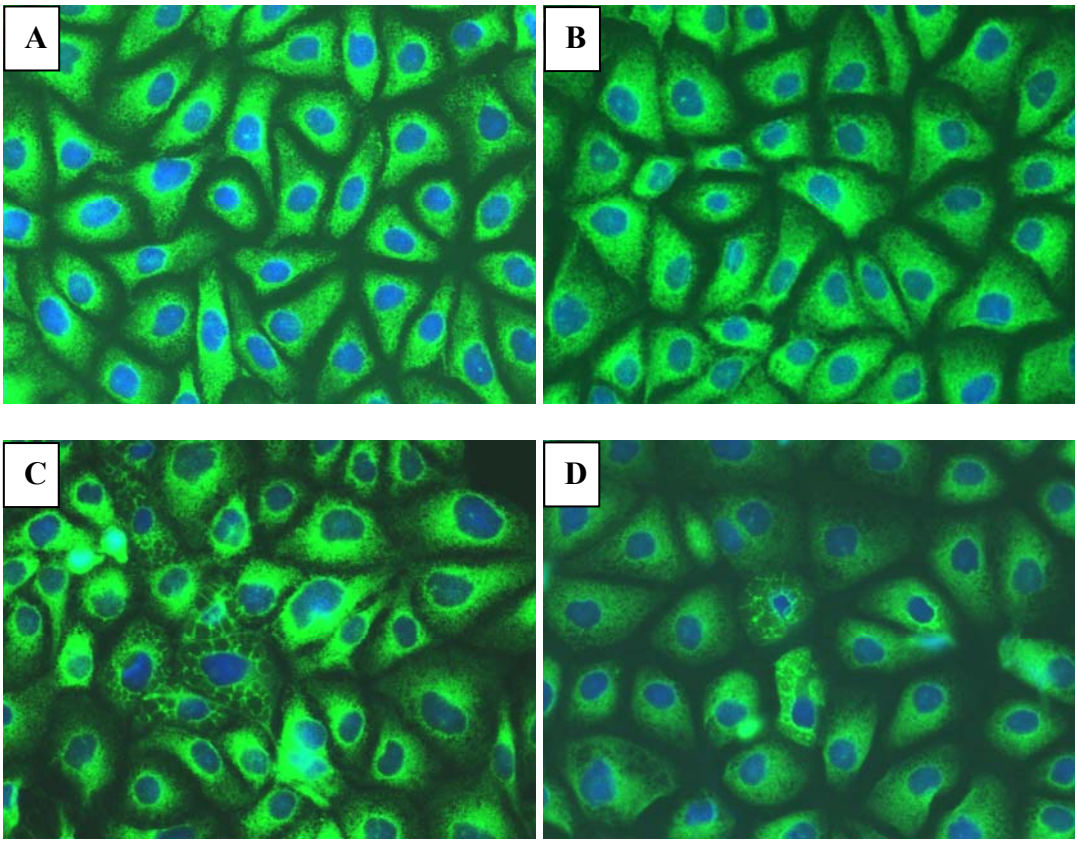

Fig (35): Immunoflorescent staining of endoplasmic reticulum: A: Control of untreated cells, **B**: LX079, **C**: LX077, **D**: LX076. PtK2 cells were incubated with 5 µg/ml of different compounds for 18 hours. In comparison with control cells, Treated cells show normal appearance after treatment with LX079, while after treatment with LX077 and LX076 cells are showing the appearance of ER stress. At the same concentration the other 2 compounds, the most of cells were died (no picture).

Thus, based on the results of *in vitro* studies, compound LX079 had the most favorable safety profile. And it was advanced into *in vivo* experiments.

4.3.2 Acute oral toxicity:

The acute oral toxicity of LX079 was evaluated in C57/BL6 mice after single oral dose. The animals were observed for 14 days after dosing. The characteristic observed signs and the survival of animals are summarized in table (17).

Table (17): Characteristic signs and survival of C57/BL6 mice at different doses of LX079.

Dose (mg/kg)	Time post dosing	Characteristic signs
62.5	30 - 240 min	Normal appearance and behavior as healthy mice
	240 min	Appearance of slight tremors
	240 min-24 hr.	Apparent recovery
	Following 14 days	Normal appearance and behavior as healthy mice
125	30 - 240 min	Three mice showed respiratory distress, tremors, lethargy and sleep. While the other 2 mice showed normal appearance and behavior.
	240 min	One of healthy mice started to show bad skin conditions
	240 min - 24 hr.	2 mice with tremors and respiratory distress start to convulse, and they were sacrificed to avoid more suffering. The others start to recover
	Following 14 days	The remaining surviving 3 mice showed normal appearance and behavior as healthy mice.
250	30 - 180 min	3 mice showed respiratory distress, tremors and sleep.
	180 - 240 min	The other 2 animals started to show tremors and sleep
	240 min	One mouse showed convulsion and it was humanely killed to avoid more suffering.
	240 min -24 hr.	Recovery of the remaining 4 animals
	Following 14 days	The remaining surviving 4 mice showed normal appearance and behavior as healthy mice.

In the acute oral toxicity studies, 100 % survival was recorded in the animals that received 62.5 mg/kg, However, the mice showed slight tremors after 4 hours of the treatment which recovered during the first 24 hours . The percentages of cumulative deaths between the animals received 125 and 250 mg/kg were 22 and 42.85 % respectively (table-18). The animals that received 125 and 250 mg/kg presented with respiratory distress and neurological

signs like tremors and sleep. These toxic manifestations recovered slowly during the first 24 hours and then the surviving animals exhibited normal appearance and behavior like the control groups. While the 3 animals that were decided to be humanely killed started to convulse. There was no significant change in the body weight between the treated and the control groups; however the animals that received 125 mg/kg showed weight loss after the first week which was increased again normally by the end of the experiment (table-19). Macroscopic examinations did not show any changes in the appearance of the organs of the treated animals compared with the control group.

Table (18): The acute oral toxicity of LX079 in C57/BL6 mice.

Group	No. of Mice	Dose (mg/kg)	No. of dead mice	% Cumulative of dead mice*	Macroscopic examination (liver, lungs, kidneys, spleen)
1	5	control	0	0	Normal
2	5	62.5	0	0	Normal
3	5	125	2	22	Normal
4	5	250	1	42.85	Normal

* using Reed–Muench method.

Table (19): Effect of administering different doses of LX079 on body weight of C57/BL6 mice over a period of two weeks.

Dose (mg/kg)	Day 0	Day 7	Day 14
Control	19.42 ± 0.53	19.62 ± 0.33	19.9 ± 0.7
62,5	19.62 ± 0.68	20 ± 0.8	20.3± 0.37
125	19.13 ± 0.49	18.87 ± 0.74	20.2 ± 0.85
250	18.88 ± 0.15	19.15 ± 0.31	19.65 ± 0.47

The results are presented as the mean ± standard deviation.

The microscopic examination of the organs illustrated in (Fig. 36) revealed no differences between the control and test groups. All the organs from the treated mice did not show any change in cell structure or any abnormal effects when visualized under the light microscope. The appearance and the coordination of cells in organs from treated groups are more or less similar with the control group.

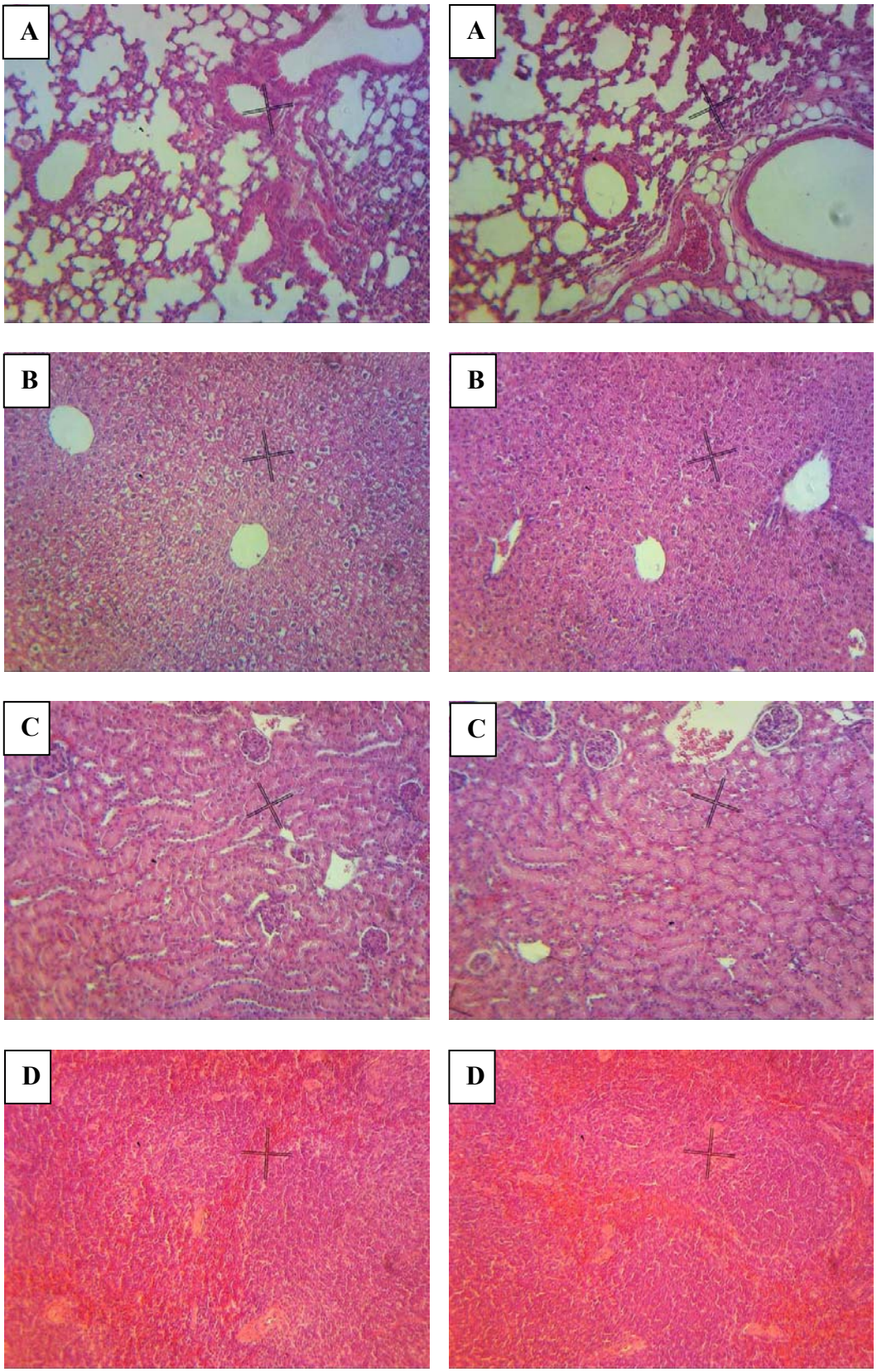

Fig. (36): Histological examination of the isolated mice organs in the acute oral toxicity experiments: left: the control group, right: the group dosed with 250 mg/kg. **A**: lung, **B**: liver, **C**: kidney, **D**: spleen. The histological features in organs from treated groups are more or less similar with the control group.

4.3.3 *In vivo* pharmacokinetics:

The *in vivo* pharmacokinetics (PK) of LX079 was evaluated in C57/BL6 mice after oral and IV administration. The plasma concentration-time profile after 12.5 mg/kg single IV dosing is shown in (Fig. 37) and the related PK parameters are listed in (table-20). The plasma concentration-time profiles of LX079 after 12.5 and 25 mg/kg single oral administration are shown in (Fig. 39). (Table -21) shows the oral bioavailability with each dose.

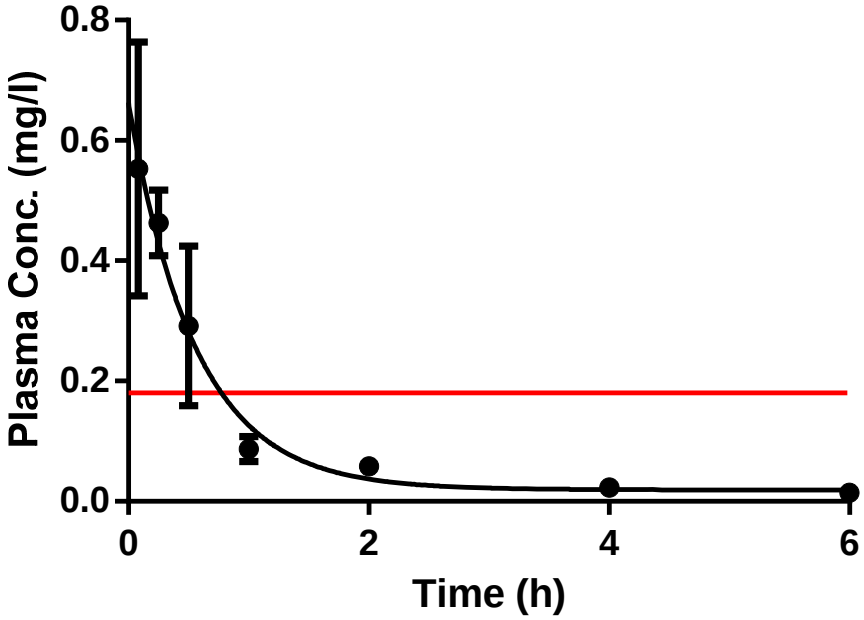

Fig. (37): Mean plasma concentration–time profile of LX079 in mice plasma following intravenous administration at 12.5 mg/kg. The red line represents the *in vitro* MIC of LX079 against *M. tuberculosis* H37Rv.

Table (20)Pharmacokinetic parameters of LX079 in mice plasma following intravenous administration at 12.5 mg/kg.

C_0 (µg/ml)	0.66 ± 0.07
AUC (h.µg.ml^{-1})	0.53 ± 0.03
$t_{1/2}$ (h)	0.43 ± 0.27
K	1.79 ± 0.44
CL (l . h^{-1} . kg^{-1})	23.64 ± 1.22

Values are represented as mean ± SD. n = 3 at each time point. AUC: Area under the 24 hour plasma concentration-time curve. $t_{1/2}$: Half-life. K: Elimination rate constant. CL: clearance.

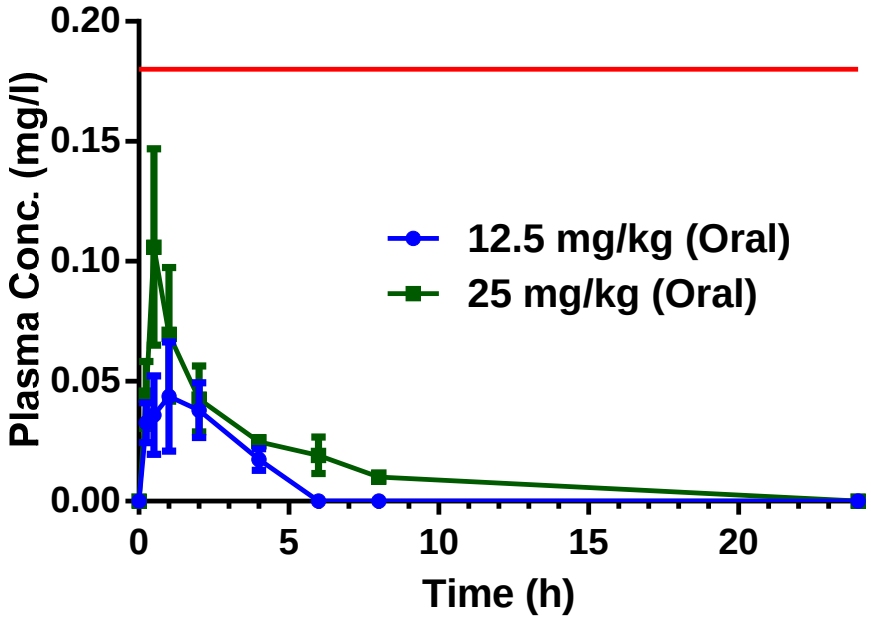

Fig. (38): Mean plasma concentration–time profiles of LX079 in mice plasma following oral administration at 12.5 and 25 mg/kg. The red line represents the *in vitro* MIC of LX079 against *M. tuberculosis* H37Rv.

Table (21): Pharmacokinetic parameters of LX079 in mice plasma following oral administration at 12.5 and 25 mg/kg.

Dose (mg/kg)	AUC (h.µg.ml^{-1})	*F* (%)
12.5	0.15 ± 0.02	27.58 ± 2.46
25	0.35 ± 0.07	32.66 ± 7.72

Values are represented as mean ± SD. n = 3 at each time point. AUC: Area under the 24 hour plasma concentration-time curve. *F*: Bioavailability.

After IV administration of LX079 intravenously, it exhibited $t_{1/2}$ of 0.43 ± 0.27 and the peak plasma concentration was 0.66 ± 0.07. The time in which the plasma concentration was exceeding the *in vitro* MIC (T > MIC) was less than 1 hour. After oral administration at 12.5 and 25 mg/kg the oral bioavailability was estimated 27.58 ± 2.46 and 32.66 ± 7.72 respectively and the plasma levels did not reach the level of the *in vitro* MIC.

4.3.4 *In vitro* pharmacokinetic studies:

The stability of the compound with hepatic microsomes was investigated. *In vitro* incubation of LX079 with pooled mice hepatic microsomes resulted in *in vitro* $t_{1/2}$ of 5.94 ± 2.36 (Fig. 40). The *in vitro* clearance ($CL_{int,\ inc}$) was calculated with the consideration of the

binding to microsomes. The hepatic intrinsic clearance (CL_{int}) was estimated by scaling up the *in vitro* $t_{1/2}$ (Table-22).

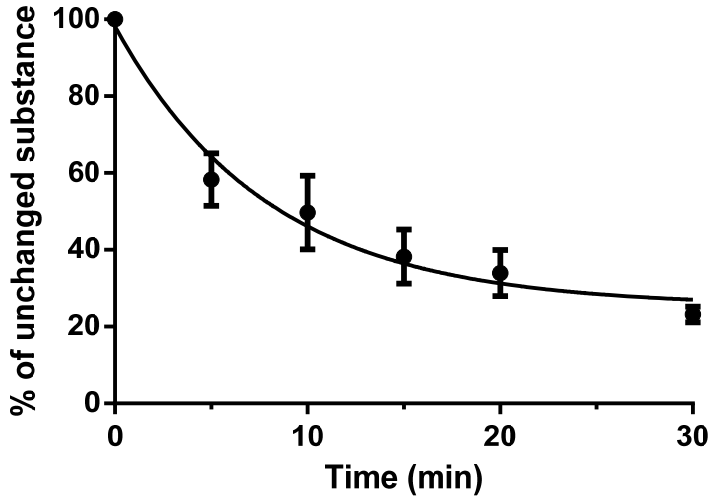

Fig. (40): *In vitro* metabolism by mouse liver microsomes of LX079: The substance was incubated with pooled mice hepatic microsomes in the presence of NADPH as a cofactor. The reaction was quenched at different time points. The percent of the parent substance was calculated in comparison to the concentration of the substance at time point 0.

Table (22): Metabolic stability parameters of LX079 in mice microsomes.

$t_{1/2}$ (min)	5.937 ± 2.36
$CL_{int,\ inc}$ (ml/min/mg protein)	2.82 ± 1.12
CL_{int} (ml/min/SMW)	221.81 ± 88.23
Stability (%)	23.14 ± 2.01

SMW: Standard mouse weight.

The extent of binding to plasma proteins was not calculated. As after quantification of the parent substance in both sides after 4 hours of dialysis, it was much lower than the starting concentration. This finding may account to instability in mice plasma.

5. Discussion:

As was introduced, this work is an approach to characterize potential drug candidates against *mycobacterium tuberculosis* (*M.tb*) in order to provide scientific database about the efficacy/safety profile for further drug development steps.

The drug research pathway is a very complicated multidisciplinary process. The success for one drug molecule to reach the patient approximately needs 12-15 years and costs US$ 400–650 million (*Panchagnula & Thomas, 2000*). The spread of resistance to anti-TB drugs represents a big challenge in front of physicians and pharmacologists. The main aim of new anti-TB drug discovery process is to find compounds that exhibit higher efficacy, could be administrated less frequent, have the ability to shorten the period of treatment and showing less drug related toxicity and drug interactions (*Sarkar & Suresh, 2011*).

5.1 Pyrazinamide:

5.1.1 *PncA* mutations and clinical pyrazinamide resistance:

Pyrazinamide (PZA), one of the first line anti-TB drugs, played a key role in shortening the duration of therapy from 12 to 6 month due to its ability to kill persisting bacilli in the acidic environment. The mycobacterial pyrazinamidase (PZase) encoded by *PncA* is involved in the activation of the prodrug PZA into its active form pyrazinoic acid POA; however the mechanism by which POA kills the mycobacterium is still not completely understood whether it is due to general acidification of the cytoplasm or via targeting specific cellular target. Numerous mutations in *PncA* gene were identified and thought to be the main cause for mycobacterial PZA-resistance (*Scorpio & Zhang, 1996*) (*Zhang et al., 2008*) (*Barco et al., 2006*) (*Portugal et al., 2004*). These mutations are located along the whole gene as well as in the upstreamed putative regulatory region with new mutations are continuously reported in new studies. The cause of this marked diversity of mutations is not clear; however it is believed that *PncA* gene is located in a hotspot for mutation in the mycobacterial genome (*Scorpio & Zhang, 1996*).

In order to assess the molecular mechanism of mycobacterial PZA-resistance, *PncA* enzymes from the native type *M. tuberculosis* H37Rv and from 5 PZA-resistant clinical strains were expressed, purified and their activity were characterized using the cell free PZase assay. The Wayne's method that was modified by (*Bhuju, 2009*) was optimized and used for

screening of the activity of different enzymes as well as to screen different analogues as prodrugs in comparison to PZA. The kinetics of the native type *PncA* with PZA was evaluated with calculated K_m 1.271 mM indicating the low specificity of PZA as a substrate for *PncA*. This can explain why the PZA is more active against non-replicating or old dormant bacilli inside macrophage. In these populations of bacilli the passive uptake of HPOA is not affected while the active efflux of POA^- is down regulated, which leads to trapping of the POA inside the bacteria regardless the slow rate of its production. This low specificity also can elucidate the lack of PZA to early bactericidal activity which was described in some previous studies (*Gumbo et al., 2009*).

In between the 5 mutants that were studied, only one mutant (mut-4 *Lys96Arg*) was found to be completely inactive. (*Zhang et al., 2008*) in their study of mutants generated by site directed mutagenesis showed that Asp8, Lys96 and Cys138 are key residues in the catalysis of PZA. In our study, in between the 5 clinical PZA-resistant mutants, the only mutant that showed complete loss of PZase activity had substitution at Lys96 amino acid which is going with the results of Zhang and his colleagues.

On the other hand, 3 mutants (mut-1 *Leu172Pro*), (mut-2 *Asp63Gly*) and (mut-3 *Leu159Val*) were still retaining different extent of activity with turnover number K_{cat} 7.2 , 16.3, 18,17 respectively in comparison to 45.05 for the wild type. Partial activity of the enzyme slows the rate by which the PZA liberate the bactericidal form POA. The rate of conversion would consequently have an important role in determining the PZA susceptibility. As well as, we revealed one mutant (mut-5 *Leu117Pro*) with higher PZase activity than the native type with K_{cat} 725.1 which means 15 times higher than the wild type. The presence of clinical mycobacterial PZA-resistant strains that retain PZase activity in spite of mutations in *PncA* gene has been reported before (*Mestdagh et al., 1999*) (*Lemaitre et al., 2001*). Other mechanisms of PZA resistance related to high active efflux for POA and lack of uptake for PZA were studied in naturally PZA-resistant, PZase positive strains as *M.smegmatis* and *M.avium* (*Sun & Zhang, 1999*) (*Sun et al., 1997*) (*Zhang et al., 1999*) (*Raynaud et al., 1999*). Such mechanisms might explain the PZA resistance observed with mut-5 which showed much higher PZase activity than the native type. In the future using such strains for whole genome sequencing, evaluation of the effect of efflux inhibitors as reserpin on retaining the sensitivity to PZA and measuring the POA intracellular should be valuable in determining the exact cause of resistance and might help to define new drug target of PZA

5.1.2 Evaluation of pyrazinoic acid amides as prodrugs using the cell free pyrazinamidase assay:

In parallel three pyrazinamides were synthesized -hexadecylpyrazinamide, tetradecylpyrazinamide and dodecylpyrazinamide- to be evaluated as prodrugs in the PZase assay. In this study the cell free PZase assay was used as a tool to evaluate the ability of different pyrazinamides to liberate POA. The three amides could not be easily activated to release POA at an appropriate rate. (*Simões et al., 2009*) by using HPLC showed the very low activation of these 3 amide by *M. smegmatis* homogenate.

5.1.3 POA esters as an alternative for pyrazinamide:

The mechanism of resistance to PZA is still a mystery to science despite of the continuous research in this field. PZA has a crucial role in achieving sterilization due to its high activity against slowly growing bacilli inside macrophage and semidormant population within the solid caseous lesions. The susceptibility of PZA-resistant strains to POA encouraged the field of molecular modification certainly the prodrug approach to find alternatives for PZA (*Dutra et al., 2012*). Lipophilic POA esters as an alternative antimycobacterial agent might have two specific advantages: 1. they would be easy to penetrate the lipophilic cell wall of mycobacterium, and 2. they can skirt the mutation in *PncA* through their activation with non-specific estrases instead of PZase. The main hindrance facing such compounds is their instability in Serum. (*Simões et al., 2009*) showed that the stability in serum can be improved with compounds which have longer side chain. From this point, we synthesized the three esters mentioned by (*Simões et al., 2009*) in order to evaluate their efficacy and safety profiles as potential drug candidates. The rationale for using *M. bovis* BCG stems from the fact that *M. bovis* BCG is a naturally PZA-resistant strain, to evaluate the effectiveness of these compounds against PZA-resistant *mycobacterium* in comparison to PZA and POA.

Hexadecylpyrazinoate, tetradecylpyrazinoate and dodecylpyrazinoate were found to have minimal inhibitory concentration (MIC) against both *M. bovis* BCG and *M. tuberculosis* H37Rv 5-10 times lower than the POA, the active counterpart of PZA. In the present study and on contrary to the results of (*Simões et al., 2009*), the three esters inhibited the mammalian cell proliferation when tested with different cell lines indicating relatively poor selectivity. Furthermore, treating Ptk2 cell line with the three esters at concentration 20 µg/ml revealed induction of the endoplasmic reticulum (ER) stress. The present study showed that

substances with higher lipophilicity had the higher cytotoxicity. The order of the IC_{50} concentrations for the three esters was the reverse order of the lipophilicity. The comparative IC_{50} values were dodecylpyrazinoate > tetradecylpyrazinoate > hexadecylpyrazinoate. In addition the three compounds showed more cellular toxicity when they were evaluated with HUVEC cells as a primary cell line.

In the double-staining assay by flow cytometry, the percentage of annexin- and PI-positive late apoptotic cells was markedly increased upon cell treatment with the three esters at a concentration of 35µg/ml for 12 hours. However there is no comparative increase of the annexin-positive and PI negative early apoptotic cells over the control untreated cells. Cells that stain positive for FITC Annexin V and negative for PI are going through apoptosis. While cells that stain positive for both FITC Annexin V and PI are either in the end stage of apoptosis, or are undergoing necrosis. So the increase of the anexin- and PI-positive cells alone reveals less information about the process by which the cells die.

Hepatotoxicity is one of the main side effects of PZA. The exact mechanism by which PZA induces the hepatic injury is still unclear. However, recent studies revealed the strong correlation between hepatic toxicity induced by anti-tuberculous treatment and oxidative stress in experimental animals (*Thattakudian Sheik Uduman et al., 2011*) (*Tostmann et al., 2008*). In addition, oxidative stress is implicated in a diversity of drug induced toxicities. ER stress and induction of intracellular reactive oxygen species (ROS) are also strongly correlated events. ROS liberate during normal oxygen-using cellular metabolic processes and have roles in cell signaling and homeostasis. The ER is considered as a unique oxidizing environment for protein folding and disulfide bond formation. But excessive ROS accumulation can happen as a consequence of different stressors as the exposure to toxicants with subsequent local oxidative stress and stimulation of adaptive responses. In another way accumulation of misfolded proteins in the lumen of the ER induces ROS production that function as a second messenger activating the unfolded protein response (UPR) and apoptosis in case of sustained stress and unresolved misfolded proteins (*Malhotra et al., 2008*) (*Deavall et al., 2012*). Our results revealed the ability of the three POA esters to produce ER stress. So we evaluated the ability of these compounds to induce intracellular ROS using the DCF assay. In our results, the three POA esters had no role in the induction of intracellular ROS.

The results of the present study demonstrate that POA esters with high lipophilicity were more toxic. The degree of reduction of cell viability was correlated with the lipophilicity which was presented as octanol/water partition coefficient (*logp*). We cannot deny that the molecular modification strategy is a promising tool in the drug discovery pathway. We can obviously recognize this from the current anti tuberculosis discovery pipeline in which the molecular modification had played an important role (*Dutra et al., 2012*). However, the physiochemical properties of the resulting compounds needs to be considered as the change of the physiochemical properties of the compound will lead to change of the efficacy/toxicity profile that can lead to rapid attrition from the discovery pathway. Lipophilicity is an important property which enhances the affinity of the compound to bind with its lipophilic binding site. On the other hand enhanced lipophilicity will increase the non specific binding in the lipophilic environments as in the cell membrane with subsequent lack of selectivity and increased nonspecific toxicity (*wang et al., 2003*) (*Leeson & Springthorpe, 2007*).

5.2 RNA polymerase inhibitors:

Bacterial DNA-dependent RNA polymerase (RNAP) is an attractive drug target. The inactivation of this crucial enzyme would lead to cell death. In addition, bacterial RNAP does not share extensive sequence homology with eukaryotic RNAP (*Bai et al., 2011*). Generally, RNAP assay as a target based screening tool has the advantage of speeding the role of medicinal chemistry to modify the compounds in a way that continue to hit the desired target (*Nuermberger et al., 2010*). The RNAP assay that was developed by (*Bhuju, 2009*) has many advantages over the previously used RNAP assays. In this study, we used this assay with few modifications. Increasing the concentration of adenosine 5′ phosphosulfate (APS) and the time of the reaction catalyzed by the ATP sulfurylase enzyme and using the half area plates improved the reproducibility of the assay. Furthermore, the assay was used to predict the inhibitory effect of different combinations that contain RNAP inhibitors (RNAPIs). The results showed the inhibitory effect of different combinations on the RNAP in a dose related manner. The OCI substances are intermediates in the synthesis of corallopyronin. They were evaluated in the RNAP assay but they did not show any inhibitory effect.

The absence of cross resistance between rifampicin (RIF) and the RNAPIs myxopyronin, corallopyronin and ripostatin make them very attractive molecules for the researchers in the field of new anti-TB drug discovery. We evaluated the *in vitro* antimycobacterial activity of the three compounds. The results revealed MIC of myxopyronin

and corallopyronin 6.25 and 12.5 μg/ml respectively, while ripostatin did not inhibit the bacterial growth up to concentration of 25 μg/ml. with the evaluation of the *in vitro* toxicity profile, corallopyronin showed low selectivity with selectivity index (SI) of 2. In addition, corallopyronin seems to be upon long storage transforms into highly toxic compound which affects the mammalian cell division through its toxic effect on the cellular microtubules leading to large multinucleated cells.

With our results and with the results of (*Mariner et al., 2011*) who showed the easy development of corallopyronin resistance, we concluded that corallopyronin is not a promising antimycobacterial drug candidate.

On the other hand, myxopyronin showed higher safety margin with SI greater than 16. Furthermore, myxopyronin showed synergistic effect with the commercially available antimycobacterial agent, ethambutol with FIC of 0.64. The rationale to investigate the synergism between the three RNAPIs and ethambutol comes from the fact that the susceptibility of *M. tb* to antibiotics is usually increased by the cell wall inhibitors. In our results, corallopyronin and ripostatin did not show synergism with ethambutol.

Additionally, the all combinations between myxopyronin and ethambutol showed high antibacterial activity against *M. bovis* BCG with wide safety margin with no detectable effect on the cellular structures with immunocytochemistry (ICC) staining even with concentrations much higher than their MIC.

Furthermore, by testing the *in vitro* MIC with the presence of 50 % fetal bovine serum (FBS), we found that myxopyronin lost its anti-TB activity even with concentrations 4 times higher than its MIC in 100 % medium indicating high binding to proteins. At the same time the combination between myxopyronin and ethambutol retained its low MIC with the presence of 50 % FBS. Depending on these results, the combination between myxopyronin and ethambutol is likely to be promising. Ethambutol is a cell wall inhibitor and its *in vitro* MIC was not affected by the addition of the FBS. This is matching with the results of (*Lee et al., 1977*) who showed that the extent of ethambutol binding to plasma proteins ranges between 20 and 30 %. Ethambutol through its action on the cell wall of the microbe may facilitate the entrance of the myxopyronin to inhibit the RNAP even with low concentration of the free fraction.

Myxopyronin was discovered more than 30 years ago. It was considered very attractive RNAPI due to the absence of cross-resistance between RIF and myxopyronin. The physiochemical properties of myxopyronin and its high binding to plasma proteins were restrictive factors to enter the subsequent stages of the discovery pathway. The extent of binding to plasma proteins can affect the antimicrobial activity of an antibiotic through different aspects. The bound antibiotic is in a temporary inactive state that cannot hit the microbe. Additionally, high binding to plasma proteins usually limits the distribution of the antibiotic. The percentage of binding determines the rate by which the antibiotic diffuses to the extravascular compartment. And for highly bound drugs, the half life ($t_{1/2}$) will determine if the drug can reach a satisfactory level in tissues or not (*Rolinson, 1980*). In the future, studying the pharmacokinetic (PK) profiles of myxopyronin *in vivo* and *in vitro*, evaluating the PK/PD parameters of myxopyronin together with ethambutol in different combinations, and the extent of their binding to proteins can help to select a suitable dose regimen to be further tested in infection animal models.

5.3 Random library of compounds:

5.3.1 *In vitro* screening:

In comparison to target-based screening approaches to discover new anti-TB agents, the whole cell based screening approaches showed more promising outcomes. All anti-TB drug candidates that are currently in clinical trials were first discovered by their antibacterial activity in whole-cell based screens. In the whole cell-based screening, the resazurin microtiter assay (REMA) was applied where ≈480 compounds were tested against *M.tb.* Based on this screening, 5 molecules inhibited the growth with micromolar concentrations were selected to evaluate their toxicity profile. Hits should be evaluated in terms of its cytotoxicity on mammalian cells before taking them ahead into the subsequent stages of the discovery chain. Here, cytotoxicity of the 5 hits was estimated against L929 cell line by using standard cell proliferation assay. It was observed that there was no significant effect on proliferation of L929 cell line at a concentration 10 times higher than MIC levels of 2 hits. After ICC staining, the LX079 was the only hit that showed no morphological changes of the treated cells at a concentration 25 times higher than the MIC. This data indicated that LX079 could be selected for further drug development.

In antimicrobial *in vitro* models, the activity of compounds is usually expressed by numeric values (IC_{50}, IC_{90}, MIC, etc.). The optimal value for whole-cell screening is 1 µg/ml.

Generally, MIC less than 2 µg/mL with a SI more than10 is assumed to be interesting for further development (*Sánchez & Kouznetsov, 2010*).

5.3.2 Acute oral toxicity:

To enable further studies, the acute toxicity of the new compound was evaluated in mice. Acute toxicity studies in animals are usually essential to give preliminary indications on the range of doses that could be toxic to the animal. Acute toxicity is the toxicity developed by a compound when it is administered in one or more doses through a period not more than 24 hours. And according to the OECD guidelines for testing toxicity of chemicals (*425-OECD guideline for testing of chemicals*), animals should be followed for 14 days after dosing to reveal any delayed toxicity. This kind of experiments should be designed to obtain the highest amount of information from the lowest number of animals. Using large number of animals to calculate lethality parameters is not recommended any more (*Federal Register of October 11, 1988, 53 FR 39650*). The information obtained from these studies together with the PK characteristics of a new compound is valuable in choosing doses for repeat-dose studies. Acute toxicity studies can provide clues about the possible target organs of toxicity and might help in selecting starting doses for phase 1 human studies. Furthermore, acute oral toxicity studies can provide relevant information about the acute overdosing in humans.

By calculating the cumulative percentage of death between the mice, the LD_{50} was estimated to be more than 250 mg/kg. However; animals that were dosed with 62.5 mg/kg manifested with slight tremors and with higher doses animals showed respiratory distress with neurological manifestations as tremors, lethargy and sleep. All manifestations in the surviving animals disappeared during the first 24 hours and no delayed toxic signs were predicted during the whole period of the experiment. As well as no significant histopathological or body weight changes were detected in all tested groups.

5.3.3 Pharmacokinetic/Pharmacodynamic (PK/PD) evaluation:

The integration between the *in vitro* efficacy expressed in MIC and the *in vivo* pharmacokinetics (PK) is very valuable in expecting the antimicrobial outcome. In addition, it has a very important role in optimizing the dosage regimens. The results of some previous studies demonstrated that the magnitude of the PK/PD parameters needed for the antimicrobial efficacy is quite similar in both human and animal model infection (*Craig,*

1998). For this reason the PK profiles for the LX079 were evaluated in mice following oral and IV administration.

The *in vivo* PK profile as well as the *in vitro* stability with hepatic microsomal enzymes was evaluated. The LX079 exhibited unfavorable *in vivo* PK pattern with short $t_{1/2}$ of 0.43 h ± 0.27 with very rapid clearance of 23.64 l . h^{-1} . kg^{-1} ± 1.22. The time in which the plasma conc. of LX079 was higher than the *in vitro* MIC (T > MIC) was less than 1 hour after IV bolus administration of the substance at 12.5 mg/kg. Following the oral administration at 12.5 and 25 mg/kg, the oral bioavailability was 27.583 ± 2.457 and 32.662 ± 7.715 respectively and the whole concentration-time curves were below the level of the *in vitro* MIC.

These findings are correlated with the low stability (23.14 % ± 2.01) of the compound when incubated with mice hepatic microsomal enzymes. LX079 exhibited very short *in vitro* $t_{1/2}$ of 5.94 ± 2.36 min with very high hepatic intrinsic clearance of 221.81± 88.23 (ml . min^{-1}/ standard mouse weight) when scaled from the *in vitro* data. Extensive first pass effect of the liver eventually leads to poor bioavailability and short $t_{1/2}$.

We did not calculate the binding of the substance to the plasma proteins. As we found that the concentration of the substance in the both chambers after 4 hours of dialysis is much lower than the starting concentration. This finding may indicate also instability of the compound in mice plasma. This observation with the very high calculated hepatic intrinsic clearance value may account to the low initial concentrations in mice plasma following administration.

In the aim to achieve better stability using the molecular modification, 20 analogues of LX079 will be further tested for lead optimization.

6. Summary:

- Pyrazinamide (PZA) is an effective sterilizing anti-TB agent. Its mechanism of action is still controversial. *PncA* mutations are responsible for PZA-resistance in the most of resistant strains.

- In order to characterize the role of *PncA* mutations in PZA-resistance, the kinetics of the pyrazinamidase (PZase) -wild type and 5 mutants from 5 resistant strains- were evaluated using the cell free PZase assay.

- We showed low specificity of PZA as a substrate for the wild type PZase. This can explain its higher activity against old dormant or non-replicating bacilli.

- In between the studied 5 mutants, only one mutant was found to be completely inactive. Three mutants were retaining different extent of activity with slower rate of conversion of PZA into pyrazinoic acid (POA) than the wild type. This indicates that the rate of conversion is an important factor in determining the susceptibility to PZA.

- One mutant was found to have higher activity than the wild type suggesting other mechanism of PZA-resistance.

- The molecular modification strategy would play an important role in achieving new anti-TB agents. And due to the susceptibility of the most PZA-resistant strains to POA, we synthesized lipophilic POA analogues -3 amides and 3 esters- in order to evaluate their efficacy/safety profiles.

- The POA amides were evaluated as prodrugs using the cell free PZase assay. They were considered very poor prodrugs as they could not liberate POA at an appropriate rate.

- The POA esters could be considered as a logic rationale to circumvent the mutations in *PncA*. But we found that the increased lipophilicity by increasing the length of the side chain was correlated to the increased toxicity of the compound, underlying the importance to consider the physiochemical properties of the new compound. Changing

the physiochemical properties will change the efficacy/toxicity profile of the resulting compound which can lead to rapid attrition from the discovery pathway.

- Prokaryotic DNA-dependent RNA polymerase (RNAP) is an attractive target for developing new anti-TB agents. It is essential for the microbe survival and shows features that make it different from mammalian RNAP.

- In this study, we used the RNAP assay to predict the inhibitory effect of different substances and combinations on the RNAP.

- Myxopyronin, corallopyronin and ripostatin are attractive RNAP inhibitors for anti-microbial drug researchers. Their mode of action is different than that of rifampicin (RIF) representing a possible solution for widespread RIF-resistance.

- The results revealed MIC of myxopyronin and corallopyronin 6.25 and 12.5 µg/ml respectively, while ripostatin did not inhibit the bacterial growth up to concentration of 25 µg/ml.

- Corallopyronin showed low selectivity with selectivity index (SI) of 2. In addition, corallopyronin seems to be upon long storage transforms into highly toxic compound which affects the mammalian cell division through its toxic effect on the cellular microtubules leading to large multinucleated cells.

- Myxopyronin showed higher safety margin with SI greater than 16. It had no effect on the cell morphology as revealed from immunocytochemistry (ICC).

- Myxopyronin showed synergistic effect with the commercially available antimycobacterial agent, ethambutol with FIC of 0.64. The all combinations between myxopyronin and ethambutol showed high antimycobacterial activity with wide safety margin with no detectable effect on the cellular structures with ICC staining even with concentrations much higher than their MIC.

- Myxopyronin is highly bound to proteins. It has MIC against *M. bovis* BCG 6.25 µg/ml in 100 % medium. In the presence of 50% FBS, it did not inhibit the bacterial

growth up to conc. 25 µg/ml. On the other hand, the antibacterial activity of the combination ethambutol with myxopyronin was not affected by adding the FBS.

- LX079 was chosen by screening of a random library of compounds. It had SI > 10 and it showed no morphological changes of the treated cell line at a concentration 25 times higher than the MIC.

- LX079 was tested for acute oral toxicity in mice. By calculating the cumulative percentage of death, the LD_{50} was estimated to be more than 250 mg/kg.

- The pharmacokinetic (PK) profiles of LX079 in mice following IV (12.5 mg/kg) and oral (12.5 & 25 mg/kg) single dosing were evaluated. After IV administration, LX079 exhibited short $t_{1/2}$ of 0.43 h ± 0.27 with rapid clearance of 23.64 l. h^{-1}. kg^{-1} ± 1.22. Theses findings were correlated with the *in vitro* results when the compound was incubated with mice pooled hepatic microsomal enzymes. LX079 had *in vitro* $t_{1/2}$ of 5.937 min ± 2.362 with hepatic intrinsic clearance of 221.81 ml . min^{-1}/SMW ± 88.23 when scaled from the *in vitro* $t_{1/2}$.

- The oral bioavailability of LX079 following single oral dosing at 12.5 and 25 mg/kg was 27.58 ± 2.46 and 32.66 ± 7.72 respectively and the whole concentration-time curves were below the level of the *in vitro* MIC.

- LX079 needs to be recycled in the lead optimization process for achieving more stability. By using the molecular modification strategy, 20 analogues of LX079 were prepared and will be further tested for this task.

7. References:

Aaron, L., Saadoun, D., Calatroni, I., Launay, O., Mémain, N., Vincent, V., Marchal, G., et al. (2004). Tuberculosis in HIV-infected patients: a comprehensive review. The European Society of Clinical Microbiology and Infectious Diseases (CMI), 10(5), 388–398.

Agren, D., Stehr, M., Berthold, C. L., Kapoor, S., Oehlmann, W., Singh, M., Schneider, G. (2008).Three-dimensional structures of apo- and holo-L-alanine dehydrogenase from Mycobacterium tuberculosis reveal conformational changes upon coenzyme binding. J Mol Biol, 377(4),1161-1173.

Allen, W. S., Aronovic, S.M., Brancone, L. M., Willians, J. H. (1953). Determination of the Pyrazinamide Content of Blood and Urine. Analytical Chemistry 25(6), 895 - 897.

Allix-Be´guec, C., Fauville-Dufaux, M., Stoffels, K., Ommeslag, D., Walravens, K., Saegerman, C., Supply, P. (2010). Importance of identifying Mycobacterium bovis as acausative agent of human tuberculosis. European Respiratory Journal, 35(3), 692-694.

American Thoracic Society (CDC) and Infectious Diseases Society of America. (2003). Treatment of Tuberculosis. 52(RR11), 1-77.

Andrews, J. R., Gandhi, N. R., Moodley, P., Shah, N. S., Bohlken, L., Moll, A. P., Pillay, M., et al. (2008). Exogenous reinfection as a cause of multidrug-resistant and extensively drug-resistant tuberculosis in rural South Africa. The Journal of Infectious Diseases, 198(11), 1582–1589.

Andries, K., Gevers, T., Lounis, N. (2010). Bactericidal potencies of new regimens are not predictive of their sterilizing potencies in a murine model of tuberculosis. Antimicrobial Agents and Chemotherapy, 54(11), 4540–4544.

Aristoff, P. A., Garcia, G. A., Kirchhoff, P. D., Hollis Showalter, H. D. (2010). Rifamycins – obstacles and opportunities. Tuberculosis (Edinburgh, Scotland), 90(2), 94–118.

Artsimovitch, I., Vassylyev, D. G. (2006). Is it easy to stop RNA polymerase?. Cell Cycle, 5(4), 399–404.

Bai, H., Zhou, Y., Hou, Z., Xue, X., Meng, J., Luo, X. (2011) Targeting bacterial RNA polymerase: promises for future antisense antibiotics development. Infectious Disorders Drug Targets,11(2), 175-87.

Balganesh, T. S., Balasubramanian, V., Kumar, S. A. (2004). Drug discovery for tuberculosis: Bottlenecks and path forward. Current Science, 86(1), 167-176.

Barco, P., Cardoso, R. F., Hirata, R. D. C., Leite, C. Q. F., Pandolfi, J. R., Sato, D. N., Shikama, M. L., et al. (2006). pncA mutations in pyrazinamide-resistant Mycobacterium tuberculosis clinical isolates from the southeast region of Brazil. The Journal of Antimicrobial Chemotherapy, 58(5), 930–935.

BD Bioscience data sheets: www.bdbioscience.com

Beer, J., Wagner, C. C., Zeitlinger, M. (2009). Protein binding of antimicrobials: methods for quantification and for investigation of its impact on bacterial killing. The AAPS Journal, 11(1), 1–12.

Bertrand-Burggraf, E., Lefevre, J. F., and Daune, M.(1984). A new experimental approach for studying the association between RNA polymerase and the tet promoter of pBR322. Nucleic Acids Research, 12(3), 1697-1706.

Bhat, J., Rane, R., Solapure, S. M., Sarkar, D., Sharma, U., Harish, M. N., Lamb, S., et al. (2006). High-throughput screening of RNA polymerase inhibitors using a fluorescent UTP Analog. Journal of Biomolecular Screening, 11(8), 968-976.

Bhuju, S. (2009). Development of novel drug screening assays and molecular characterization of rifampicin and pyrazinamide resistance in Mycobacterium tuberculosis. Braunschweig University, Ph.D.

Bradford, M. M. (1976). A rapid and sensitive method for the quantitation of microgram quantities of protein utilizing the principle of protein-dye binding. Analytical Biochemistry, 72, 248–254.

Brennan, P. J., Nikaido, H. (1995). The envelope of mycobacteria. Annual Review of Biochemistry, 64, 29–63.

Bujnowski, K., Synoradzki, L., Dinjus, E., Zevaco, T., Augustynowicz-Kopeć, E., Zwolska, Z. (2003). Rifamycin antibiotics—new compounds and synthetic methods. Part 1: Study of the reaction of 3-formylrifamycin SV with primary alkylamines or ammonia. Tetrahedron, 59(11), 1885–1893.

Campbell, E. A., Korzheva, N., Mustaev, A., Murakami, K., Nair, S., Goldfarb, A., Darst, S. A. (2001). Structural mechanism for rifampicin inhibition of bacterial RNA polymerase. Cell, 104(6), 901–912.

Changsen, C., Franzblau, S. G., Palittapongarnpim, P. (2003). Improved green fluorescent protein reporter gene-based microplate screening for antituberculosis compounds by utilizing an acetamidase promoter. Antimicrobial Agents and Chemotherapy, 47(12), 3682–3687.

Chao, M. C., Rubin, E. J. (2010). Letting sleeping dos lie: does dormancy play a role in tuberculosis?. Annual Review of Microbiology, 64, 293–311.

Cheng, S., Thibert, L., Sanchez, T., , Heifets, L. (2000). pncA mutations as a major mechanism of pyrazinamide resistance in mycobacterium tuberculosis: spread of a monoresistant strain in Quebec , Canada. Antimicrobial Agents and Chemotherapy, 44(3), 528–532.

Chopra, I. (2007). Bacterial RNA polymerase: a promising target for the discovery of new antimicrobial agents. Curr Opin Investig Drugs, 8(8), 600-607.

Chopra, I., Hesse, L., O'Neill, A. J. (2002). Exploiting current understanding of antibiotic action for discovery of new drugs. Journal of Applied Microbiology Symposium Supplement, (92), 4S–15S.

Clark-Curtiss, J. E., Haydel, S. E. (2003). Molecular genetics of Mycobacterium tuberculosis pathogenesis. Annual Review of Microbiology, 57, 517–549.

Collins, L., Franzblau, S. G. (1997). Microplate alamar blue assay versus BACTEC 460 system for high-throughput screening of compounds against Mycobacterium tuberculosis and Mycobacterium avium. Antimicrobial Agents and Chemotherapy, 41(5), 1004–1009.

Corbett, E. L., Watt, C. J., Walker, N., Maher, D., Williams, B. G., Raviglione, M. C., Dye, C. (2003). The growing burden of tuberculosis. Arch Intern Med, 163, 1009–1021.

Cordice, J. W. V., Hill, L. M., Wright, L. T. (1953). Use of pyrazinamide (Aldinamide) in the treatment of tuberculous lymphadenopathy and draining sinuses. Journal of the National Medical Association, 45(2), 87-98.

Craig, W. A. (1998). Pharmacokinetic/Pharmacodynamic Parameters: Rationale for antibacterial dosing of mice and men. Clinical Infectious Diseases, 26(1), 1–10.

Cynamon, M. H., Klemens, S. P., Chou, T. S., Gimi, R. H., Welch, J. T. (1992). Antimycobacterial activity of a series of pyrazinoic acid esters. Journal of Medicinal Chemistry, 35(7), 1212–1215.

Daele, I., Calenbergh, S. (2005). Patent developments in antimycobacterial small-molecule therapeutics. Expert Opin. Ther. Patents, 15(2), 131-140.

Daniel,V., Grimberg, J., Zeevi, M. (1975). In vito synthesis of tRNA precursors and their conversion to matur size tRNA. Nature, 257, 193–197.

Davies, B. and Morris, T. (1993). Physiological parameters in laboratory animals and humans. Pharmaceutical Research, 10(7), 1093-1095.

Davies, G.R., Cerri, S., Richeldi, L. (2007). Rifabutin for treating pulmonary tuberculosis, Cochrane Database of Systematic Reviews 2007, Issue 4.

Deavall, D. G., Martin, E. A., Horner, J. M., Roberts, R. (2012). Drug-induced oxidative stress and toxicity. Journal of Toxicology, 2012(2012), ID 645460.

Debouck, C., Goodfellow, P. N. (1999). DNA microarrays in drug discovery and development. Nature genetics, 21(1 suppl), 48–50.

Derendorf, H., Chaikin, P., Lee, P., Miller, R., Powell, R., Rhodes, G., Stanski, D., et al. (2000). Pharmacokinetic/Pharmacodynamic modeling in drug research and development. The Journal of Clinical Pharmacology, 40(12), 1399-1418.

Dhar, N., McKinney, J. D. (2010). Mycobacterium tuberculosis persistence mutants identified by screening in isoniazid-treated mice. Proceedings of the National Academy of Sciences of the United States of America, 107(27), 12275–12280.

Di, L., Kerns, E. H., Hong, Y., Kleintop, T. a, McConnell, O. J., Huryn, D. M. (2003). Optimization of a higher throughput microsomal stability screening assay for profiling drug discovery candidates. Journal of Biomolecular Screening, 8(4), 453–462.

Dickinson, J. M., Mitchison, D. a. (1970). Suitability of rifampicin for intermittent administration in the treatment of tuberculosis. Tubercle, 51(1), 82–94.

Dorman, S. E., Chaisson, R. E. (2007). From magic bullets back to the magic mountain: the rise of extensively drug-resistant tuberculosis. Nature Medicine, 13(3), 295–298.

Dutra, L. A., Regina, T., Melo, F. D., Chin, C. M., Leandro, J. (2012). Antitubercular drug discovery: the molecular modification as promise tool. International Research of Pharmacy and Pharmacology, 2(1), 1–9.

East African/British Medical Research Councils. (1971). Streptomycin plus PAS plus pyrazinamide in the treatment of pulmonary tuberculosis in east Africa. Tubercle, 52(3), 191-198.

East and central African/British Medical Research Councils. (1986). Controlled clinical trial of 4 short-course regimens of chemotherapy (three 6-month and one 8-month) for pulmonary tuberculosis: final report. East and Central African/British Medical Research Council Fifth Collaborative Study. Tubercle, 67(1), 5-15.

Elamin,A. A., Stehr,M., Oehlmann,W.; Singh,M. (2009). The mycolyltransferase 85A, a putative drug target of Mycobacterium tuberculosis: development of a novel assay and quantification of glycolipid-status of the mycobacterial cell wall. Journal of Microbiological Methods, 79 (3), 358- 363.

Elamin, A.A., Stehr, M., Spallek, R., Rohde, M., Singh, M.The Mycobacterium tuberculosis Ag85A is a novel diacylglycerol acyltransferase involved in lipid body formation. (2011). Mol. Microbiol., 81, 1577–1592

Ellard, G. A., Haslam, R. M. (1976). Observations on the reduction of the renal elimination of urate in man caused by the administration pyrazinamide. Tubercle, 57(2), 97-103.

Federal Register of October 11, 1988, Department of services, Food and Drug Administration. 53 FR 39650

Fenhalls, G., Stevens, L., Moses, L., Bezuidenhout, J., Betts, J. C., Helden, P., Lukey, P. T., Duncan, K. (2002). In situ detection of mycobacterium tuberculosis transcripts in human lung granulomas reveals differential gene expression in necrotic lesions. Infect Immun, 70(11), 6330-6338.

Flynn, J. L., Chan, J. (2001). MINIREVIEW Tuberculosis: Latency and Reactivation. Infection and Immunity, 69(7), 4195-4201.

Flynn, J. L. (2006). Lessons from experimental Mycobacterium tuberculosis infections. Microbes and Infection, 8(4), 1179–1188.

Gandhi, N. R., Moll, A., Sturm, a W., Pawinski, R., Govender, T., Lalloo, U., Zeller, K., et al. (2006). Extensively drug-resistant tuberculosis as a cause of death in patients co-infected with tuberculosis and HIV in a rural area of South Africa. Lancet, 368(9547), 1575–1580.

Geraldes Santos, M. D. L. S., Figueiredo Vendramini, S. H., Gazetta, C. E., Cruz Oliveira, S. A., Scatena Villa, T. C. (2007). Poverty: socioeconomic characterization at tuberculosis. Revista latino-americana de enfermagem, 15 Spec No, 762–767.

Girling, D. J.(1978). The hepatic toxicity of antituberculosis regimens containing isoniazid, rifampicin and pyrazinamide. Tubercle, 59(1), 13-32.

Gumbo, T., Dona, C. S., Meek, C., Leff, R. (2009).Pharmacokinetics-pharmacodynamics of pyrazinamide in a novel in vitro model of tuberculosis for sterilizing effect: a paradigm for faster assessment of new antituberculosis drugs. Antimicrobial Agents and Chemotherapy, 53(8), 3197-3204.

Haebich, D., Von Nussbaum, F. (2009). Lost in transcription-inhibition of RNA polymerase. Angewandte Chemie (International ed. in English), 48(19), 3397–3400.

Haydel, S. E. (2010). Extensively drug-resistant tuberculosis: a sign of the times and an impetus for antimicrobial discovery. Pharmaceuticals (Basel, Switzerland), 3(7), 2268–2290.

Heep, M., Rieger, U., Beck, D., , Lehn, N. (2000). Mutations in the beginning of the rpoB gene can induce resistance to rifamycins in both Helicobacter pylori and Mycobacterium tuberculosis. Antimicrobial Agents and Chemotherapy, 44(4), 1075–1077.

Hong Kong Chest Service/British Medical Research Council. (1991). Controlled trial of 2, 4, and 6months of pyrazinamide in 6-month, three-times-weekly regimens for smear-positive pulmonary tuberculosis, including an assessment of a combined preparation of isoniazid, rifampin, and pyrazinamide. Results at 30 months. The American Review of Respiratory Disease. 143(4 Pt 1),700-706.

Houston, J. B. (1994). Utility of in vitro drug metabolism data in predicting in vivo metabolic clearance. Biochemical Pharmacology, 47(9), 1469-1479.

Hutter, B., Singh, M. (1998). Host vector system for high-level expression and purification of recombinant, enzymatically active alanine dehydrogenase of Mycobacterium tuberculosis. Gene,212(1),21-29.

immunocytochemistry methods, techniques & protocols: www.ihcworld.com

Irschik, H., Jansen, R., Höfle, G., Gerth, K., Reichenbach, H. (1985). The corallopyronins, new inhibitors of bacterial RNA synthesis from myxobacteria. The Journal of Antibiotics (Tokyo), 38 (2), 145-152.

Irschik, H., Augustiniak, H., Gerth, K., Höfle, G., Reichenbach, H. (1995). The ripostatins, novel inhibitors of eubacterial RNA polymerase isolated from myxobacteria. The Journal of Antibiotics (Tokyo), 48(8), 787–792.

Jayaram, R., Gaonkar, S., Kaur, P., Suresh, B.L., Mahesh, B.N., Jayashree, R., Nandi, V. et al. (2003). Pharmacokinetics-pharmacodynamics of rifampin in an aerosol infection model of tuberculosis. Antimicrobial Agents Chemotherapy, 47(7), 2118-2124.

Jayaram, R., Shandil, R. K., Gaonkar, S., Kaur, P., Suresh, B. L., Mahesh, B. N., Jayashree, R et al. (2004). Isoniazid Pharmacokinetics-Pharmacodynamics in an Aerosol Infection Model of Tuberculosis. Antimicrobial Agents Chemotherapy, 48(8), 2951–2957.

Jiunn, H. L., Anthony, Y. H. L. (1997). Role of pharmacokinetics and metabolism in drug discovery and development. Pharmacological Reviews, 49(4), 403-449.

Jureen, P. (2008). Molecular characterization of antibiotic resistance in mycobacterium tuberculosis. Swedish institute for infectious disease control, Solna, Sweden.

Karlsson M., Kurz T., Brunk, U., Nilsson, S., Frennesson, C. (2010). What does the commonly used DCF-test for oxidative stress really show?. The Biochemical Journal, 428(2), 183–190.

Kerns, E. H., Di, L. (2003). Pharmaceutical profiling in drug discovery. Drug Discovery Today, 8(7), 316–323.

Khachatourians, G. G., Tipper, J. (1974). Inhibition of messenger ribonucleic acid synthesis in escherichia coli by thiolutin. Journal of Bacteriology, 119(3), 795-804.

Kinnings, S. L., Liu, N., Buchmeier, N., Tonge, P. J., Xie, L., Bourne, P. E. (2009). Drug discovery using chemical systems biology: repositioning the safe medicine Comtan to treat multi-drug and extensively drug resistant tuberculosis. PLoS Computational Biology, 5(7), e1000423.

Kohl ,W., Irschik, H., Reichenbach, H., Höfle, G. (1983). Myxopyronin A und B - zwei neue Antibiotika aus Myxococcus fuluus Stamm Mx f50. European Journal of Organic Chemistry, 1983(10), 1656–1667.

Koul, A., Arnoult, E., Lounis, N., Guillemont, J., Andries, K. (2011). The challenge of new drug discovery for tuberculosis. Nature, 469, 483–490.

Kozlov, M., Bergendahl, V., Burgess, R., Goldfarb, A., Mustaev, A. (2005). Homogeneous fluorescent assay for RNA polymerase. Analytical Biochemistry, 342(2), 206–213.

Kuhlman, P., Duff, H. L., Galant, A. (2004). A fluorescence-based assay for multisubunit DNA-dependent RNA polymerases. Analytical Biochemistry, 324(2), 183–190.

Laemmli , U. K. (1970).Cleavage of Structural Proteins during the Assembly of the Head of Bacteriophage T4. Nature, 227, 680 - 685.

Lee, C.S., Gambertoglio ,J.G., Brater, D.C., Benet, L.Z. (1977). Kinetics of oral ethambutol in the normal subject. Clin Pharmacol Ther, 22(5 Pt 1),615-21.

Lee, R. E., Protopopova, M., Crooks, E., Slayden, R. A, Terrot, M., Barry, C. E. (2003). Combinatorial lead optimization of [1,2]-diamines based on ethambutol as potential antituberculosis preclinical candidates. Journal of Combinatorial Chemistry, 5(2), 172–187.

Leeson, P. D., Springthorpe, B. (2007). The influence of drug-like concepts on decision-making in medicinal chemistry. Nature Reviews. Drug discovery, 6(11), 881–890.

Leimane, V., Riekstina, V., Holtz, T. H., Zarovska, E., Skripconoka, V., Thorpe, L. E., Laserson, K. F., et al. (2005). Clinical outcome of individualised treatment of multidrug-resistant tuberculosis in Latvia: a retrospective cohort study. Lancet, 365(9456), 318–326.

Lemaitre, N., Callebaut, I., Frenois, F. D., Jarlier, V., Sougakoff, W. (2001). Study of the structure–activity relationships for the pyrazinamidase (PncA) from Mycobacterium tuberculosis. Biochem. J., 353, 453–458.

Lenaerts, A. J., Degroote, M. A., Orme, I. M. (2008). Preclinical testing of new drugs for tuberculosis: current challenges. Trends in Microbiology, 16(2), 48–54.

Ley, S. V., Priour, A. (2002). Total Synthesis of the Cyclic Peptide Argyrin B. European Journal of Organic Chemistry, 2002(23), 3995–4004.

Lindup, W.E., L'eorme, M.C. (1981). Clinical Pharmacology Plasma protein binding of drugs. British Medical Journal (Clin Res Ed), 282(6259), 212–214.

Liu, J., Barry, C. E., Besra, G. S., Nikaido, H. (1996). Mycolic acid structure determines the fluidity of the mycobacterial cell wall. The Journal of Biological Chemistry, 271(47), 29545–29551.

Malhotra, J. D., Miao, H., Zhang, K., Wolfson, A., Pennathur, S., Pipe, S. W., Kaufman, R. J. (2008). Antioxidants reduce endoplasmic reticulum stress and improve protein secretion. Proceedings of the National Academy of Sciences of the United States of America, 105(47), 18525–18530.

Mariner, K., McPhillie, M., Trowbridge, R., Smith, C., O'Neill, A. J., Fishwick, C. W. G., Chopra, I. (2011). Activity of and development of resistance to corallopyronin A, an inhibitor of RNA polymerase. Antimicrobial Agents and Chemotherapy, 55(5), 2413–2416.

Marriner, G. A., Nayyar, A., Uh, E., Wong, S. Y., Mukherjee, T., Via, L. E., Carroll, M., et al. (2011). The medicinal chemistry of tuberculosis chemotherapy. Top Med Chem, 7, 47–124.

McClure, W. R. (1980). Rate-limiting steps in RNA chain initiation. Proceedings of the National Academy of Sciences of the United States of America, 77(10), 5634–5638.

McKinnon, P. S., Davis, S. L. (2004). Pharmacokinetic and pharmacodynamic issues in the treatment of bacterial infectious diseases. European Journal of Clinical Microbiology, 23(4), 271–288.

Mestdagh, M., Fonteyne, P. A., Realini, L., Rossau, R., Jannes, G., Mijs, W., De Smet, K. A., et al.(1999).Relationship between Pyrazinamide Resistance, Loss of Pyrazinamidase Activity, and Mutations in the pncA Locus in Multidrug-Resistant Clinical Isolates of Mycobacterium tuberculosis Antimicrobial Agents and Chemotherapy, 43(9), 2317–2319.

Mitchison, D. A. (1985). The action of antituberculosis drugs in short-course chemotherapy. Tubercle, 66(3), 219-225.

Mitchison, D. A., Davies, G. R. (2008). Assessment of the efficacy of new anti-tuberculosis drugs. The Open Infectious Diseases Journal, 2, 59–76.

Moghazeh, S. L., Pan, X., Arain, T., Stover, C. K., Musser, J. M., , Kreiswirth, B. N. (1996). Comparative antimycobacterial activities of rifampin, rifapentine, and KRM-1648 against a collection of rifampin-resistant Mycobacterium tuberculosis isolates with known rpoB mutations. Antimicrobial Agents and Chemotherapy, 40(11), 2655–2657.

MondaL, S. K., Mazumder, U. K., Mondal, N. B, Banerjee, S. (2008). Optimization of rat liver microsomal stability assay using HPLC. Journal of Biological Sciences, 8(6), 1110–1114.

Moore-Gillon, J. (2001). Multidrug-Resistant Tuberculosis: This Is the Cost. Annals New York Academy of Sciences,953b, 233–240.

Mukhopadhyay, J., Das, K., Ismail, S., Koppstein, D., Jang, M., Hudson, B., Sarafianos, S., et al. (2008). The RNA polymerase " switch region " is a target for inhibitors. Cell, 135(2), 295–307.

Musser, J. M. (1995). Antimicrobial agent resistance in mycobacteria: molecular genetic insights. Clinical Microbiology Reviews, 8(4), 496–514.

Muthaiah, M., Jagadeesan, S., Ayalusamy, N., Sreenivasan, M., Prabhu, S. S., Muthuraj, U., Senthilkumar, K., et al. (2010). Molecular epidemiological study of pyrazinamide-resistance in clinical isolates of mycobacterium tuberculosis from south India. International Journal of Molecular Sciences, 11(7), 2670–2680.

Naritomi, Y., Terashita, S., Kimura, S., Suzuki, A., Kagayama, A., Sugiyama, Y. (2001). Prediction of human hepatic clearance from in vivo animal experiments and in vitro metabolic studies with liver microsomes from animals and humans. Drug Metab Dispos. ,29(10),1316-24.

Nassar, A. F., Hollenburg, P. F., Scatina, J. (2009). Drug metabolism handbook: concepts and applications. John Wiley and Sons.

Nishimura, K., Takenaka, Y., Kishi, M., Tanahashi, T., Yoshida, H., Okuda, C., Mizushina, Y. (2009). Synthesis and DNA polymerase alpha and beta inhibitory activity of alkyl p-coumarates and related compounds. Chemical & pharmaceutical bulletin (Tokyo), 57(5), 476–480.

Nuermberger, E. L., Yoshimatsu, T., Tyagi, S., Williams, K., Rosenthal, I., O'Brien, R. J., Vernon, A. a, et al. (2004). Moxifloxacin-containing regimens of reduced duration produce a stable cure in murine tuberculosis. American Journal of Respiratory and Critical Care Medicine, 170(10), 1131–1134.

Nuermberger, E., Rosenthal, I., Tyagi, S., Williams, K. N., Almeida, D., Peloquin, C. a, Bishai, W. R., et al. (2006). Combination chemotherapy with the nitroimidazopyran PA-824 and first-line drugs in a murine model of tuberculosis. Antimicrobial Agents and Chemotherapy, 50(8), 2621–2625.

Nuermberger, E. (2008). Using animal models to develop new treatments for tuberculosis. Semin Respir Crit Care Med, 29(5),542-551.

Nuermberger, E. L., Spigelman, M. K., Yew, W. W. (2010). Current development and future prospects in chemotherapy of tuberculosis. Respirology, 15(5), 764–778.

Nwaka, S., Hudson A. (2006). Innovative lead discovery stratigies for tropical diseases. Nature reviews-drug discovery, (5), 941-955.

O'Brien, R. J., Nunn, P. P. (2001). Pulmonary Perspective: The need for new drugs against tuberculosis obstacles, opportunities, and next steps. Am J Respir Crit Care Med, 162, 1055–1058.

OECD guideline for testing of chemicals: Acute Oral Toxicity – Up-and-Down Procedure. (2001), 425 (December).

Ohno, H., Koga, H., Kohno, S., Tashiro, T., Hara, K. (1996). Relationship between rifampin MICs for and rpoB mutations of Mycobacterium tuberculosis strains isolated in Japan. Antimicrobial agents and chemotherapy, 40(4), 1053–1056.

Oliva, B., Neill, A. O., Wilson, J. M., Peter, J., Hanlon, O., Chopra, I., Hanlon, P. J. O., et al. (2001). Antimicrobial Properties and Mode of Action of the Pyrrothine Holomycin Antimicrobial Properties and Mode of Action of the Pyrrothine Holomycin. Antimicrobial Agents and Chemotherapy, 45(2),532-539.

O`Neill, A. O., Oliva, B., Storey, C., Hoyle, A., Fishwick, C., Chopra, I., Chopra, I. A. N. (2000). RNA polymerase inhibitors with activity against rifampin-resistant mutants of staphylococcus aureus RNA polymerase inhibitors with activity against rifampin-resistant mutants of staphylococcus aureus. Antimicrobial Agents And Chemotherapy, 44(11), 3163-3166.

Palomino, J., Martin, A., Camacho, M., Guerra, H., Swings, J., Portaels, F. (2002). Resazurin microtiter assay plate: simple and inexpensive method for detection of drug resistance in Mycobacterium tuberculosis. Antimicrobial Agents and Chemotherapy. 46(8), 2720-2722.

Panchagnula, R., Thomas, N. S. (2000). Biopharmaceutics and pharmacokinetics in drug research. International journal of pharmaceutics, 201(2), 131–150.

Petrella, S., Gelus-Ziental, N., Maudry, A., Laurans, C., Boudjelloul, R., Sougakoff, W. (2011). Crystal structure of the pyrazinamidase of Mycobacterium tuberculosis: insights into natural and acquired resistance to pyrazinamide. PloS one, 6(1), e15785.

Portugal, I., Barreiro, L., Moniz-Pereira, J., Brum, L. (2004) pncA mutations in pyrazinamide-resistant mycobacterium tuberculosis isolates in Portugal, Antimicrobial Agents And Chemotherapy, 48(7), 2736–2738.

Prentis, R. a, Lis, Y.,Walker, S. R. (1988). Pharmaceutical innovation by the seven UK-owned pharmaceutical companies (1964-1985). British Journal of Clinical Pharmacology, 25(3), 387–96.

Raman, K., Yeturu, K., Chandra, N. (2008). targetTB: A target identification pipeline for Mycobacterium tuberculosis through an interactome, reactome and genome-scale structural analysis. BMC systems biology, 2, 109.

Rastogi, N., Goh, K. S., David, H. L. (1990). Enhancement of drug susceptibility of Mycobacterium avium by inhibitors of cell envelope synthesis. Antimicrobial Agents and Chemotherapy, 34(5), 759–764.

Raynaud, C., Lanéelle, M. A., Senaratne, R. H., Draper, P., Lanéelle, G., Daffé, M. (1999). Mechanisms of pyrazinamide resistance in mycobacteria: importance of lack of uptake in addition to lack of pyrazinamidase activity. Microbiology, 145(pt 6), 1359-1367.

Reed, L.J., & Muench, H. (1938). A simple method of estimating fifty percent endpoints. American Journal of Hygiene, 27, 493-497

Rolinson, G. N. (1980). The significance of protein binding of antibiotics in antibacterial chemotherapy. Journal of Antimicrobial Chemotherapy, 6, 311-317.

Römmele, G., Wirz, G., Solf, R., Vosbeck, K., Gruner, J., Wehrli, W. (1990). Resistance of Escherichia Coli to rifampicin and sorangicin A-a comparison. The Journal of Antibiotics (Tokyo), 43 (1), 88-91.

Rosenthal, I. M., Zhang, M., Williams, K. N., Peloquin, C. a, Tyagi, S., Vernon, A. a, Bishai, W. R., et al. (2007). Daily dosing of rifapentine cures tuberculosis in three months or less in the murine model. PLoS Medicine, 4(12), e344.

Rowland, K. (2012). Totally drug-resistant TB emerges in india discovery of a deadly form of TB highlights crisis of 'mismanagement'. Nature News, (13 January).

Sacchettini, J. C., Rubin, E. J., Freundlich, J. S. (2008). Drugs versus bugs: in pursuit of the persistent predator Mycobacterium tuberculosis. Nature Reviews. Microbiology, 6(1), 41–52.

Salfinger, M., , Heifets, L. B. (1988). Determination of pyrazinamide MICs for Mycobacterium tuberculosis at different pHs by the radiometric method. Antimicrobial Agents and Chemotherapy, 32(7), 1002–1004.

Sánchez, J. G. B., Kouznetsov, V. V. (2010). Antimycobacterial susceptibility testing methods for natural products research. Brazilian Journal of Microbiology, 41(2), 270-277.

Sánchez, F., López Colomés, J. L., Villarino, E., Grosset, J. (2011). New drugs for tuberculosis treatment. Enferm Infecc Microbiol Clin, 29(Supl 1), 47-56.

Sarkar, S., Suresh, M. R. (2011). An overview of tuberculosis chemotherapy - a literature review. Journal of pharmacy & pharmaceutical sciences, 14(2), 148–161.

Schmidt, S., Röck, K., Sahre, M., Burkhardt, O., Brunner, M., Lobmeyer, M. T., , Derendorf, H. (2008). Effect of protein binding on the pharmacological activity of highly bound antibiotics. Antimicrobial agents and chemotherapy, 52(11), 3994–4000.

Schmidt, S., Gonzalez, D., , Derendorf, H. (2010). Significance of protein binding in pharmacokinetics and pharmacodynamics. Journal Of Pharmaceutical Sciences, 99(3), 1107–1122.

Scorpio, A., Zhang, Y. (1996). Mutations in pncA, a gene encoding pyrazinamidase/nicotinamidase, cause resistance to the antituberculous drug pyrazinamide in tubercle bacillus. Nature Medicine, 2(6), 662-667.

Shaaban, S. (2010). Synthesis and Biological Activity of Multifunctional Sensor/Effector Catalysts. Chemie, Pharmazie, Bio- und Werkstoffwissenschaften der Universität des Saarlandes, Saarbrücken, Germany.

Shahab, F.M., Kobarfard, F., Shafaghi, B., Dadashzadeh, S. (2010). Preclinical pharmacokinetics of KBF611, a new antituberculosis agent in mice and rabbits, and comparison with thiacetazone. Xenobiotica , 40 (3), 225-234.

Sharma, S. K., Mohan, a. (2004). Extrapulmonary tuberculosis. The Indian Journal of Medical Research, 120(4), 316–353.

Shi, C., Shi, J., Xu, Z. (2011). A review of murine models of latent tuberculosis infection. Scandinavian Journal of Infectious Diseases, 43(11-12), 848–856.

Sigma-aldrich protocols: www.sigmaldrich.com

Simões, M. F., Valente, E., Gómez, M. J. R., Anes, E., Constantino, L. (2009). Lipophilic pyrazinoic acid amide and ester prodrugs stability, activation and activity against M. tuberculosis. European journal of pharmaceutical sciences, 37(3-4), 257–263.

Singh, P., Mishra, a K., Malonia, S. K., Chauhan, D. S., Sharma, V. D., Venkatesan, K., , Katoch, V. M. (2006). The paradox of pyrazinamide: an update on the molecular mechanisms of pyrazinamide resistance in Mycobacteria. The Journal of Communicable Diseases, 38(3), 288–298.

Sousa, M., Pozniak, A., Boffito, M. (2008). Pharmacokinetics and pharmacodynamics of drug interactions involving rifampicin, rifabutin and antimalarial drugs. The Journal of Antimicrobial Chemotherapy, 62(5), 872–878.

Stabb, E. V., Handelsman, J. (1998). Genetic analysis of zwittermicin A resistance in Escherichia coli: effects on membrane potential and RNA polymerase. Molecular Microbiology, 27(2), 311–322.

Stehr, M., Elamin ,A. A , Singh, M. (2012). Cytosolic lipid inclusions formed during infection by viral and bacterial pathogens. Microbes and Infection, XX (2012), 1-11.

Sun, Z., Scorpio, A, Zhang, Y. (1997). The pncA gene from naturally pyrazinamide-resistant Mycobacterium avium encodes pyrazinamidase and confers pyrazinamide susceptibility to resistant M. tuberculosis complex organisms. Microbiology, 143(Pt 10), 3367–3373.

Sun, Z., Zhang, Y. (1999). Reduced pyrazinamidase activity and the natural resistance of Mycobacterium kansasii to the antituberculosis drug pyrazinamide. Antimicrobial Agents and Chemotherapy, 43(3), 537–542.

Thattakudian Sheik Uduman, M. S., Sundarapandian, R., Muthumanikkam, A., Kalimuthu, G., Parameswari S, A., Vasanthi Srinivas, T. R., Karunakaran, G. (2011). Protective effect of methanolic extract of Annona squamosa Linn in isoniazid-rifampicin induced hepatotoxicity in rats. Pakistan journal of pharmaceutical sciences, 24(2), 129–134.

Tostmann, A., Boeree, M. J., Aarnoutse, R. E., de Lange, W. C. M., van der Ven, A. J. A. M., Dekhuijzen, R. (2008). Antituberculosis drug-induced hepatotoxicity: concise up-to-date review. Journal of Gastroenterology and Hepatology, 23(2), 192–202.

Valim, A. R. M., Rossetti, M. L. R., Marta, O., Zaha, A., Valim, I. A. R. M. (2000). Mutations in the rpoB Gene of Multidrug-Resistant Mycobacterium tuberculosis Isolates from Brazil. Journal of Clinical Microbiology, 38(8), 3119-3122.

Van Bambeke, F., Barcia-Macay, M., Lemaire, S., Tulkens, P. (2006). Cellular pharmacodynamics and pharmacokinetics of antibiotics: Current views and perspectives. Current Opinion in Drug Discovery & Development, 9(2), 218-230.

Van den Boogaard, J., Kibiki, G. S., Kisanga, E. R., Boeree, M. J., , Aarnoutse, R. E. (2009). New drugs against tuberculosis: problems, progress, and evaluation of agents in clinical development. Antimicrobial Agents and Chemotherapy, 53(3), 849–862.

Vassiliou, W., Epp, J. B., Wang, B. B., Del Vecchio, A. M., Widlanski, T., Kao, C. C. (2000). Exploiting polymerase promiscuity: A simple colorimetric RNA polymerase assay. Virology, 274(2), 429-437.

WHO. (2007). Tuberculosis facts.

WHO. (2010), Treatment of tuberculosis guidelines (4th ediation).

WHO. (2011). Global tuberculosis control.

Wang, S., Sim, T. B., Kim, Y.-S., , Chang, Y.-T. (2004). Tools for target identification and validation. Current Opinion in Chemical Biology, 8, 371–377.

Wang, Y., Mathis, C. a, Huang, G.-F., Debnath, M. L., Holt, D. P., Shao, L., Klunk, W. E. (2003). Effects of lipophilicity on the affinity and nonspecific binding of iodinated benzothiazole derivatives. Journal of Molecular Neuroscience, 20(3), 255–260.

Watterson, S. A., Wilson, S. M., Yates, M. D., Drobniewski, F. A. (1998). Comparison of three molecular assays for rapid detection of rifampin resistance in mycobacterium tuberculosis. Journal of Clinical Microbiology, 36(7), 1969-1973.

Weissman, K. J., Müller, R. (2010). Myxobacterial secondary metabolites: bioactivities and modes-of-action. Natural Product Reports, 27(9), 1276–1295.

Wu, P., Daniel-Issakani, S., LaMarco, K., Strulovici, B. (1997). An automated high throughput filtration assay: Application to polymerase inhibitor identification. Analytical Biochemitry, 245(2), 226-230.

Xu, K.-H., Lu, D.-P. (2010). Plumbagin induces ROS-mediated apoptosis in human promyelocytic leukemia cells in vivo. Leukemia research, 34(5), 658–665.

Xu, M., Zhou, Y. N., Goldstein, B. P., & Jin, D. J. (2005). Cross-resistance of Escherichia Coli RNA polymerases conferring rifampin resistance to different antibiotics. Journal Of Bacteriology, 187(8), 2783–2792.

Yamamoto, S., Toida, I., Watanabe, N., Ura, T. (1995). In vitro antimycobacterial activities of pyrazinamide analogs. Antimicrobial agents and chemotherapy, 39(9), 2088–2091.

Young, D., Dye, C. (2006). The development and impact of tuberculosis vaccines. Cell, 124(4), 683–687.

Yuen, L. K. W., Leslie, D., Coloe, P. J. (1999). Bacteriological and Molecular Analysis of Rifampin-Resistant Mycobacterium tuberculosis Strains Isolated in Australia. Journal of Clinical Microbiology, 37(12), 3844-3850.

Zhang, H., Deng, J.-Y., Bi, L.-J., Zhou, Y.-F., Zhang, Z.-P., Zhang, C.-G., Zhang, Y., et al. (2008). Characterization of Mycobacterium tuberculosis nicotinamidase/pyrazinamidase. The FEBS journal, 275(4), 753–762.

Zhang, Y., Scorpio, A., Nikaido, H., Sun, Z. (1999). Role of acid pH and deficient efflux of pyrazinoic acid in unique susceptibility of mycobacterium tuberculosis to pyrazinamide. Journal of Bacteriology, 181(7), 2044–2049.

Zhang, Y., Permar, S., Sun, Z. (2002). Conditions that may affect the results of susceptibility testing of Mycobacterium tuberculosis to pyrazinamide. Journal of Medical Microbiology, 51(1), 42–9.

Zhang, Y., Wade, M. M., Scorpio, A., Zhang, H., Sun, Z. (2003). Mode of action of pyrazinamide: disruption of Mycobacterium tuberculosis membrane transport and energetics by pyrazinoic acid. The Journal of antimicrobial chemotherapy, 52(5), 790–795.

Zhang, Y., Mitchison, D. (2003). The curious characteristics of pyrazinamide: a review. The International Journal of Tuberculosis and Lung Disease. 7(1), 6–21.

Zimhony, O., Cox, J. S., Welch, J. T., Vilchèze, C., Jacobs, W. R. (2000). Pyrazinamide inhibits the eukaryotic-like fatty acid synthetase I (FASI) of Mycobacterium tuberculosis. Nature Medicine, 6(9), 1043–1047.

www.admescope.com

www.cyprotex.com

8. Appendix:

Immunocytochemistry (ICC):

Different combinations of myxopyronin and ethambutol at different concentrations were investigated in the ICC to confirm their safety and to predict if they could produce any changes in the cell morphology. Endoplasmic reticulum (ER) (Fig. 40), microtubules (Fig. 41) and actin stress fibres (Fig. 42) were stained after 18 hours incubation with the test compounds.

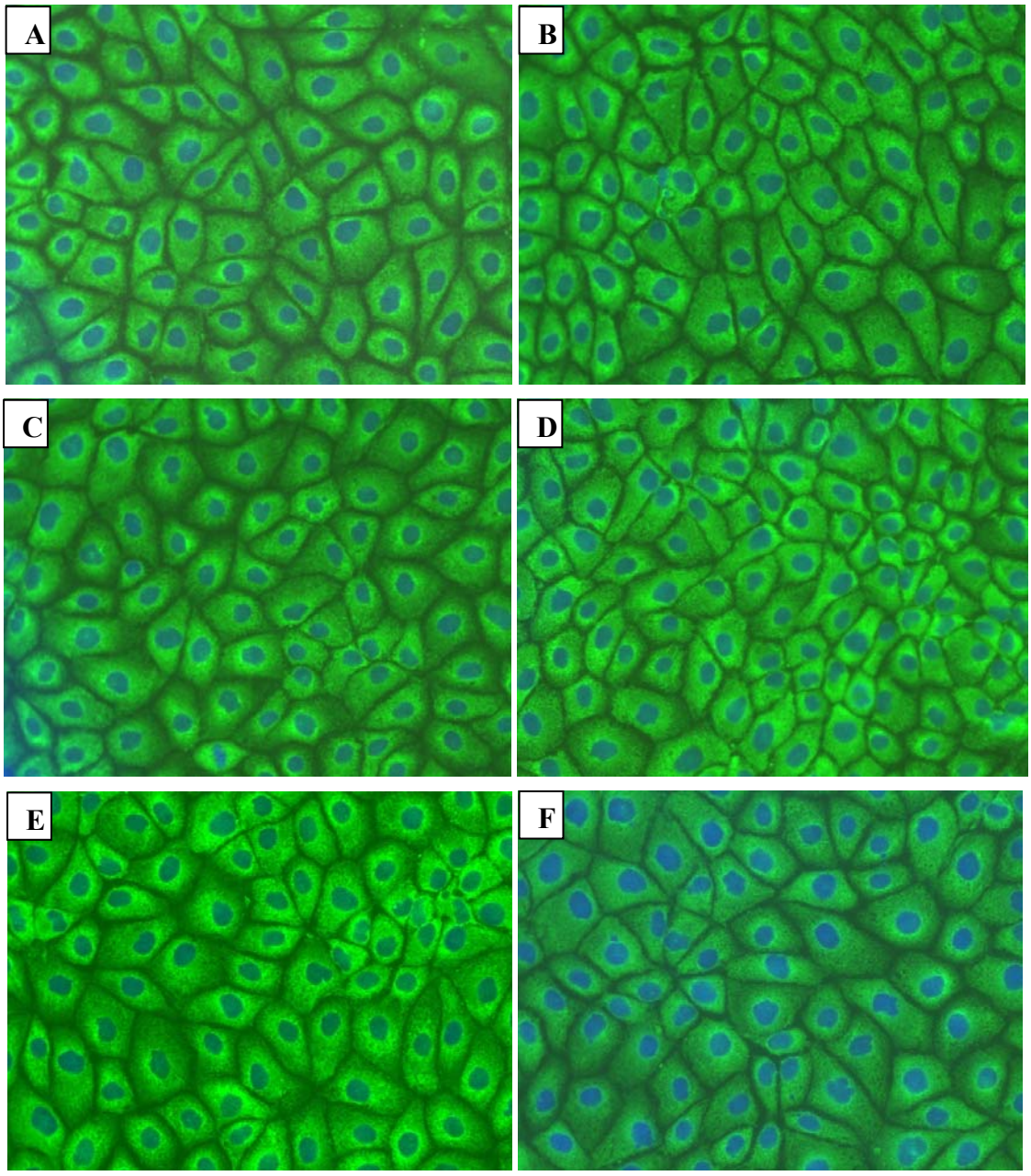

Fig (40): Immunoflorescent staining of endoplasmic reticulum: A: Control, B: LX018, C: LX019, D: LX021, E: LX004, F: LX024. PtK2 cells were incubated with 20 µg/ml of different combinations for 18 hours. In comparison with control cells, treated cells show also normal appearance of the endoplasmic reticulum.

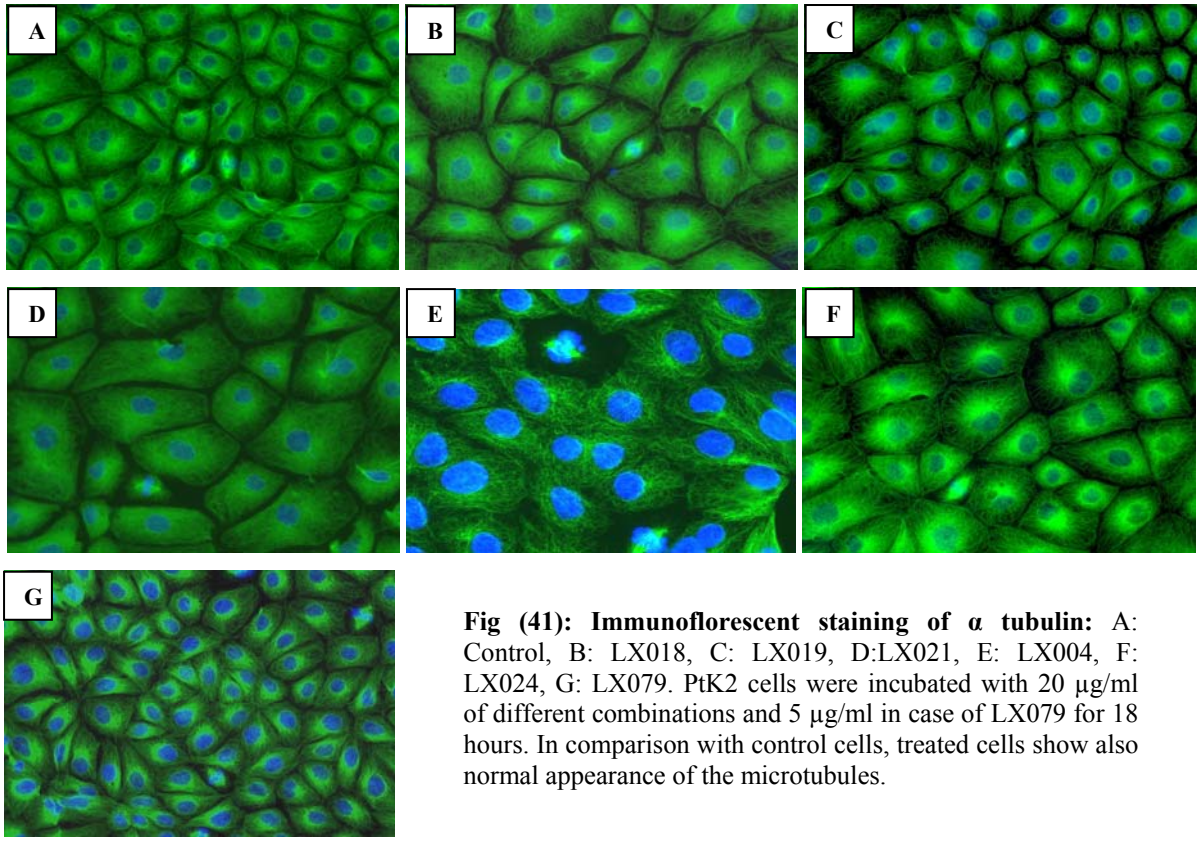

Fig (41): Immunoflorescent staining of α tubulin: A: Control, B: LX018, C: LX019, D:LX021, E: LX004, F: LX024, G: LX079. PtK2 cells were incubated with 20 µg/ml of different combinations and 5 µg/ml in case of LX079 for 18 hours. In comparison with control cells, treated cells show also normal appearance of the microtubules.

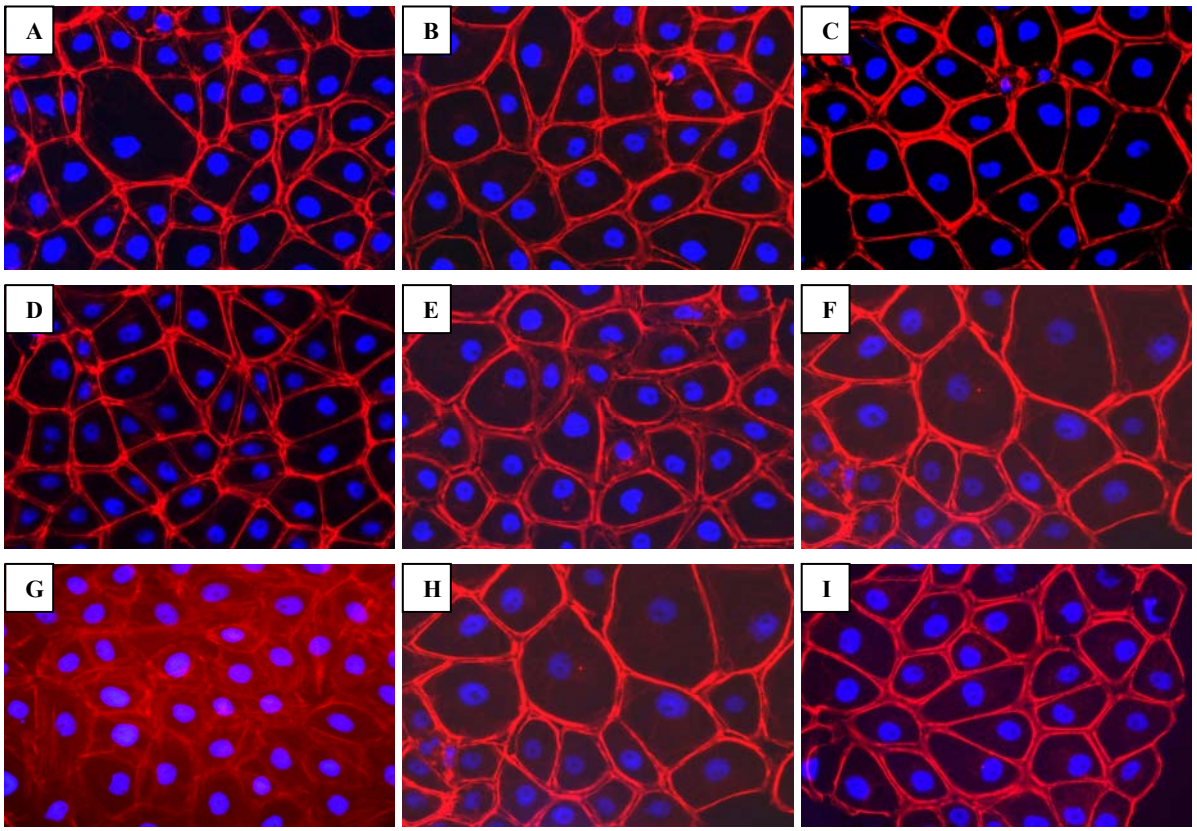

Fig. (42): Immunoflorescent staining of actin: A: Control, B: myxopyronin, C: ethambutol, D: LX018, E: LX019, F: LX021, G: LX004, H: LX024, I: LX079. PtK2 cells were incubated with 20 µg/ml of different combinations and 5 µg/ml in case of LX079 for 18 hours. In comparison with control cells, treated cells show also normal appearance of the actin stress fibres.

In addition, (Fig. 41) shows the staining of microtubules after the treatment with LX079, the substance that was selected from the library of compounds to be further investigated. (Fig. 42) shows also the staining of actin stress fibres after the treatment with myxopyronin and ethambutol individually and the compound LX079. All treated cells show normal morphological appearance.

9. Abbreviations:

ADME	Absorption, distribution, metabolism, and excretion
APS	Adenosine 5´ phosphosulfate
ATP	Adenosine triphosphate
AUC	Area under the curve
BCG	Bacille Calmette-Guérin
BSA	Bovine serum albumin
CC	Column chromatography
CL	Clearance
C_{max}	peak concentration
CYP	Cytochrome P450 enzymes
DCF	2′,7′-dichlorofluorescein
DCFH	2`,7`-dichlorodihydrofluorescein
DCFH-DA	2`,7`-dichlorodihydrofluorescein diacetate
DMSO	Dimethyl sulfoxide
DNA	Desoxiribonucleic acid
DOTS	Directly observed treatment short-course
EBA	Early bactericidal activity
ED	Equilibrium dialysis
EDTA	Ethylenediamine tetraacetic acid
FASI	Fatty acid synthetase I
FITC	Fluorescein isothiocyanate
FPLC	Fast protein liquid chromatography
h	Hour
His	Histidine
HIV	Human immunodeficiency virus
HMS	Hepatic microsomal stability
ICC	Immunocytochemistry
IMAC	Immobilized metal affinity chromatography
INH	Isoniazid
kDa	Kilodalton
LB	Luria Bertani medium

Log*Pow*	Octanol–water partition coefficient
Luc	Luciferin
min	Minute
mM	Millimolar
M	Molar
MDR-TB	multi-drug resistant TB
M. TB	*Mycobacterium tuberculosis*
MTT	(3-[4,5-dimethylthiazol-2-yl]-2,5-diphenyl tetrazolium bromide
NADPH	Nicotinamide adenine dinucleotide phosphate
NTP	Nucleotides (ATP, UTP, GTP& CTP)
OADC	Oleic acid, albumin, dextrose, catalase
OD	Optical density
OECD	Organisation for Economic Co-operation and Development
PAGE	Polyacrylamide gel electrophoresis
PBS	Phosphate buffered saline
PD	pharmacodynamics
PI	Propidium Iodide
PK	Pharmacokinetics
POA	Pyrazinoic acid
PPB	Plasma protein binding
PPi	Pyrophosphate
PTFE	Polytetrafluoroethylene
PS	Phospholipid phosphatidylserine
PZA	Pyrazinamide
QSAR	Quantitative structure activity relationship
RED	Rapid equilibrium dialysis device
REMA	Resazurin microtiter assay
RIF	Rifampin
RLU	Relative light unit
RNA	Ribonucleic acid
RNAP	DNA-dependent RNA polymerase
RNAPI	RNA polymerase inhibitors
ROS	Reactive oxygen species
rpm	Rounds per minute

SDS	Sodium dodecyl sulphate
SMW	Standard mouse weight
$t_{1/2}$	Half-life
TAE	Tris-Acetate-EDTA
TB	Tuberculosis
TLC	Thin layer chromatography
U	Unit
UPR	Unfolded protein response
UV	Ultraviolet light
V_d	Volume of distribution
WHO	World Health Organization
XDR-TB	Extensively drug-resistant TB